AN ANALOGUE COMPUTER FOR THE INVESTIGATION OF THE TRAJECTORIES OF COSMIC RAY PARTICLES IN THE GEOMAGNETIC FIELD

THESIS

submitted by

CLIFFORD JOHN BLAND

for the degree of

DOCTOR OF PHILOSOPHY

in the

UNIVERSITY OF LONDON

October 1961

ABSTRACT.

Using a small scale model of the geomagnetic field (a terrella), the cosmic radiation was simulated by means of a stream of electrons leaving its surface. Under certain conditions of field strength and electron energies these electrons are trapped in the terrella field and travel from the electron gun anode to the terrella surface. By use of scaling equations it is clear that this process is analagous to the screening of the low rigidity portion of the cosmic ray spectrum by the geomagnetic field at the so-called threshold or cut-off rigidity.

Investigation of the way in which this trapping occurs when the field is represented by a centred dipole reveals the main cone and the penumbra close to that predicted by VALLARTA et al. The width and transparency of the penumbra has been compared with theoretical predictions. Some discrepancy in the transparencies was found.

The augmentation of the main dipole field by radial dipoles produces regional anomaly fields similar to those existing at the surface of the earth. By this means, the effect of these anomaly fields on the penumbra has been studied. It appears that the centred dipole penumbra is not seriously affected by the higher order terms. In the region of latitude 10° - 20°, the penumbra seems to be that

appropriate to the latitude at which the threshold rigidity measured would occur in a centred dipole field. The Quenby and Webber method of predicting threshold rigidities has been checked and found to be no more than 10% in error at latitudes up to 30°.

The effect of an external uniform field in the direction of the dipole axis has been briefly investigated.

CONTENTS

CHAPTER 1. THE EFFECT OF GEOMAGNETISM UPON THE COSMIC RAY INTENSITY OBSERVED AT THE EARTH.

1.1 General Introduction.

The setting up of a large number of cosmic ray observatories in the last few years, particularly during the International Geophysical Year, has provided a means of studying the conditions existing in regions of space as yet inaccessible to space probes. Among the quantities that may now be more accurately measured are the energy spectrum and the direction and spatial scale of the modulation mechanisms responsible for the time variations of the cosmic ray intensity. A knowledge of these quantities permits models of the interplanetary conditions to be proposed and tested against world wide observations.

Not least among the diagnostic aids to this research is the geomagnetic field itself. This field controls the distribution of particles over the surface of the earth according to their energy, charge, and orientation upon entering the field. It is therefore important to have a good understanding of this controlling mechanism before ascribing various features of the cosmic radiation 'picture' to extraterrestrial influences.

In particular, a knowledge of the portion of the radiation spectrum prevented from reaching a given point on the earth is essential. This 'screening' occurs at the so-called 'threshold' or 'cut-off' rigidity*. A comprehensive knowledge of these threshold rigidities has been the aim of much research in recent years. The following text will describe experimental work undertaken to answer some questions arising from this work. Before doing so we shall indicate the inadequacies of earlier theoretical work and also show the importance of geomagnetism in this field, by reference to the 'time-variations' in the cosmic ray intensity.

* The term 'rigidity', here introduced, is defined by:-

$$P = \frac{pc}{Ze} \qquad (1.1)$$

where:

p is the momentum

c is the velocity of light

Z is the unit charge of a given component of the cosmic radiation.

and e is the electronic charge.

1.2 The Theory of Geomagnetic Effects.

Introduction.

Towards the end of the 1920's it was discovered that the primary radiation consisted of charged particles. SKOBELZYN (1929) investigated tracks in a cloud chamber and found them consistent with a source of charged particles outside the earth. Soon afterward, BOTHE and KOLHORSTER (1929), using the recently developed Geiger-Muller tubes, verified that the cosmic radiation did consist of charged particles. Almost simultaneously CLAY (1928) sent an ionization chamber around the world and discovered the latitude effect. This at once gave an indication of the momentum of the primary charged particles, and showed that it was necessary to bring geomagnetic effects into any discussion of intensity measurements.

Several years earlier, STORMER had begun an extensive series of theoretical investigations into the motion of charged particles in the field of a magnetic dipole, in order to explain the polar aurorae. This theoretical work was immediately applied to the field of cosmic rays by LEMAITRE and VALLARTA (1933).

1.3 Stormer Treatment of the Motion of Charged Particles in the Field of a Centred Dipole.

STORMER (1955) assumed that to a first approximation, the magnetic field of the earth resembled that of a centred dipole. The

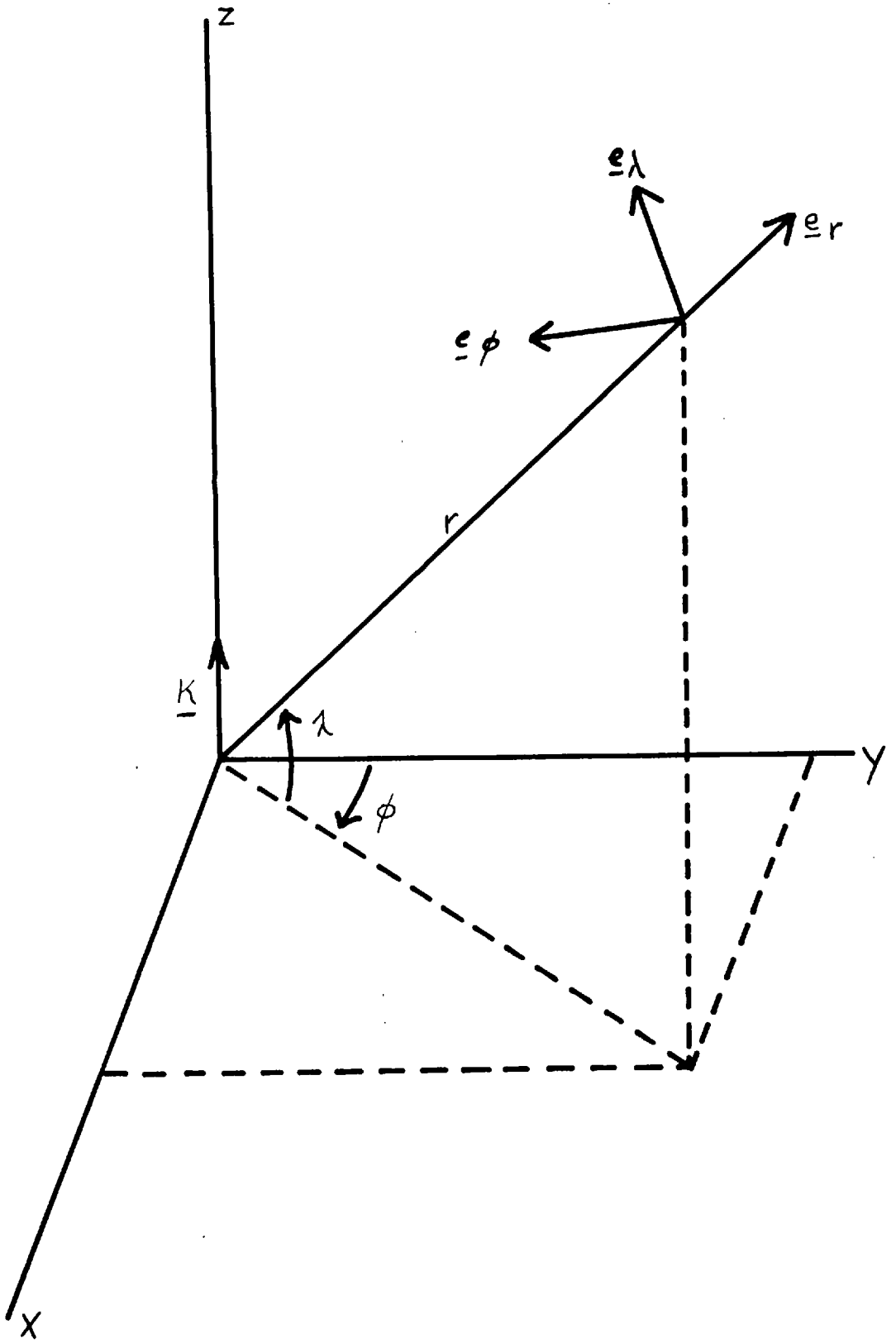

Fig. 1.1 Coordinate System used in derivation of Stormer Threshold Rigidities.

validity of this approximation will be dealt with in the section devoted to the description of the geomagnetic field.

The centred dipole approximation will be used in the following treatment in which spherical polar coordinates are adopted. These are illustrated in figure 1.1 in which the dipole axis lies along the z axis, and angles λ , φ refer to the geomagnetic latitude and longitude respectively. The Lagrangian of a charged particle moving in this field may be written as:-

$$L = -m_o c^2 \sqrt{1 - B^2} + \frac{e}{c} \underline{A}.\underline{v} \qquad (1.2)$$

where $\underline{A}$ is the vector potential of the magnetic field,

m_o the rest mass,

e the charge,

and $\underline{v}$ the velocity of the particle.

The generalised equation of motion

$$\frac{d}{dt}\left(\frac{dL}{dq}\right) = \frac{dL}{dq}$$

when evaluated for the φ coordinate yields the following integral equation as a consequence of $P_\varphi = \frac{dL}{d\varphi}$ being a constant of the motion.

$$r \cos\lambda \sin\theta + \frac{M}{P} \frac{\cos^2\lambda}{r} = \text{constant} \qquad (1.3)$$

where r is the distance of the particle from the origin

M is the dipole moment and

θ is the angle between $\underline{v}$ and $\underline{e}_\varphi$

e_φ being the unit vector specified in figure 1.1

This equation describes the motion of particles in the meridian plane i.e. a plane at right angles to the equatorial plane containing a line drawn from the centre of the dipole to the particle. The substitution of $r = \sqrt{\frac{M}{P}}\, R$ yields the following dimensionless equation:-

$$R \cos\lambda \sin\theta + \frac{\cos^2\lambda}{R} = 2\gamma \qquad (1.5)$$

γ is a constant which is proportional to the impact parameter of a particle relative to the dipole axis at infinity. R is now measured in units called Stormers.

As $\sin\theta$ must lie between + 1 and - 1 the substitution of either value yields an equation which describes a boundary line in the r, plane. This line is symmetrical about the R = 0 axis. This boundary divides two regions of space, one in which the particle is everywhere allowed and one in which the particle is everywhere forbidden. The shape of the boundary is determined by the value of γ.

In general there are two allowed regions, an outer one extending to infinity and an inner one containing the dipole. For $\gamma < 1$ the regions connect; for $\gamma > 1$ they do not. $\gamma = 1$ therefore defines critical conditions for the particle to enter the inner allowed region. The scale of the allowed regions with respect to the radius of the earth is determined by the momentum of the particle.

Substitution of $R = R_e = r_e \sqrt{\frac{P}{M}}$ and $\gamma = 1$ thus yields a critical value of P_c in terms of λ and θ, below which particles cannot arrive at a given point on the earth. P_c is given by the

following equation:-

$$P_c = \frac{4M_e c}{r_e^2 Ze} \left[\frac{1 - \sqrt{1 - \cos\theta \cos^3\lambda}}{\cos\theta \cos\lambda} \right]^2 \qquad (1.6)$$

For vertical incidence, $\theta = 90^\circ$ and the equation reduces to:-

$$P_c = \frac{4M_e c \cos^4\lambda}{r_e^2 Ze} \simeq 15 \cos^4\lambda \quad GV \qquad (1.7)$$

Alternatively one can find the critical angle of arrival ' θ ' when $\gamma = 1$ and $r = r_e$ for a given rigidity. This angle is the complement of a half angle defining the so-called 'Stormer cone', within which particles are allowed. LIOUVILLE'S theorem requires that the flux seen through this cone is the same as the flux at infinity (LEMAITRE & VALLARTA, 1933). Thus the boundaries of the allowed cone determine the intensity of radiation arriving at a given point.

The simple theory reviewed above gives necessary conditions for particles to arrive at a given point on the surface of the earth. These conditions, however, are not sufficient; step by step integration of many orbits reveals that some orbits are asymptotic to a whole series of periodic and semi-periodic orbits (LEMAITRE, 1935). Thus one can only say with certainty that those orbits up to the asymptotic "connect" between the observer and infinity. Moreover the effect of an impenetrateable earth has not been taken into account.

Elaboration of the original theory to take these latter effects into account was first attempted by LEMAITRE and VALLARTA (1933, 1936a,b). They found that the family of asymptotic orbits define another cone,

which they called the main cone, within which all radiation is unconditionally allowed. Trajectories of particles arriving within the main cone are relatively simple and arrive at the surface without making loops. Those particles arriving between the main and Stormer cone, in general have complicated trajectories, some of which are obstructed by the earth. The region between the main and Stormer cone is made up of bands of alternating allowed and forbidden regions. By analogy to optics it is known as the penumbra.

The transparency of the penumbra is zero at the equator and one hundred per cent at the pole. The percentage transparency in other latitudes has been calculated by SCHWARTZ (1959), HUTNER (1939) and others. In general such investigations required the use of computers to integrate the equations of motion of the particle. LEMAITRE and VALLARTA also found that in the region near the main cone, relatively simple trajectories may define a 'shadow cone' which further restricts the arrival of particles at the surface. This problem has been tackled by SCHREMP (1938) and more recently by KASPER (1959).

Experimental Evidence on the Distribution of the Cosmic Radiation over the Surface of the Earth.

The cosmic ray intensity at a given point may be expressed as:-

$$N(P,x,t) = \sum_{Z} \int_{P(\lambda\,\varphi)}^{\infty} S_Z(P,x) \left(\frac{dj_Z(p,t)}{dP}\right)_t dP \qquad (1.8)$$

$\left[\frac{dj_Z(P,t)}{dP}\right]_t$ $(p = P)$ being the differential rigidity spectrum at time t. and $S_z(P,x)$ being the specific yield function for a component of charge z at atmospheric depth x. $p(\lambda\,\varphi)$ is the threshold rigidity at latitude λ , and longitude φ .

Assuming that $S_Z(P,x)$ tends to zero at a certain value P_A (the atmospheric cut-off), then the minimum intensity occurs at a position of maximum threshold rigidity P_{max} if $P_A < P_{max}$.

The locus of minimum intensity thus defines a locus of maximum threshold rigidity (the so-called cosmic ray equator). The position of this locus is therefore a test of geomagnetic theory. Threshold rigidities may be evaluated by measuring the rigidity at which the differential rigidity spectrum tends to zero. In order to minimize atmospheric effects, these measurements are done at high altitudes (where $S(P,x) \rightarrow 1$) using for example, balloon borne Cerenkov-scintillation counters (McDONALD, 1956) or photographic emulsion (WADDINGTON, 1956).

In the centered dipole theory, lines of equal cosmic ray

intensity should be along circles of geomagnetic latitude. Early in the investigation of geomagnetic effects, serious discrepancies were observed (MILLIKAN and NEHER, 1937). Further inconsistencies from the predicted zenith angle distribution were observed by JOHNSON and READ (1938) using inclined telescopes. A thorough check of the centered dipole approximation was made by NEHER (1952) who found, amongst other things, that the observed threshold rigidities varied significantly from the pure dipole case, but found the values consistent if the eccentricity of the dipole were taken into account. The effects of the eccentricity of the dipole were first calculated by VALLARTA (1935).

Various authors have prepared tables of threshold rigidities assuming the geomagnetic field to be that of an eccentric dipole, in particular by KODAMA, KONDO and WADA (1957). However the results of WADDINGTON (1956) and McDONALD (1957) did not agree with the eccentric dipole model. These authors found startling differences in the threshold rigidities over North America and Europe. They ascribed these differences to a longitude shift in the eccentric dipole by 40° to the west. This model was suggested by SIMPSON et al. (1956) to explain the 'phase shift' observed in the cosmic ray equator in their world wide survey. KODAMA and MIYAZAKI (1957) provided experimental evidence in support of this view.

Surveys carried out in the region of South Africa, where a large magnetic anomaly exists, by ROTHWELL and QUENBY (1958)

indicated that a strong correlation exists between the local field and the cosmic ray intensity.

ROTHWELL (1958) suggested that the threshold rigidities should be calculated by using the magnetic dip latitude. Confirmation of this view was provided by the experiments of SANDSTROM (1958) and STOREY (1959) who found that the intensities observed during ~~aird~~ aero plane flights are better accounted for if the dip latitude is used rather than the geomagnetic latitude. This model also accounted for the results of ROSE et al. and KODAMA et al. Evidence against the westward shift of the effective magnetic coordinates was provided by PFOTZER (1956, 1957) from measurements made during the flare increase in 1956.

The good correlation of intensity observations with threshold rigidities calculated from the dip latitude suggests that the higher order terms in the geomagnetic field must be taken into account in the calculation of threshold rigidities.

Several authors have considered the effect of the quadrapole terms in the geomagnetic field. In particular, VALLARTA (1951) suggested that the 'phase shift' of the geomagnetic equator could be accounted for by the inclusion of quadrapole terms, in the calculation of threshold rigidities. JORY (1956), however, found that the dipole plus quadrapole cosmic ray equator was little different from the eccentric dipole cosmic ray equator. VALLARTA, GALL and LIFSHITZ (1948) considered the effect of the quadrapole terms on the shadow cones of SCHREMP and found it to be small. Later, GALL and LIFSCHITZ

(1956) calculated the effect of the quadrapole terms on the cosmic ray albedo. This work is difficult to check owing to lack of experimental evidence.

QUENBY and WEBBER (1959) developed an approximation for calculating threshold rigidities, which takes into account higher order terms, up to the sixth. At high geomagnetic latitudes ($\lambda > 40^{\circ}$), they argue that the particle is little affected by the non dipole field until it has close contact with a line of force as it approaches the earth's surface. This line of force therefore largely determines the point of arrival of the particle. If this line of force were approximated to by a line of force originating from a centred dipole, then the point of arrival would effectively have a new geomagnetic latitude. The threshold rigidity of this point would then be that appropriate to a latitude $\bar{\lambda}$ in a centred dipole field. The effective latitude $\bar{\lambda}$ is determined by an expression giving the 'best-fit' tilted dipole line of force to the actual line of force. This expression takes into account terms up to the sixth order. The relevant equations are developed in the paper by QUENBY and WEBBER (1959). The threshold rigidity is given by an equation analagous to that used to find the 'Stormer' threshold rigidity in the centred dipole case i.e.:-

$$Pc = \frac{M}{4r_e^2} \cos^4 \bar{\lambda} \qquad (1.9)$$

At equatorial latitudes ($\lambda < 20^{\circ}$), a different approach to the problem is used. It will be remembered that in the original Stormer treatment the inner and outer allowed regions were divided at $\gamma = 1$.

At equatorial latitudes the 'jaws' meet at about two earth's radii from the dipole centre, and are therefore distorted by the non dipole contribution to the geomagnetic field. QUENBY and WEBBER calculate the distortion of the boundary between the allowed and forbidden region and derive a modified magnetic moment:

$$M^1 = M(1 + 0.6 \frac{\Delta H}{H_c}) \qquad (1.10)$$

where ΔH is the difference between the actual horizontal field and that due to a centred dipole H_c. The factor 0.6 is calculated by weighting the multipole terms according to their average magnitude over the earth. They also argue that the effective latitude $\bar{\lambda}$ should be used in the expression for the threshold rigidity at equatorial latitudes instead of the geomagnetic latitude λ. The threshold rigidities in the region $\pm 20^\circ$ are therefore given by:-

$$P = \frac{M}{4r_e^2} (1 + 0.6 \frac{\Delta H}{H_c}) \cos^4 \bar{\lambda} \qquad (1.11)$$

Between latitudes 20° and 40°, no single expression for the threshold rigidity can be derived and therefore interpolation between the high and low latitude values is used.

The 'Quenby-Webber' treatment has been successful in accounting for many of the discrepancies of the 'Stormer' treatment. Values of threshold rigidities calculated in this manner are given in tables by QUENBY and WEBBER (1959) and COGGER (1960). These values are consistent with the observed cosmic ray equator, the auroral zones

and the distribution of the 1956 flare increase (QUENBY, 1958). Moreoger, their values are consistent with the threshold rigidities calculated in limited equatorial regions by KELLOGG (1960), using a digital computer. Further successes of the theory will be mentioned in the chapter dealing with the influences of geomagnetism on the interpretation of the time variations of the cosmic ray intensity. Recently, QUENBY and WENK (1961) have used the results of some work by HULTQVIST (1958) to obtain better values of the effective latitude $\bar{\lambda}$ at higher altitudes. HULTQVIST calculated the point of intersection of lines of force leaving high latitudes, with the equatorial plane.

The Quenby Webber treatment suffers from the disadvantage that it can only predict the 'Stormer cone' threshold rigidity. It is therefore necessary to make an estimate of the correction to be made for the penumbra. The investigation of the penumbra has been undertaken by many workers. SCHWARTZ (1958) has made extensive calculations on the penumbra at latitudes above 30°. His results agree well with experimental investigations by WINKLER and ANDERSON (1954) and DANIELSON and FREIER (1958). SCHWARTZ also confirms experimental evidence that some of the earlier shadow cone calculations by SCHREMP (1938) are grossly in error. The equatorial aeroplane flights by KATZ, MEYER and SIMPSON (1958) afford an estimate of the penumbral corrections if 'Quenby-Webber' threshold rigidities are subtracted from the observed threshold rigidities. Tables of

threshold rigidities containing these penumbral corrections have recently been prepared by QUENBY & WENK (1961). It is found that the average behaviour of the penumbra is that to be expected from the centred dipole approximation. However, there are serious differences in some regions. The question arises whether these differences are due to the fact that the penumbral corrections are estimated by subtracting possibly incorrect threshold rigidities from the observed threshold rigidities, or whether they are due to the use of penumbral corrections calculated for a dipole field, when we know that the geomagnetic field deviates substantially from that of a dipole.

To summarize: the Quenby-Webber method appears to be successful in accounting for some of the major defects of the original centred dipole theory, but evidence is lacking on the penumbral corrections that should be applied. It is hoped that the present work will throw new light on some aspects of this field.

CHAPTER 2. THE EFFECT OF GEOMAGNETISM ON THE OBSERVED TIME VARIATIONS IN THE COSMIC RAY INTENSITY.

2.1 Introduction.

The major intensity variations observed in the primary radiation are all ascribable to modulation mechanisms of solar origin.

In this chapter we shall deal with the influence of geomagnetism on the observation and interpretation of each of the following well established 'time variations':-

1. The solar flare increase
2. The Forbush decrease and associated 27 day recurrence phenomena.
3. The 11 year variation.
4. The daily variation.

Any theory of the modulation processes must adopt some specific model of the interplanetary environment. It is the testing of these models against observation that determines the particular model to be adopted. A comparison of the expected and observed distribution of particles moving in the geomagnetic field of internal origin will restrict the choice of external fields that may be adopted in any particular model. Moreover the predicted spectrum of a given

variation must agree with the observed spatial dependence of the variation at the earth. It is clear therefore that the geomagnetic field plays no small part in the testing of these models.

2.2. The Solar Flare Increase.

Several times a year the cosmic ray intensity is augmented by streams of low rigidity particles (< 10 GV) ejected from the sun. This process is well correlated with a number of associated phenomena, in particular the observation of an optical flare in white light and in the H_α. Other associated phenomena include X-ray and R.F. emission.

The particles emitted consist mainly of protons, although an α-particle component has been established (FREIER, NEY and WINKLER, 1959).

The screening effect of the atmosphere effectively inhibits the detection of primaries much below 2 GV, so that flare increases are seldom seen at sea level. The flare increases are generally observed by balloon-borne equipment and riometers. The latter instruments measure the cosmic noise absorption (CNA) due to the ionization occurring in the ionosphere by incoming solar particles (BAILEY, 1959; REID & LEINBACH, 1959). The rigidities of the flare particles are such that the geomagnetic field confines them to high

latitudes ($> 60^{\circ}$ geomagnetic), although there have been a few flares where the 'tail' of the spectrum was long enough for the flare increase to be seen at equatorial latitudes e.g. February, 1956. Owing to their steep spectrum, solar flare increases are strongly latitude dependent and thus afford a crucial test of the values of threshold rigidities assigned to the various cosmic ray observatories.

WEBBER (1961) shows that on the average, a riometer situated at geomagnetic latitude $\lambda = 65^{\circ}$ should be about ten times more sensitive than one situated at $\lambda = 62^{\circ}$ to flare radiation. The threshold rigidities at these two stations are 0.32 GV and 0.49 GV respectively, assuming a geomagnetic field due to a centred dipole. However, the tables of threshold rigidities by QUENBY and WENK (1961) reveal that the threshold rigidity at $\lambda = 62^{\circ}$ may vary between $\sim$1.4 GV and $\sim$ 0.1 GV, depending on the geomagnetic longitude. This example illustrates the necessity of using the correct threshold rigidities before any comparison of observations at different stations can be used as a basis for determining the flare spectrum.

The flare spectrum can be represented by a smooth power law function of rigidity tending to zero at low rigidities ($\sim$ 0.1 GV). The exponent of the flare spectrum may be determined by measuring the flare enhancement as a function of threshold rigidity. This is found to vary between p^{-4} to p^{-7}, the spectrum steepening as the flare progresses. The use of the Quenby-Webber threshold rigidities facilitates this determination, as the experimental points form a

Fig. 2.1 JULY 17, 1959 SOLAR ACTIVITY vs. ECCENTRIC DIPOLE THRESHOLD RIGIDITIES.
Points are taken from several stations. (After Carmichael and Steljes)

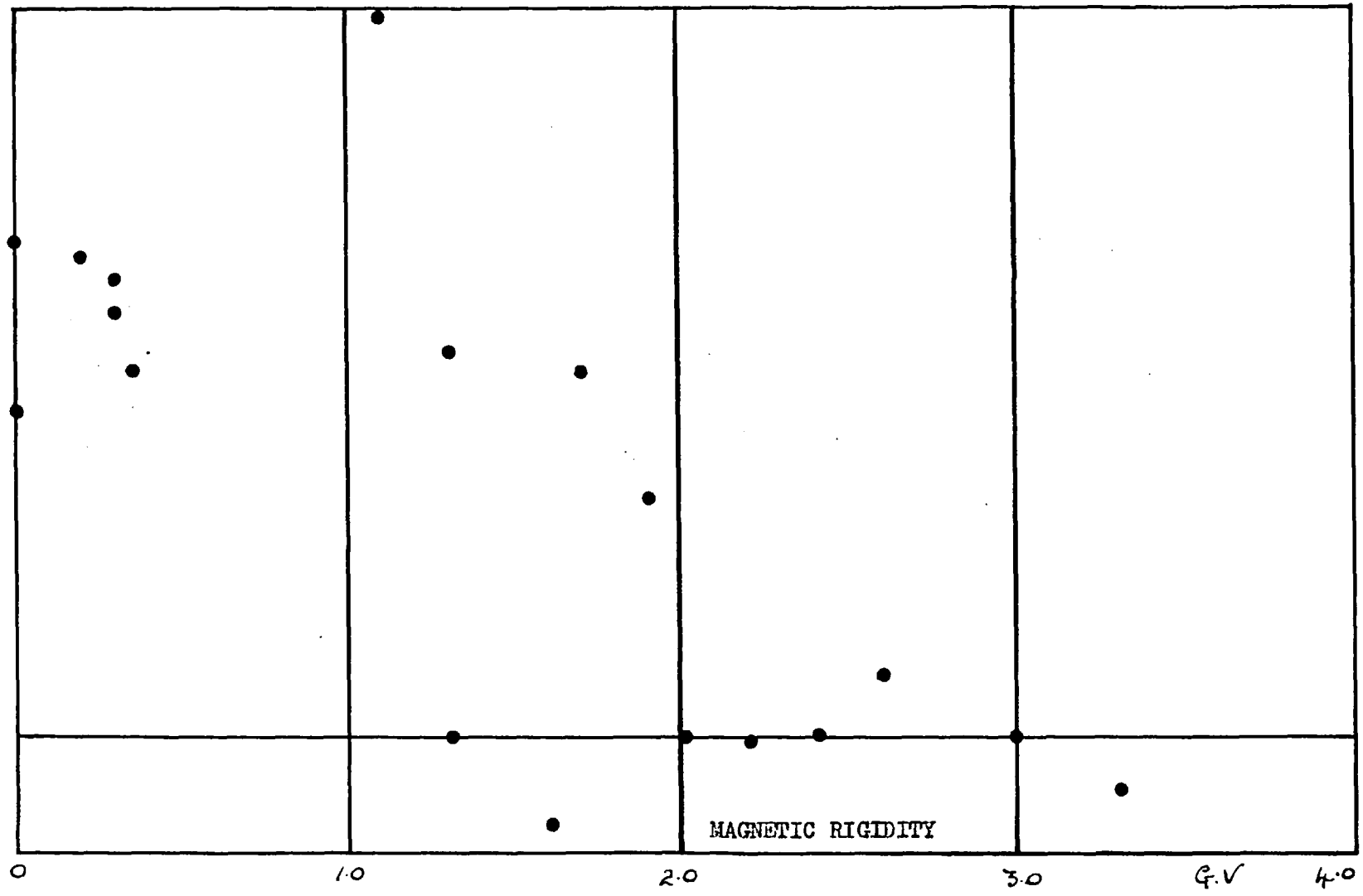

Fig. 2.2 JULY 17, 1959 SOLAR ACTIVITY vs. QUENBY & WEBBER THRESHOLD RIGIDITIES.
Points are taken from several stations. (After Carmichael and Steljes)

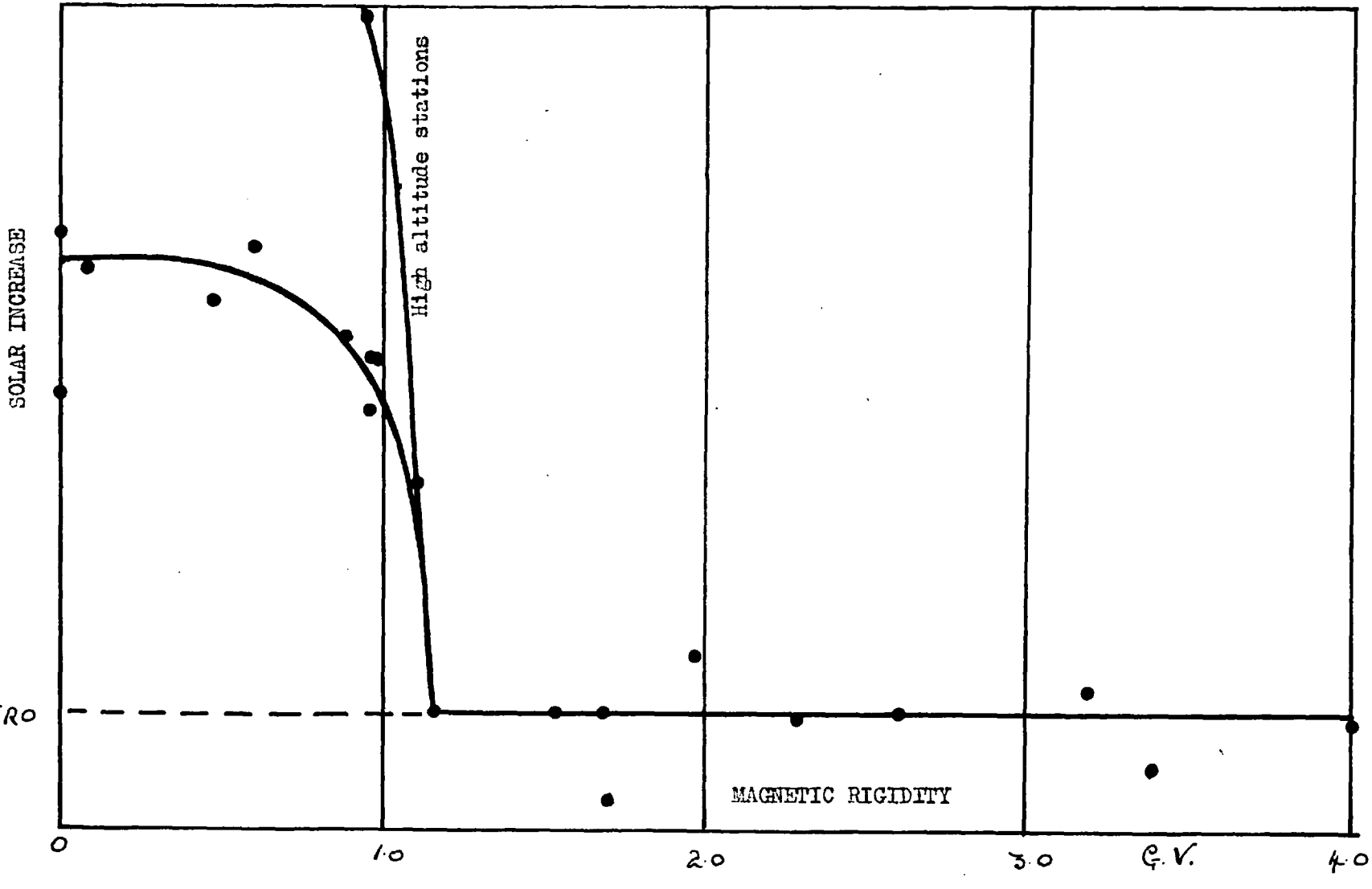

smooth curve of flare enhancement as a function of threshold rigidity. If the centred or eccentric dipole threshold rigidities are used there is a large amount of scatter due to the errors inherent in the dipole approximations. Data collected from the flare increase of July, 1959 by CARMICHAEL & STELJES (1960) illustrate this point. Figs. 2.1 & 2.2 shows the flare increases, plotted as a function of the eccentric dipole threshold rigidities. Figure 2.2 shows the flare increases, plotted as a function of Quenby-Webber threshold rigidities. The lack of scatter about a smooth curve in the latter case clearly indicates that the Quenby-Webber threshold rigidities are the more accurate.

Recently FREON & McCRACKEN (1961) have used the flare effects of November, 1960 as a further test of the Quenby-Webber approximation. They find that the flare enhancements at several stations are a smooth function of threshold rigidity with the exception of the flare enhancement at Port-au-Francais. This station lies close to the severe South African anomaly. The threshold rigidity predicted by the Quenby-Webber approximation may be improved if a better fit to the magnetic line of force through the station is used. WENK (1961) has calculated the threshold rigidity for this station using the computations of HULTQVIST which allow a better determination of the effective latitude λ (defined in the paper by QUENBY & WEBBER, 1959) and finds a value of threshold rigidity which is consistent with the smooth curve obtained from other stations. It is interesting that

the value obtained by WENK'S refinement of the Quenby-Webber treatment is not significantly different from the value obtained by McCRACKEN (1961). McCRACKEN used a computer to integrate the equations of motion of negatively charged particles in the FINCH & LEATON (1957) simulation of the geomagnetic field.

In the early stages of a flare, it often happens that the flare increase is only seen at certain stations, even though these stations may have the same effective threshold rigidity (either geomagnetic or atmospheric). This fact indicates that the flare radiation at this time is anisotropic. The flare increases may be confined to certain broad areas of the earth's surface called impact zones. If the assymptotic directions of particles arriving at these points are computed, it is found that they all intersect with the sun, and define a rather narrow source region.

The relevant theory of impact zones has been developed by JORY (1956), FIROR (1954), SCHLUTER (1958) and McCRACKEN (1961). SCHLUTER shows that at infinity only certain values of the angular momentum about the dipole axis 2γ (cf. Chapter 1) pertain to trajectories passing through the dipole origin. These trajectories the so-called 'Nullbahn' define the impact zones. The existence of impact zone phenomena evidenced in the data collected by GOLD & ELLIOT (1957) for the February 23rd, 1956 event places certain restrictions on the electromagnetic state of interplanetary space, in particular a lack of severe scattering which would tend to 'smear out' any

impact zone effects. Conversely the absence of impact zone effects during the November 12th, 1960 event together with other evidence, has led STELJES et al. (1961) to postulate a model of the inner solar system in which there exist regions of chaotic fields.

As in the evaluation of threshold rigidities, the calculation of impact zones requires an estimation of the effects of higher order terms in the geomagnetic field. A simple expedient may be adopted, that is to use the effective latitude $\bar{\lambda}$, as derived by QUENBY & WEBBER in the application of the centred dipole predictions. Such a procedure has been used by McCRACKEN (1961) as a means of qualitatively checking computations, made with an electronic computer, for the analysis of the May and November 1960 events.

2.3 The Forbush decrease and 27 day recurrence Phenomena.

A day or two after a solar flare, a sharp decrease in galactic cosmic radiation intensity (maximum value $\sim$15% observed by sea level neutron monitors) is sometimes observed. This event is known as the 'Forbush' decrease.

There is a strong correlation between Forbush decreases and magnetic storms, particularly if the latter have sudden commencements (KITAMURA, 1954). The disturbance of the geomagnetic field must modify the prestorm threshold rigidities but these modifications,

however large, could not account for the observed features of the decrease in cosmic ray intensity. For this reason, it is evident that the geomagnetic storm is not the cause of the Forbush decrease, but that both are symptomatic of some large scale modulation process at work at this time.

The Forbush decrease is observed on a world wide scale. FENTON et al. (1959) have compared the percentage decrease in counting rate observed by neutron monitors at Ottawa ($\lambda = 56.8^{\circ}$) and Hobart ($\lambda = 51.6^{\circ}$) and found them strongly correlated for 11 events between November, 1956 and January, 1958. It is also observed that the Forbush decrease characteristics are similar in both the proton and α-particle components (MEYER, 1960; McDONALD & WEBBER, 1960).

The latitude dependence of the Forbush decrease affords a convenient check on any proposed modulation mechanism, since if the correct threshold rigidities be used, this data may be used to obtain the modulation spectrum. The modulation mechanism proposed recently by ELLIOT (1960) has been tested in this way with data from the March, 1958 event and also with the data for the July, 1959 event compiled by CARMICHAEL & STELJES (1960).

Besides the large scale modulation of the cosmic radiation intensity during a Forbush decrease, there is evidence of fluctuations of a local character. In particular ROSE has noted fluctuations occurring after the initial sharp decrease which seem to be longitude dependent, (WILSON, ROSE & POMERANTZ, 1960) roughly corresponding to

the same local time at each station. It may be that there exist allowed paths of propagation for solar particles during this time along which little scattering occurs. In addition to these local effects, second order effects due to the modification of the geomagnetic field are sometimes observed.

The theory of magnetic storms (CHAPMAN & FERRARO, 1931; MARTYN, 1951) supposes that a westward flowing ring current is set up as the solar plasma interacts with the geomagnetic field. This ring current must modify the threshold rigidities calculated for the geomagnetic field of internal origin. The extent of their modification has been calculated by TREIMAN (1953) and RAY (1956) who show that a lowering of the threshold rigidities should be observed. The effect is in general seen in conjunction with the main phase of a large ($\sim 200\gamma$) magnetic storm. The latitude dependence of the increase is consistent with a ring current of the order indicated by the space probe measurements made by SONNET, JUDGE, COLEMAN & SMITH (1960)

It should be noted however, that a temporary uniform field in the opposite sense to that of the dipole component of the geomagnetic field would produce a similar phenomena. KONDO, YOSHIDA & WADA (1959) have accounted for the events of September 13th, 1957 and February 11th, 1958 in this manner.

WINCKLER, BHAVSA & PETERSON (1960) found evidence of the lowering of threshold rigidities by observing particles below the normal threshold rigidities at Minneapolis during the July 1959 event.

This event was remarkable in that three successive Forbush decreases occurred within a few days. The cumulative effect was to magnify the intensity variations normally seen, in particular those due to the world wide lowering of threshold rigidities. Other events in which this process seems to have occurred are those of March 26th, 1958 (WINKLER, 1960) and May 12th, 1959 (WINKLER & BHAVSA, 1960).

There is also some evidence to suggest an increase of thresholds at the time of the sudden commencement, perhaps due to an easterly flowing ring current (WINKLER, BHAVSA & PETERSON, 1961).

Whilst we have only indicated some of the major features of the Forbush decrease and coincident small flare increases, it is certainly clear that there exists sufficient data to warrant a much fuller understanding of how the threshold rigidities may be modified by internal higher order fields and more particularly, by external fields of various configurations.

The 27 day recurrence phenomena was discovered by GILL (1939). As its period agrees well with the synodic rotational period of the sun, one would expect that the modulation mechanism responsible is of the same type as the Forbush decrease (VAN HEERDEN & THAMBYAHPILLAI, 1955). The fact that that the 27 day phenomena is not of geomagnetic origin was established by SIMPSON (1954) who found that the 27 day variations of neutron intensities just below the 'knee' of the latitude curve are very similar to those observed at lower latitudes.

2.4 The 11 Year Variation.

This variation has been successfully correlated with the 11 year sunspot cycle. It appears that towards sunspot maximum the whole cosmic ray spectrum is depressed and that particles of low rigidity ($<\sim 2$ GV) are removed (see ELLIOT et al., 1960). This process is exhibited by the shift in the 'knee' of the latitude curve (STOREY, 1959). Again any quantitative data to be gained from the latter occurrence requires a knowledge of the correct threshold rigidities.

It is possible that, over a solar cycle, the threshold rigidities systematically change. The analysis of the unusual event of November 10th-16th, 1960 by MATHEWS, THAMBYAHPILLAI, and WEBBER (1961) revealed some interesting features. These authors argue that the apparent flattening of the flare spectrum in this event compared with the February 23rd, 1956 event, was due to the change of threshold rigidities over a solar cycle. Only with a precise theoretical knowledge of how the threshold rigidities should change, can such a hypothesis be tested. In this context, we should mention that COCCONI et al. (1957) have suggested that a radial field exists between the sun and the earth during a flare. This field, of course, would modify the threshold rigidities. Since such a field destroys the cylindrical symmetry of the geomagnetic dipole, its effects is not easily calculable.

2.5 The Daily Variation.

After correcting for meteorological effects, there remains a daily variation of $\sim 0.2\%$ for vertical meson telescopes at sea level. The maximum occurs at 10 to 18 hours U.T. The amplitude and phase of the daily variation undergo long term changes having a major period of 22 years (ELLIOT & THAMBYAHPILLAI, 1953; HYNDS, 1961). These changes are world wide and sensibly independent of latitude. During the recovery phase of the Forbush decrease the daily variation increases in amplitude and the time of maximum occurs earlier (SEKIDO & YOSHIDA, 1950).

In any theoretical treatment of the daily variation, it is necessary to assess the mean rigidity of the radiation responsible.

Three approaches to this problem are possible:-

(1). A comparison of the variation observed by telescopes pointing in different directions.

(2). A comparison of the variation observed with telescopes having different opening angles.

(3). A comparison of the variation observed by telescopes at different atmospheric depths.

A full account of the first method has been published by BRUNBERG & DATTNER (1954). These authors use the results of their experiments on the trajectories of electrons moving in a dipole field to determine the direction of the source of the variation (BRUNBERG &

DATTNER, 1953). The hour of maximum, for a given telescope determines directions of the anisotrophy for particles of various rigidities. A comparison of this relationship for telescopes pointing in different directions defines a range of rigidities responsible for the variation. The range indicated is 20 to 40 GV. This range lies within that of the variation of threshold rigidity with zenith angle at equatorial latitudes. Thus the second method would be an effective one in determining the rigidities responsible. SARABHAI (1956) has noted that the daily variation is a function of the opening angle of a telescope in the equatorial region.

As the daily variation is due to particles having rigidities above most geomagnetic threshold rigidities, the latitude effect is negligibly small. Therefore, no simple expedient exists for the determination of the spectrum of the daily variation. The only methods are those mentioned above and also by reference to the difference in the daily variation observed by detectors having dissimilar differential response curves.

These methods indicate that the spectrum is flat and lies somewhere between 15 and 50 GV.

The estimation of the rigidities responsible for the daily variation allows the use of the BRUNBERG and DATTNER DIAGRAMS, to obtain the asymptotic directions. These diagrams account, for example, for the two hour phase difference between high and low latitude stations after atmospheric corrections have been made. However,

these diagrams are based on measurements made in a dipole field. The effect of higher order terms is difficult to calculate. As a first approximation QUENBY & THAMBYAHPILLAI (1960) use the BRUNBERG and DATTNER diagrams, but substituting an effective latitude instead of the geomagnetic latitude. The effective latitude($\bar{\lambda}$)is the same as that developed in the paper on threshold rigidities by QUENBY & WEBBER (1959). QUENBY and THAMBYAHPILLAI have dealt with the case of the daily variation observed at Mawson. The geomagnetic latitude of Mawson is 73°, the effective latitude is 67.2°. The effect of including the non-dipole part of the geomagnetic field into the calculation is to bring the assymptotic directions for 15 GV and 20 GV closer together. The agreement is then better between the phase angles of these two rigidities.

2.6 Conclusion.

The importance of a knowledge of geomagnetic effects in the interpretation of the time variations of the cosmic ray intensity has been illustrated in this chapter. The estimation of the effect of the higher order terms has been shown to have become increasingly necessary in the evaluation of threshold rigidities, impact zones, and assymptotic directions. It is therefore hoped that the justification for the present experiment is apparent.

CHAPTER 3. THE USE OF A LABORATORY MODEL FOR THE INVESTIGATION OF THRESHOLD RIGIDITIES.

3.1 General.

The use of mechanical and electronic computers in this field has yielded much valuable information. LEMAITRE and VALLARTA, HUTNER, SCHREMP and others investigated some of the problems of the main cone and penumbra by using a mechanical computer known as a Bush analyser. (For a summary of this early work see VALLARTA, 1961). Recently several workers have programmed fast electronic computers to calculate orbits of charged particles in the geomagnetic field.

For example, McCRACKEN (1961) has investigated impact zones and threshold rigidities in this way, using an IBM 707 computer. McCRACKEN uses the Finch and Leaton (1957) approximation to the geomagnetic field which accounts for multipole fields up to the sixth order. However, even using fast computers, the time required to compute fairly straightforward threshold rigidities is comparatively long. A figure of four minutes per trajectory is quoted by McCRACKEN. It is thus difficult to obtain a qualitative idea of the general features of geomagnetic effects over many points without investing in a large quantity of computer time.

The approach that was used in this work was to scale the whole geomagnetic field down to laboratory dimensions and to simulate

cosmic rays by electrons. These particles move in an analagous way to cosmic ray particles; we therefore feel justified in calling the apparatus an analogue computer.

3.2 Historical.

The laboratory simulation of geomagentic effects is not new. In fact, the original work of STORMER was stimulated by the model experiments of BIRKELAND (1901). BIRKELAND'S experiment was essentially an investigation into the structure of a glow discharge in a magnetic dipole field. The magnetic dipole field was generated by a permanent magnet enclosed in a spherical casing, this object being known as a terrella. The name has since been used in other model experiments. BIRKELAND noticed a structure in the glow discharge not unlike that deduced from observations of the aurorae. The observation of this phenomena led STORMER to begin his theoretical work on the motion of charged particles in the field of a magnetic dipole.

This early work was repeated by later workers using more refined apparatus in particular by VILLARD (1906), BRUCHE (1931) and BLOCK (1955).

Quantitative results from a model terrella were obtained by MALMFORS (1945) who investigated the asymptomatic directions of electrons leaving the surface. In this way he accounted for some

features of the daily variation in cosmic ray intensity. Later, BRUNBERG and DATTNER (1953) improved on MALMFORS' apparatus and performed more extensive and accurate experiments on the same subject. To a large extent, the success of this experiment prompted the present work.

The only other recent application of model experiments in this field that has come to our notice is that of BENNETT (1959) who constructed a device known as a 'Stormertron' to investigate the orbits of solar particles in the geomagnetic field. BENNETT has produced several photographs which show periodic orbits previously predicted by STORMER.

3.3 The Validity of the Experiment.

The investigation of physical problems using scaled down versions of the actual situation is widespread. In particular, the testing of model ships and aircraft may be cited. This is a perfectly valid approach as long as all the equations describing the state of the system yield the same scaling factor when any of the three variables of mass, length and time are reduced in magnitude.

In practice this never occurs since certain typical quantities are invariant, e.g. the size of gas molecules, the lifetime of excited atomic states, and the wavelength of emitted light. As a result of this fact, it is difficult to simulate such variables as the

conductivity of interstellar space, if it is scaled to laboratory dimensions.

ALFVEN (1950) has produced a table of the various similarity transformations applicable to different physical quantities in the laboratory simulation of electrical discharges. These tables indicate that the conductivity of interstellar space would be simulated by a highly ionized gas at a pressure of 100 atmospheres.

In this experiment we are solely interested in the interaction of the cosmic radiation with the geomagnetic field. It is therefore necessary to minimize the interaction of the electrons with the residual gas i.e. the m.f.p. for electrons moving round the terrella must be much longer than the length of a typical electron trajectory. A low pressure is therefore required; how this pressure was decided and attained will be discussed in the chapter dealing with the apparatus in detail.

3.4 The Scaling Equations.

We will now show how the scaling equations applicable to this experiment were obtained.

The threshold rigidity for a cosmic ray is given by:-

$$P_e = \frac{M_e}{4r_e^2} \cos^4 \lambda \qquad (3.1)$$

in the case of a centred dipole where:

M_e is the dipole moment of the earth

r_e is the radius of the earth

and λ is the geomagnetic latitude,

and a similar expression holds for electrons moving in the terrella field viz.

$$P_t = \frac{M_t}{4r_t^2} \cos^4\lambda \qquad (3.2)$$

where the suffix t denotes quantities appropriate to the terrella. Now the rigidity of an electron of charge 'e' accelerated through a voltage V is given by:-

$$P_t^2 = V^2 + \frac{2m_e c^2 V}{e} \qquad (3.3)$$

where m_e = rest mass of electron and

c = velocity of light.

In the non-relativisitic case this expression reduces to:-

$$P_t^2 = \frac{2m_e c^2 V}{e} \qquad (3.4)$$

$2m_e c^2$ is the rest mass energy of two electrons i.e. one Mev. Substitution of (4) into (2) and division into (1) leads to the following equation:-

$$\frac{P_e}{10^3 \ V} = \frac{M_e}{M_t} \frac{r_t^2}{r_e^2} \qquad (3.5)$$

$$P_e = \frac{M_e}{M_t} \frac{r_t^2}{r_e^2} \sqrt{V} \ 10^3 \text{ volts} \qquad (3.6)$$

$$\text{or} \qquad P_e = \frac{M_e}{M_t}\,\frac{r_t^2}{r_e^2}\,\sqrt{V}\;10^{-6}\;\text{G.V.} \qquad (3.7)$$

Substitution of $M_e = 8.01 \times 10^{10}$ gauss. cm^3

and $r_e = 6.4 \times 10^{8}$ cm.

yields the following equation:-

$$P_e = \frac{198 r_t^2}{M_t}\,\sqrt{V}\;\text{GV.} \qquad (3.8)$$

The choice of r_t, M_t, and V was decided by several factors to be described in the next chapter. However, suitable values of r_t and M_t indicated that V should vary over a range of 200-1000 volts. As the wavelength of electrons in this range, $\sim 10^{-8}$cm, is many times less than the typical dimensions of the apparatus, any effects of diffraction may be ignored. The electrons move as particles in an analagous way to protons in the earth's field and it is therefore perfectly valid to use them to investigate geomagnetic effects.

CHAPTER 4. THE APPARATUS.

4.1 Introduction.

Close study of the scaling equations reveals that the requirements in regard to voltage, magnetic fields, and dimensions are practically manageable for the laboratory simulation of geomagnetic effects.

In order to make the apparatus as versatile as possible, it was necessary to compromise between many competing design requirements. In the first place, an upper limit had to be put on the size of the vacuum chamber together with the necessary degaussing coils. Having decided these dimensions, most of the remaining design parameters were fixed as a consequence. We shall therefore describe the major components of the apparatus in sequence showing how these parameters were decided upon. A photograph of the complete apparatus is shown in fig. 4.1.

4.2 The Vacuum Chmaber.

When $\gamma = 1$ (where γ is the constant proportional to the impact parameter for motion in the equatorial plane cf. Chapter 1) and particles from the terrella fail to escape from the inner allowed region, the 'jaws' of the forbidden region meet at a distance r

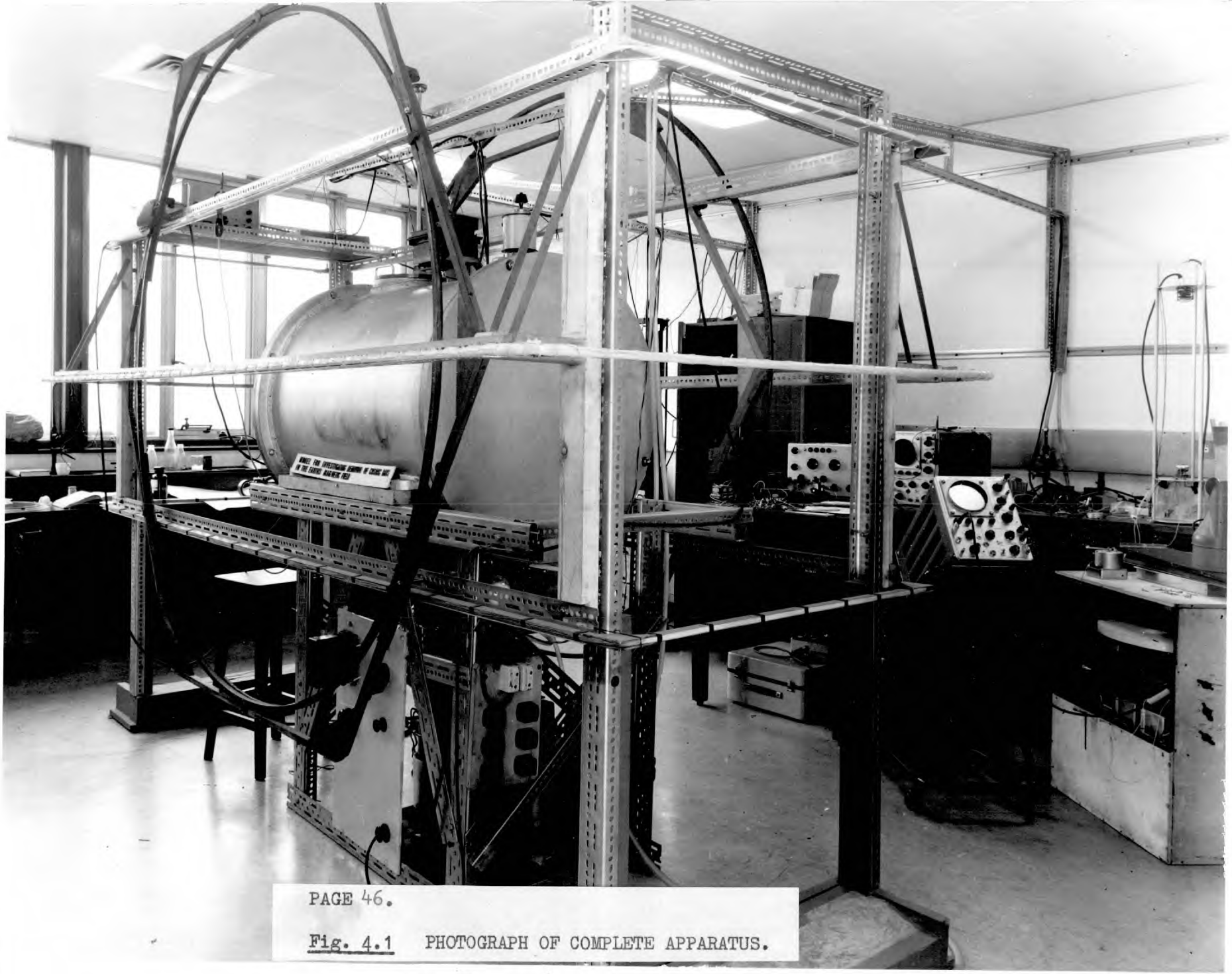

PAGE 46.

Fig. 4.1 PHOTOGRAPH OF COMPLETE APPARATUS.

given by:-

$$r = \frac{2r_t}{\cos^2\lambda} \qquad (4.1)$$

where r_t is the radius of the terrella and λ is the geomagnetic latitude of the point where electrons leave the terrella surface. For this reason, only threshold rigidities up to the point where the jaws approach very closely to the tank walls, may be investigated. Therefore the larger the tank, the higher the latitudes at which threshold rigidities may be investigated. However an upper limit is placed on the size of the tank by three factors: the space available, the size of the degaussing coils and the vacuum pump requirements. Bearing these factors in mind, as well as cost, it was decided that a tank with major dimensions of about a metre was practical. As the vessel was to withstand external atmospheric pressure, a cylindrical tank seemed to be the obvious choice. This shape has the added advantage that, if it is made long compared with the terrella dimensions, one may use one end to investigate the asymptotic directions of electrons leaving a terrella at the other end.

If the investigation of threshold rigidities is required up to $\lambda = 45^\circ$ with a terrella of 8 cm. radius*, substitution into

.....

* Due to difficulties in construction, the radius of the finished terrella was $\sim$10 cm. as opposed to the design estimate of 8 cm. Therefore threshold rigidities could only be investigated up to $\lambda = 33^\circ$.

equation 4.1 requires r to be $\frac{2 \times 8}{\cos^2 45^\circ}$ = 32 cm.

A cylinder was therefore made with dimensions 80 cm. diameter and 120 cm. long. From the non-ferrous materials available, aluminium alloy NP 5/6 was chosen as having the advantages of being non-porous, light in weight, relatively cheap, and having a high tensile strength. The thickness of the cylindrical shell was found by equating the tangential stress to the pressure per unit area, using the following equation:-

$$\frac{2T}{r} = \frac{P}{t} \qquad (4.2)$$

where T is the maximum safe stress appropriate to the material

r is the radius of the cylinder

P is the atmospheric pressure

t is the thickness of the shell.

Taking very pessimistic values for the maximum safe stress, a thickness of a quarter of an inch was decided upon. The tank was fitted with flanges each end with fitted neoprene O-rings on which one inch thick circular end pieces were held by stainless steel half inch nuts and bolts. In the middle of one end piece, a 17 inch viewing window of "Armourplate" glass was fitted, again the sealing was by means of an O-ring. The two end pieces made metal to metal contact with the end flanges under pressure, thus providing very satisfactory sealing.

The main body of the vacuum tank had three ports, one, was tapped to receive the diffusion pump. The other two held the

terrella assembly and the ionization gauge.

The tank is of welded construction and was made to specification by the A.P.V. company.

4.3 The Vacuum Pumping System.

Before deciding on the ultimate pressure required, it was necessary to consider the mean free paths of electrons at the energies proposed. As will be shown, the typical electron energies used were $\sim$ 250 volts.

The intensity per unit area I, after an electron beam, with an original intensity I_o, has traversed a distance x, is given by:-

$$I = I_o e^{-\alpha x} \qquad (4.3)$$

where

$$\alpha = \frac{1}{L} \qquad (4.4)$$

and L is a typical scattering length.

Also

$$\alpha = \frac{n \pi \delta^2}{4} \qquad (4.5)$$

where n is the number of air molecules per unit volume and δ is their effective radius for scattering. The quantity δ is in fact a function of energy which rises rapidly at those energies at which large excitation cross sections occur for the different constituents of the residual gas. Evidence on this subject is far from complete but a value of $\delta \simeq 5 \times 10^{-7}$ cm. was adopted (DUSHMANN, 1947).

If L is required to be $\sim$100 times the dimensions of the tank i.e. 100 metres, then substituting into equations 4.4 and 4.5 and equating, one obtains

$$\frac{1}{10000} = \frac{n \pi \times 25 \times 10^{-14}}{4}$$

whence $n = 4 \times 10^{10}$ per cm^2.

Using the equation of state

$$p = nKT \qquad (4.6)$$

$p = \sim 2 \times 10^{-6}$ mm. Hg.

The vacuum system was therefore designed with this pressure as a target. The choice of the size of diffusion pump depends on the area of surface under vacuum and its outgassing characteristics. The pump chosen was an 'Edwards F603' three stage oil diffusion pump. This has an unbaffled pumping speed of 600-800 litres per minute. The pumping speed of this pump tends to zero at 5×10^{-7} mm. Hg.

As vacuum oil molecules have a high cross section for electrons, it was necessary to reduce 'backstreaming' to an absolute minimum. For this reason, a water cooled chevron baffle was fitted as well as a 'guard-ring'. This latter device is virtually a fourth stage of the diffusion pump. These expedients reduced the pumping speed to an estimated 300-400 litres per minute.

The diffusion pump was backed by an 'Edwards 1SC 150B' single stage rotary pump, which was fitted with an 'air ballast' facility for preventing vapours condensing in the pump oil. Phosphorus

pentoxide vapour traps were fitted.

In the absence of leaks the systen could be pumped down to $\sim 2 - 3 \times 10^{-6}$ mm. Hg from atmospheric pressure in about four hours.

All the vacuum sealing was done by means of neoprene O-rings which were thinly coated with 'Apiezon M' vacuum grease. The pumping system was cleaned thoroughly with detergent and acetone before assembly. No trouble with leaks in the system has been experienced since its initial assembly.

4.4 The Terrella Assembly.

We shall not touch upon the construction of the terrella coil and magnet assembly as this will be dealt with later.

If the electron gun is fixed one must arrange for the rotation of the terrella in two perpendicular directions so that the gun can be positioned over several different points on the terrella. This could be achieved by suspending the terrella on gimbles. It was considered that there were three objections to this:-

(a) The obstruction of the beam by the gimbles.

(b) The difficulty of having bearing surfaces in vacuum.

(c) The necessity of having at least two vacuum seals for the current leads.

Therefore it was decided to place the coil assembly in a spherical shell and to have an outside pressure sphere in which the former could revolve. This has the great advantage that all the bearing

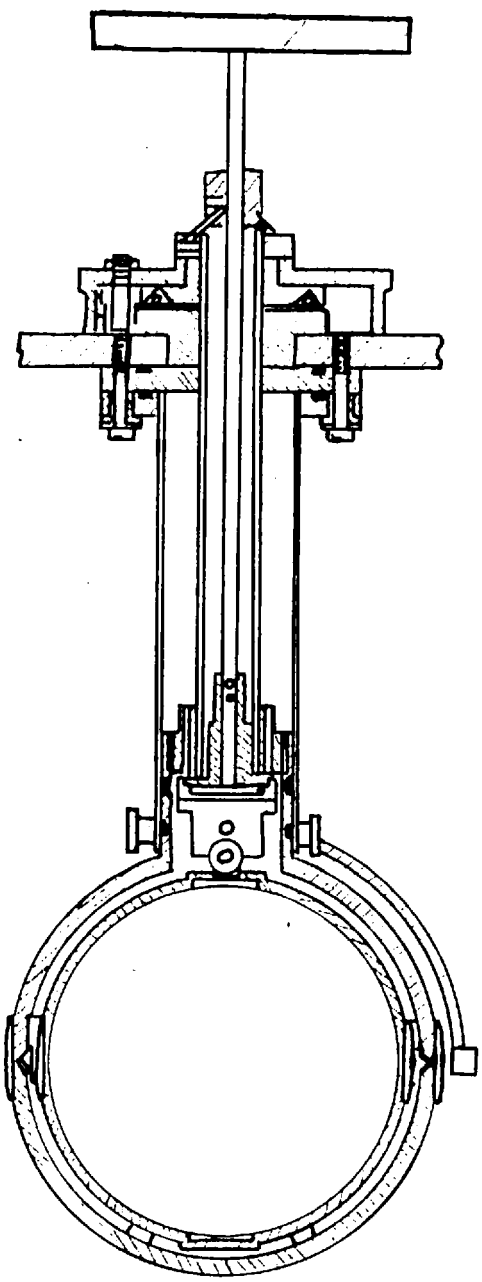

Fig. 4.2 DIAGRAM OF TERRELLA AND ELECTRON GUN ASSEMBLY.

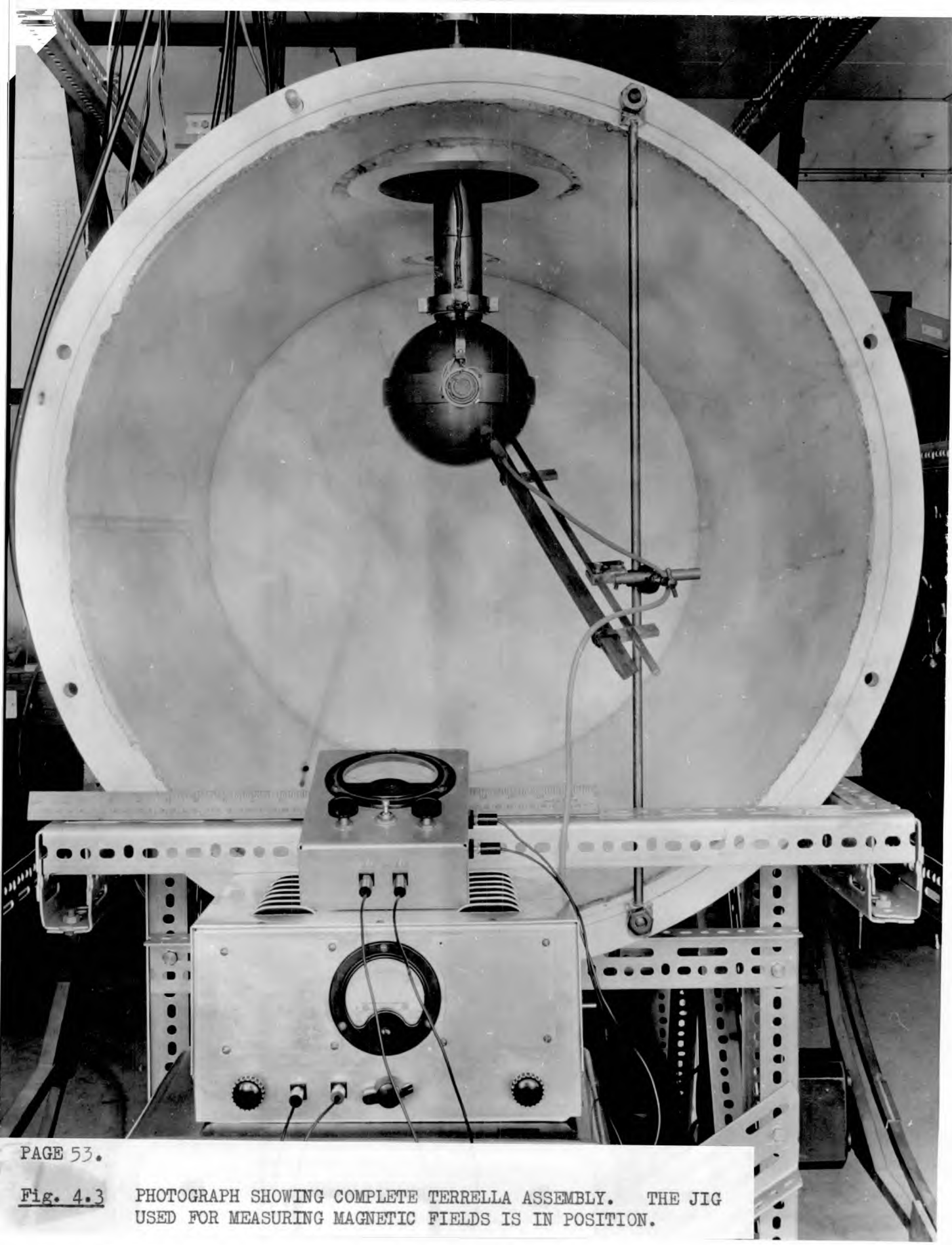

Fig. 4.3 PHOTOGRAPH SHOWING COMPLETE TERRELLA ASSEMBLY. THE JIG USED FOR MEASURING MAGNETIC FIELDS IS IN POSITION.

surfaces as well as the coil itself are open to the atmosphere. Moreover the outside pressure sphere presents an almost unobstructed spherical surface around which the electrons may move.

The spherical shell was machined out of the solid brass for accuracy, and so that the porosity one sometimes encounters in castings, should be avoided.

The inner sphere was moved in latitude by means of a worm and rack device and moved over P.T.F.E. bearing surfaces. The latter were not seriously affected by the temperature of the terrella which at times exceeded 100°C. The whole of this sub-assembly rotated in longitude in a hollow shaft fixed to the main supporting flange. The latitude could be varied from plus to minus 45°, one complete turn of the control knob moving the terrella ½° in latitude. A ten to one reduction gearing was fitted in the longitude control. A diagram of the terrella assembly is shown in figure 4.2.

The pressure sphere was made in two halves which screwed together compressing a silicone rubber O-ring seal. The electron gun was held in position by a circular cantilever homocentric to the spherical surface. This cantilever was insulated from the terrella assembly by a "Fluorosint" washer so that current to it could be measured.

The leads to the electron gun were brought through metal-ceramic vacuum seals. These leads were made from P.T.F.E. covered connecting wire This has been found completely satisfactory from the point of

view of outgassing at low pressures. As little insulation surface as possible was exposed to the electron beam to prevent any electrostatic potentials building up.

4.5 The Electron Gun.

The electron gun requirements are difficult to fulfill since the gun must be kept very short for two reasons. In the first place the magnetic deflection inside the gun must be minimized and secondly it is necessary to make the exit point of the gun as close to the terrella surface as possible since this point defines the effective radius.

The first gun used was analogous to a pinhole camera. The idea being to limit the large emission current from an oxide cathode to a small solid angle by the use of a very small hole in the anode. The emission was limited by a perforated plane electrode near to the cathode. The characteristics of this gun were quite satisfactory, the beam being limited to a total exit angle of about 7°. At low voltages $\sim$200 volts the spot acquired several satellites probably due to space charge effects.

One serious drawback was found to be that the cathode became seriously 'poisoned' even under vacuum, probably because of vacuum oil molecules present in the system. Moreover emission dropped after each exposure to the air even though the cathode was kept at $\sim 100^{\circ}$C during this time, following the suggestions in a paper by HAAS and JENSEN (1957). Although it was possible to recoat the cathode after exposure to the atmosphere, it was found that the time taken to form

Fig. 4.4 DIAGRAM OF THE ELECTRON GUN.

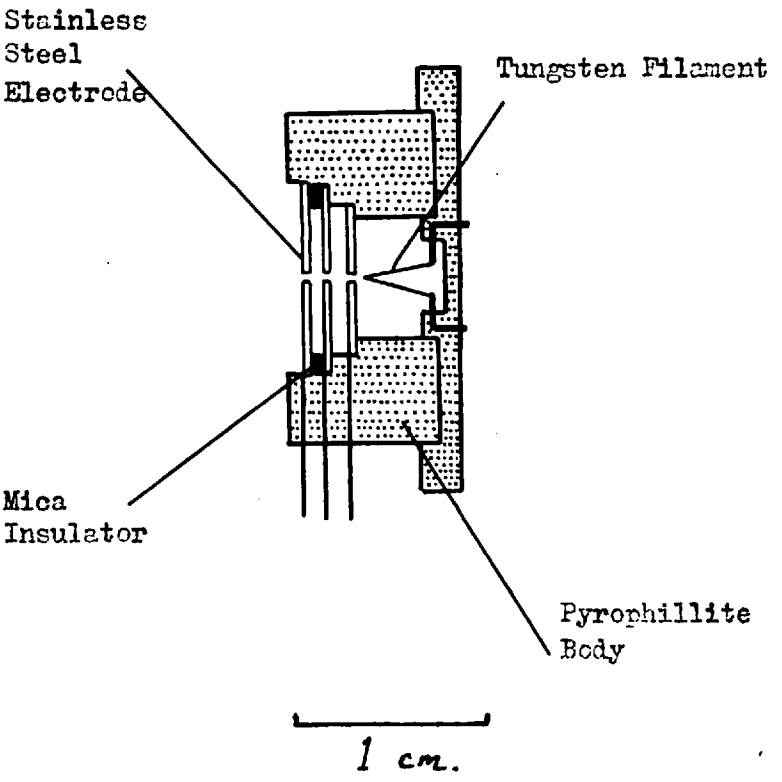

an emissive cathode was too excessive.

It was decided therefore, to make a focussing gun using a tungsten "hairpin" cathode. The lens was of the three electrode variety, the first anode being effectively the lens, if the holes in the other electrodes are kept small. The focal length is given approximately by the equation:-

$$f = \frac{4V_c}{E^1 - E}$$

where $E = \frac{V_A - V_c}{a}$ and $E^1 = \frac{V_C - V_B}{b}$

and V_A = voltage on grid

V_B = voltage on 2nd Anode

and V_C = voltage on 1st Anode

a = distance between grid and 1st Anode

and b = distance between 1st and 2nd Anode.

A diagram of the gun is shown in Figure 4.4

The gun should focus over a wide range of final anode voltages provided that the ratios of three electrode voltages are kept constant. This was achieved by a potential divider connected across the gun. The

ratio was set by trial and error, initially looking at the spot on a post-accelerating target coated with zinc sulphide. A total exit angle of about 4° was achieved, although the optics seriously deteriorated below $\sim$ 200 volts, no doubt due to space charge effects.

The body of the gun was turned from "Pyrophillite", which was fired at $\sim 1400^{\circ}C$ after machining. The electrodes were accurately cut from stainless steel sheet. They were drilled in situ so that the holes were accurately centred. The electrodes were held in place with gun cement which is made from a mixture of potassium silicate and aluminium oxide. The whole gun was baked at $800^{\circ}C$ in a vacuum furnace to remove all volatile constituents. The tungsten 'hairpin' filament was made by the standard technique of using a cork and razor blade. The 'hairpin' formed was then spot welded to eureka support leads. The gun was held in a brass collar. The leads to it came down underneath the circular cantilever and were crimped and soldered on to the electrode tags.

4.6 The Degaussing Coils.

The field in the laboratory is nearly uniform except near the floor and ceiling where there are disturbing fields due to the steel frame of the building.

The vertical field is ~~0.6~~ 0.39 gauss and the horizontal field 0.10 gauss. It is possible to line the apparatus up in an East-West position. Therefore it is only necessary to provide a compensating

field in two mutually perpendicular directions. The size of the apparatus precludes the use of coils in the Helmholtz configuration for the compensation of the vertical field with any degree of accuracy.

The vertical compensating system therefore used three rectangular coils. This system has been applied by HAYNES and WEDDING (1951) in the construction of a β - ray spectrometer. The three rectangular coils have dimensions such that their edges lie on the surface of a right circular cylinder. The system is symmetrical about the middle coil, the upper and lower coils are arranged such that the angle subtended by the corners at the centre of the middle coil is 45° (see figure 4.5). The number of windings in the upper and lower coils are $1/\sqrt{2}$ times the number of windings of the middle coil. With the same current through all the coils this system approximates to a cylindrical current sheet with the current density varying as the cosine of the angle of elevation. This system produces a uniform field within itself and an approximately dipole field without. The magnitude of the field produced in three perpendicular directions is given by the following equations:-

$$H_x = \frac{8i}{a}\left\{\left(\frac{r}{a}\right)^6 \sin 6\theta - \left(\frac{3}{2}\right)\left(\frac{a}{L}\right)^4\left(\frac{r}{a}\right)^2 \sin 2\theta \quad ----\right\}$$

$$H_y = \frac{8i}{a}\left\{1 + \frac{a^2}{2L^2} - \frac{3a^4}{8L^4} + \left(\frac{r}{a}\right)^6 \cos 6\theta - \frac{3a^4}{8L^4}\left(\frac{r}{a}\right)^2(2 - 2\cos 2\theta) + \frac{3a^2}{2L^2}\,\frac{Z^2}{L^2}\right\}$$

$$H_z = \frac{8i}{a}\,\frac{3a^3}{L^3}\,\frac{z}{L}\,\sin\theta$$

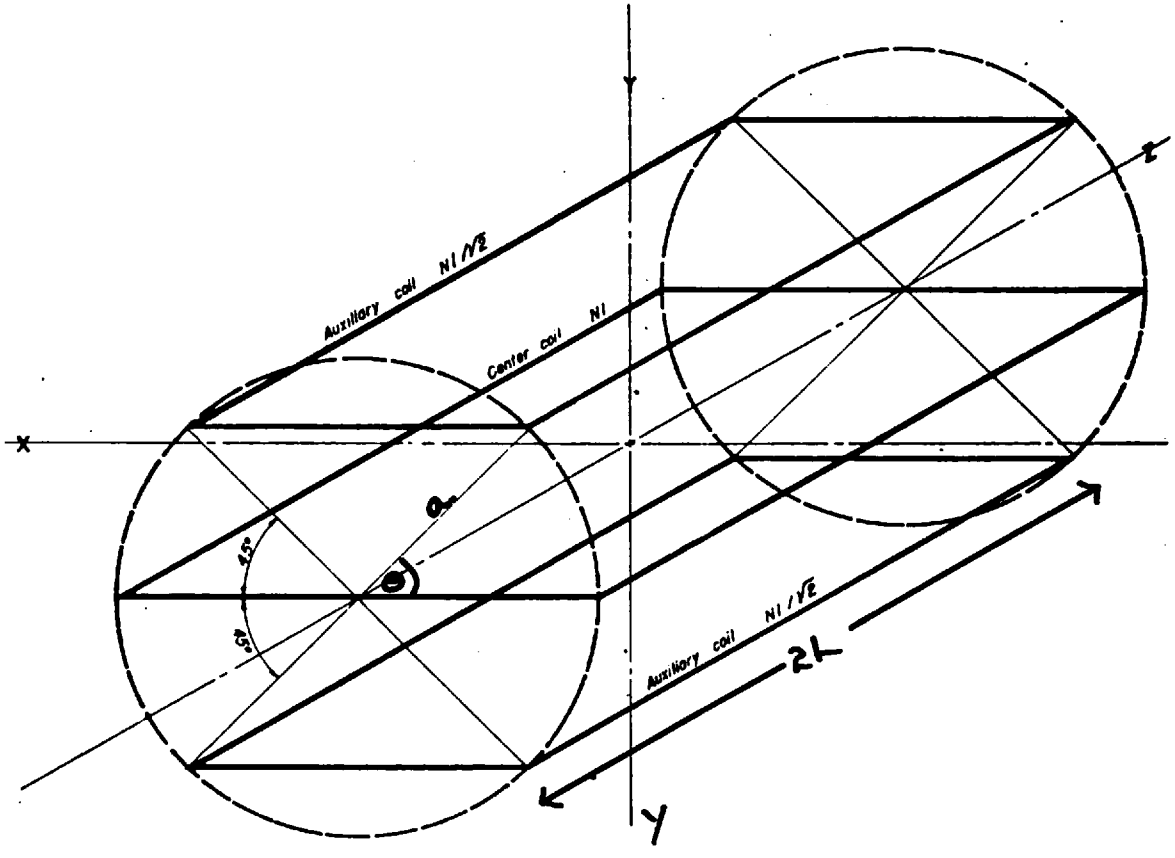

Fig. 4.5 DIAGRAM ILLUSTRATING THE GEOMETRY OF THE VERTICAL DEGAUSSING COILS.

where i is the current through the coils and the remaining dimensions are illustrated in figure 4.5. It will be seen that if a << L the field is almost uniform. The quantity 'a' is fixed by the size of the tank, the quantity 'L' was made as large as possible consistent with the requirements of space available and cost. The terrella was situated at the centre of the coil system, 'a' was chosen as 5¼ feet and 'L' as 10½ feet, with this configuration the variation of 'H_y' over a sphere of radius 25 cm. concentric with the terrella is of a little over 1%. The horizontal field was compensated by means of two circular coils. Each coil is 1.1 metre in radius. The distance apart was made slightly larger than the radius as in the Helmholtz configuration ir order to optimize the uniformity of the field over the largest volume. (see CRAIG, 1947). Before the full size coil system was built, a small scale model was made and the field inside it was thoroughly checked by means of a varipermeability magnetometer. This magnetometer will be described in a subsequent chapter, but the results of these measurements showed that the coil systen was suitable for the purpose described. The residual field being $\sim$ .02 gauss over the entire region that the electrons traversed.

4.7 The Instrumentation of the Model Experiment.

(a) Pressure Gauges.

In the backing line, two thermocross gauges were fitted. These gauges consist of two 1 cm. lengths of 0.1 mm. diameter wire.

One wire is made of 'Eureka', the other of 'Nichrome'. The two wires are laid across each other to form a cross, and spot welded where they touch. The four ends are soldered to porcelain insulated vacuum terminals. If A.C. current is passed into two of the terminals connected to dissimilar wires, the thermal E.M.F. across the other two terminals is a function of the pressure. This form of gauge, developed by KLEMPERER (1960), has the advantage that it is easy to construct and requires no calibration.

In the high vacuum part of the system an "Elliott" Cold Cathode Ionization gauge was fitted, this is a commercial form of the Penning Gauge but has the advantage that a solenoid replaces the conventional permanent magnet. The latter, of course, could easily affect the electron trajectories.

(b) Current detection.

The electron current was usually easily measured with a lamp and scale galvanometer. However in order to investigate small currents going to the gun holder or the stem of the gun an electrometer amplifier was constructed.

The electrometer amplifier is based on a circuit published by LECK and AUSTIN (1960) which consists of an electrometer pentode, the anode current of which is fed into the base of a silicon transistor. The output current of this transistor is fed into a conventional three transistor D.C. amplifier. A high degree of negative feedback is applied over the complete circuit. The whole instrument was built

in a sealed box, which also contained a small accumulator to supply the filament of the valve. The electrometer was capable of measuring currents down to 10^{-9}A with ease.

(c) Power Supplies.

The power supplies were conventional AC/DC converters with heavy smoothing. The terrella supply had cascaded filter circuits to reduce the hum level to $\sim$0.1% of the applied D.C. voltage. The filament supply was fitted with a constant voltage transformer so that a steady emission current was maintained. The high tension supply to the electron gun was either from a 'Phillips' stabilized power supply or from 120 volt dry batteries, according to whether or not a supply insulated from earth was required.

(d) Measurements of the Terrella Temperature.

Because of the ohmic losses and lack of convection cooling, a means of checking the temperature of the terrella was fitted. This consisted of a bridge which compared the voltage dropped across a standard resistor in series with the terrella coil, with the voltage appearing across the terrella coil. The bridge, at balance, therefore measured the resistance of the terrella coil which in turn depended on its mean temperature.

CHAPTER 5. THE PRODUCTION OF A FIELD ANALAGOUS TO THE GEOMAGNETIC FIELD.

5.1 General Considerations.

In some previous model experiments (BIRKELAND, 1901; BRUCKE, 1931; MALMFORS, 1945), the centred dipole features of the earth's field were produced by permanent magnets. This method has the disadvantage that the magnetic moment cannot be varied as a means of altering the effective or scaled rigidity of the electrons.

In the model experiment of BRUNBERG and DATTNER (1953) the dipole field was produced by a coil wound so that the current density varied as the cosine of the latitude. The theory involved in the construction of such coils is developed in Appendix 2. BRUNBERG and DATTNER made a coil system by winding a series of concentric cylindrical coils as described by BROWN and SWEER (1945). In this experiment some coil system was required in which regional anomalies could be introduced. For this reason a hollow coil system was devised. Figure 5.1 shows how the coil was wound by means of twenty circular segments. Each segment was wound with a different diameter of wire, so that the current density varied approximately as the cosine of the latitude. The coil former was made of brass and turned from the solid for accuracy. The dimensions of the coil former were chosen so that the interior spherical region had a radius

Fig. 5.1 DIAGRAM SHOWING CONSTRUCTION OF THE TERRELLA COIL AND THE POSITIONS OF THE ANOMALY MAGNETS.

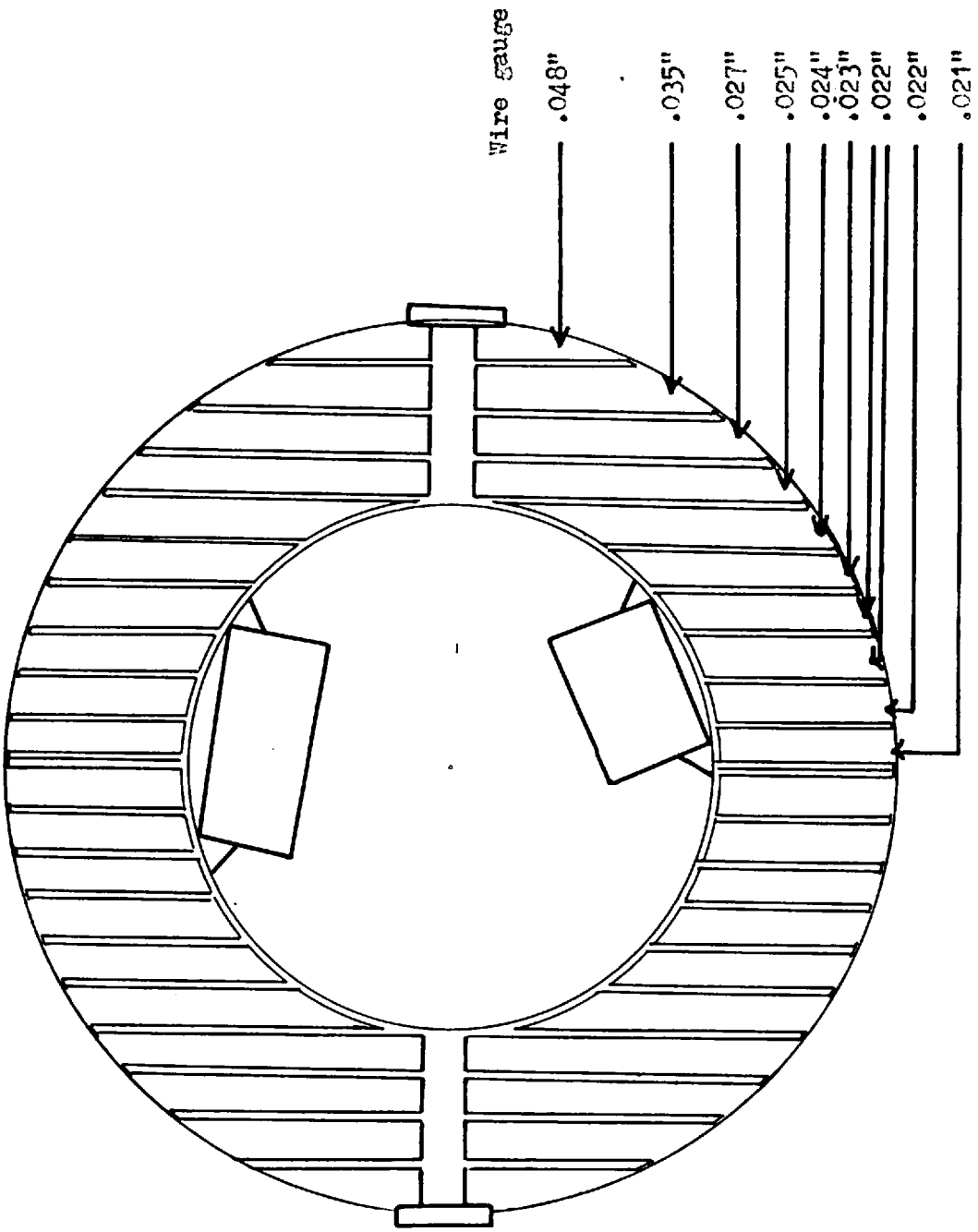

of about half that of the complete coil system. This dimension was chosen because it is possible to reproduce the regional anomalies in the geomagnetic field by means of radial dipoles positioned half a radius below the surface of the earth (McNISH, 1940).

The production of the anomaly field can be accomplished to a high degree of accuracy, according to McNISH, by the use of thirteen subsidiary anomaly dipoles. It is difficult, however, to achieve the dipole moments necessary for all thirteen dipoles within in the space available. For this reason, the number of anomaly dipoles used was reduced to three, thus it was only possible to reproduce the gross features of the geomagnetic field. In order to obtain a better approximation to the geomagnetic field, the field windings were offset to produce an eccentric dipole, by the amount indicated by the analysis of the geomagnetic field. This modification also off-centres the anomaly dipoles, but this is a second order effect, and does not substantially alter the gross features of the terrella field produced.

5.2. The Winding of the Dipole Coil.

Before describing in detail the terrella fields produced, we will deal briefly with the practical aspects of making the terrella coil.

As we have already mentioned the coil former was turned from the solid brass. The winding surface was then coated with a silicone

varnish and baked. The latter process produced a coating which remains non-conducting to 180°C. In order to reinforce this insulation, thin P.T.F.E. tape (.002 inches thick) was placed between the windings and the coil former. The synthetic enamel coating of the wire used for the coils (Lewkanex M) also remains non-conducting up to 180°C.

5.3. The Anomaly Magnets.

An attempt was made to produce the anomaly dipole fields by means of electromagnets. These electromagnets could have been placed in series with the main dipole coil and the magnitude of the complete terrella field simply varied by means of a series rheostat.

Unfortunately, air cooled coils were unsuitable owing to the power dissipation necessary to produce the requisite dipole moments. Some experiments were carried out to see if the effective dipole moment could be increased by winding the coil on a core of high permeability material.

The effective permeability* of a given core depends on its

.....

* The term effective permeability is often applied to the ratio B/H_o. Its relation to the intrinsic permeability is given by:-

$$\frac{1}{\mu} = \frac{1}{\mu_1} - \frac{N}{4\pi}$$

$\frac{N}{4\pi}$ is known as the demagnetising factor.

geometry. This is due to the demagnetising effect of the induction field. Results of measurements and calculations reported by BOZORTH (1951) show that, for a cylinder of reasonable length to diameter ratio, the demagnetising factor is large. This fact indicated the use of very high permeability materials as the only means of achieving an increase in dipole moment.

The results of experiments conducted using these high permeability cores showed that the effective magnetic moment could be increased by factors up to $\sim$ 12. Despite these increases, however, the power dissipation necessary for the production of the appropriate anomaly fields was considered to be excessive. Moreover the dipole moment of these coils was not a linear function of the current through them. Therefore there was no simple way of using the magnetic field as a variable to change the rigidity of the electrons.

The use of permanent cylindrical magnets in conjunction with the dipole coil was adopted.

This has the disadvantage that the magnets tend to demagnetise each other, and moreover must work in the uniform field inside the terrella. For these reasons it is only possible to make a crude estimate of the dipole moments and positions necessary for the best approximation to the geomagnetic field. The best compromise can only be found by trial and error.

In the design of the permanent magnets used for the anomalies, four competing factors were taken into account, these are:-

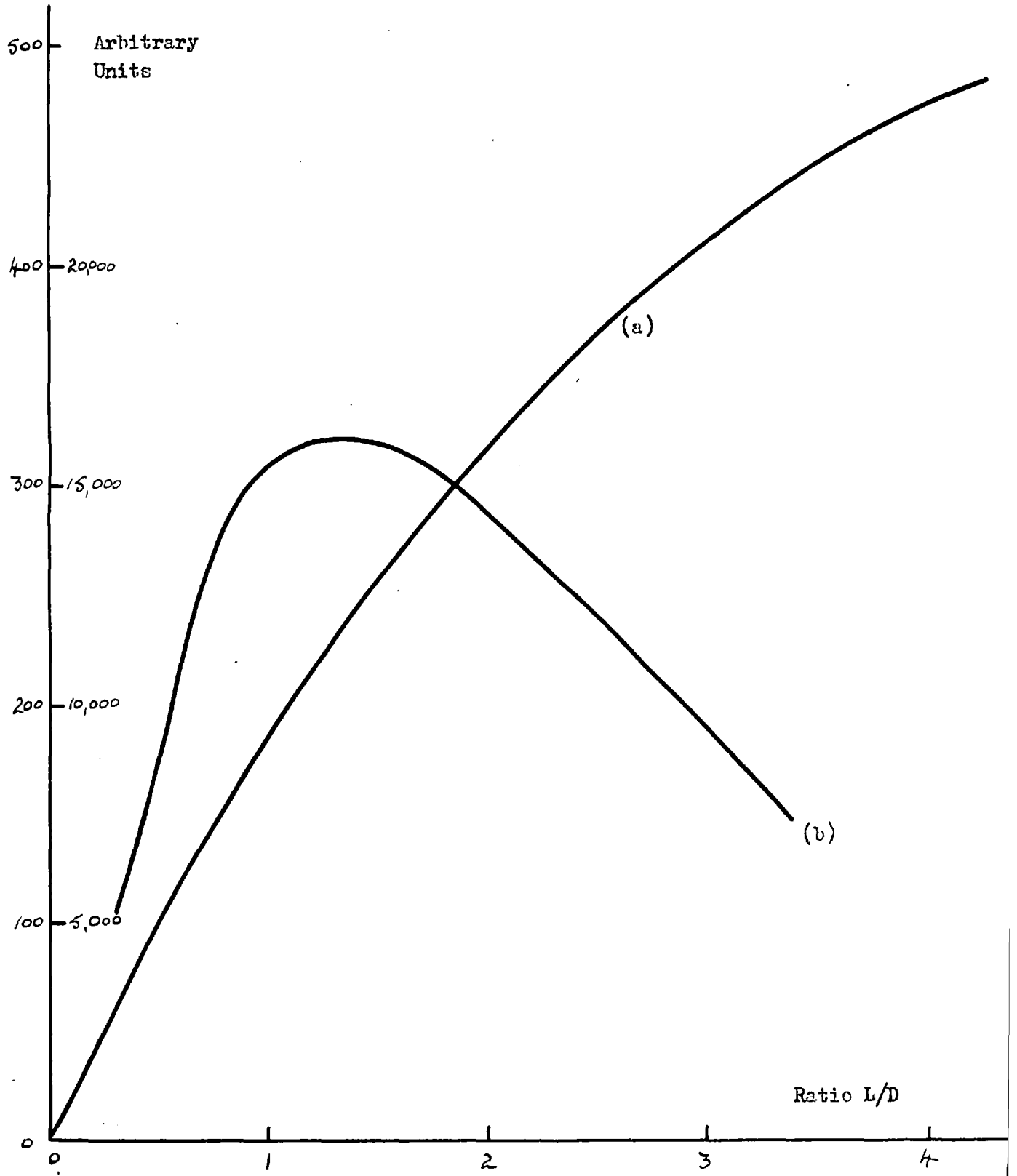

Fig. 5.2 a) MAGNETIZATION PER UNIT VOLUME AS A FUNCTION OF LENGTH TO DIAMETER RATIO FOR TICONAL G. b) MAGNETIC MOMENT AS A FUNCTION OF LENGTH TO DIAMETER RATIO WHEN TICONAL G MAGNET IS CONSTRAINED TO FIT INSIDE A GIVEN SPHERE.

(1) The magnetic moment varies as the volume for a given magnetic moment per unit volume m_v.

(2) The magnetic moment per unit volume varies as the ratio of the length to the diameter of a cylindrical magnet.

(3) The centre of the anomaly magnet defines the position of the magnetic centre of tne anomaly dipole with respect to the centre of the terrella. For this reason the anomaly magnets should be kept as short as possible.

(4) The three magnets must all fit within the given spherical surface at the positions which are chosen for the best match to the geomagnetic field.

If these magnets had been designed solely with the object of obtaining a maximum magnetization then the ratio of length to diameter ratio would have been chosen to obtain BH max. However, the ratios indicated for some magnetic materials, for example 'Magnadur 2', are too small to allow the magnets to fit into the positions they must occupy to generate the regional anomaly fields. The material eventually chosen was 'Ticonal G', the relevant curves are shown in Figure 5.2 The lower curve indicates the magnetic moment per unit volume as a function of length to diameter ratio, the upper curve the total magnetic volume when one dimension of the magnet is fixed at some arbitrary value. As the number of samples of magnetic materials was limited, it was not possible to adopt a strictly formal approach

to the problem of the choice of material, shape and size of the anomaly magnets. Therefore the above considerations simply served as a guide to the final choice of magnets which was made by trial and error from the limited quantity of magnetic material readily available. After the magnets were ground to a suitable dimension they were megnetised in the extremely uniform ($\sim$ 1 part in 10^6) field of a 'Newport' electromagnet at a field of $\sim$ 10,000 gauss.

The three anomaly magnets were placed in the centre of the terrella assembly. Care was taken to ensure that they were kept as far apart from each other as possible so that demagnetization inter alia was minimized. The magnets were fixed in jigs inside the terrella made from fibreglass paste, which upon hardening, held them rigidly in position.

The interior field of the main dipole coil is equal to the polar field. In order that the magnets remained magnetically stable, this field was increased to beyond the normal working field after the magnets were fitted and before any measurements were made. Likewise, the temperature of the coil was allowed to rise to a value in excess to that normally encountered during use, so that any deterioration in magnetisation occurred before measurements were made.

5.4 The measurement of the Terrella Field.

In choosing the field measuring device to be used in this experiment, the following types of magnetometers were considered:-

(i) Moving coil

(ii) Hall effect

(iii) Proton resonance

(iv) Variable permeability.

The reason for rejecting the first type is that suitable sensitivity could not be achieved without the use of coils of the same order of size as the typical dimensions of the field gradients to be measured. For example in making a survey of the radial field along a line of latitude, the field could change over 5° of longitude by as much as 20% near a regional anomaly. In order therefore to record this difference the radius of the coil must subtend an angle several times smaller than 5° at the centre of the terrella. Assuming for example, we made it subtend an angle of 1° at the centre, then with a terrella of 10 cm. radius, the diameter of the coil must be $\sim$ 3 mm. radius. In the equatorial region the radial field may be $\sim$ 1 gauss in some regions. If such a coil were rotated in this field and the output fed into a valve voltmeter, then in order to get 1 MV. output at a rotation of 5000 r.p.m. it would be necessary to have $\sim$ 2000 turns on the search coil. Such a number of windings is clearly impracticable

on a coil of these dimensions. Another disadvantage is that the rotating search coil responds to the field in the two directions at right angles to the axis of rotation. Since it was necessary to measure the field of three mutually perpendicular components independently the rotating coil system was ruled out.

Very similar considerations ruled out the use of the Hall effect probe, i.e. lack of directionality and sensitivity. Moreover the Hall probes at present commercially available are only linear over a limited field range and are also sensitive to temperature changes.

The proton resonance magnetometer would have been suitable on the grounds of accuracy and sensitivity but the typical dimensions of the probe would have been too large. Moreover such instruments respond to the total field and not to a given component of the field.

The variable permeability magnetometer generally takes the form of the well known 'flux gate' magnetometer. The flux gate magnetometer depends on the measurement of a second harmonic which appears when a first harmonic is applied to a coil wound on some high permeability material core. The strength of the second harmonic depends on the steady magnetic field surrounding the core. The instrument is extremely accurate but generally is rather complex, and has a probe too large for use in this experiment. An instrument developed originally by GREGG (1947) seemed to fulfill all the requirements for this experiment. The original design has been extensively modified and improved by Mr. P.C. Hedgecock of this laboratory.

Fig. 5.3 BLOCK DIAGRAM OF VARI-PERMEABILITY MAGNETOMETER.

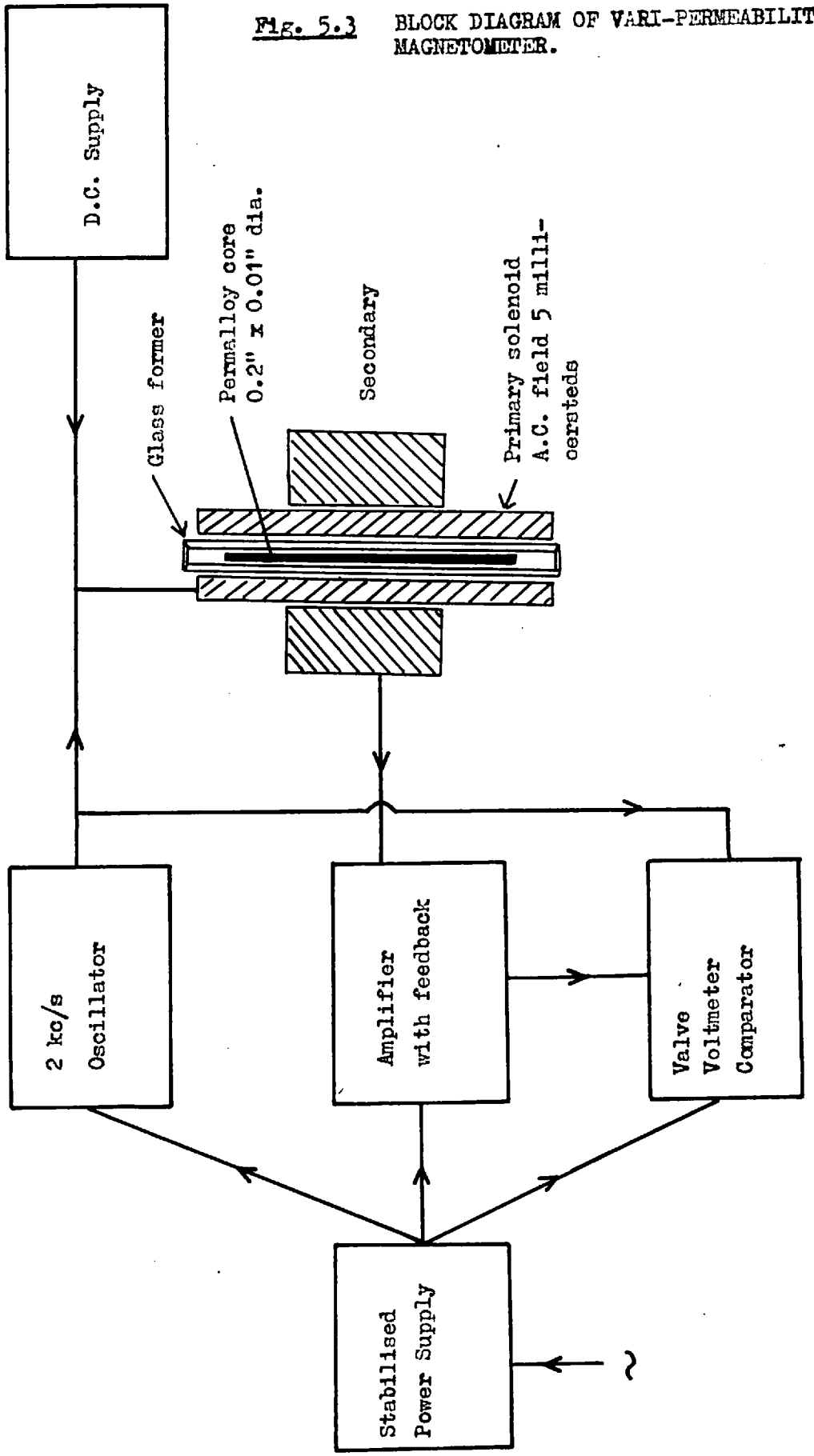

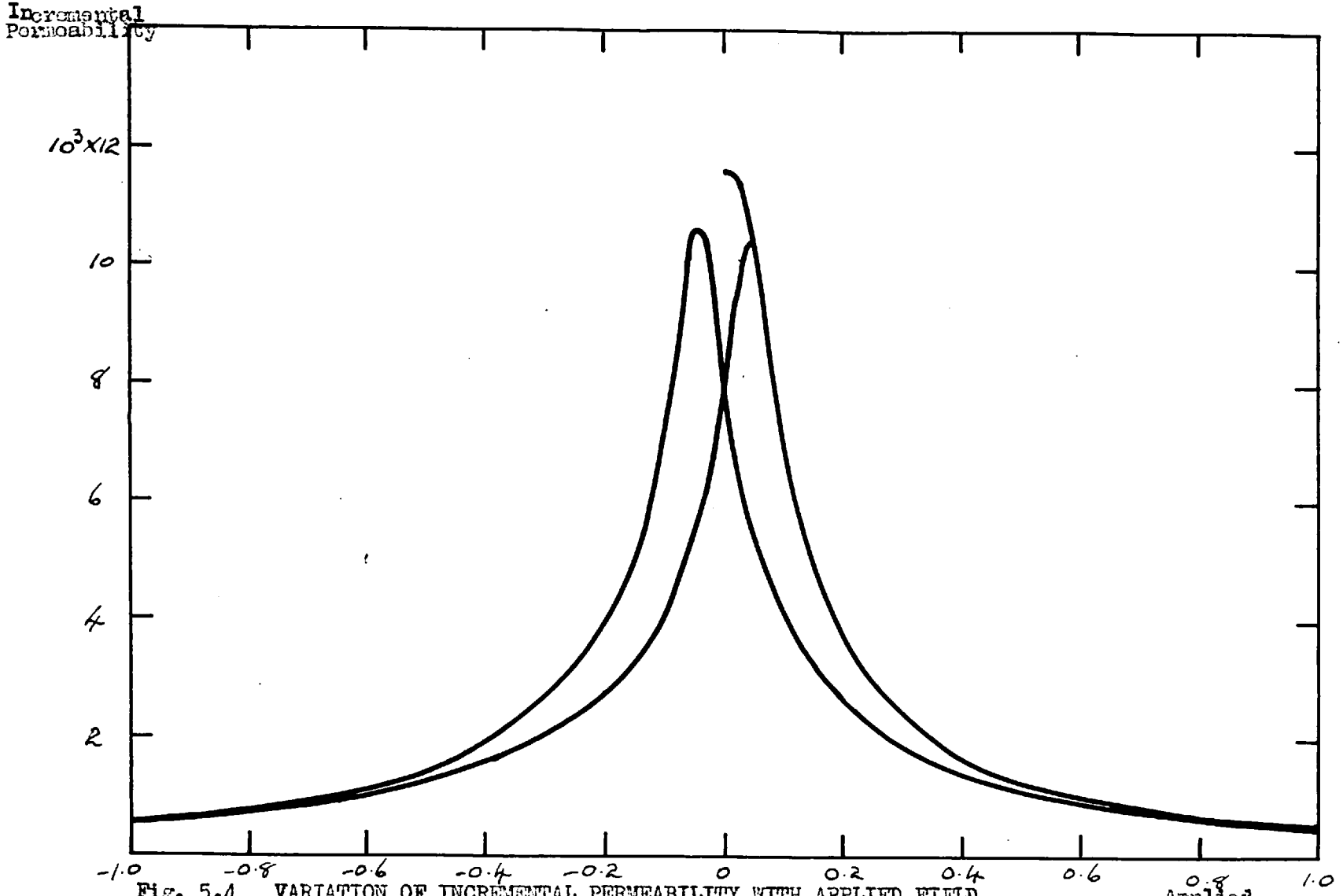

Fig. 5.4 VARIATION OF INCREMENTAL PERMEABILITY WITH APPLIED FIELD.

The magnetometer consists basically of a miniature transformer having a core of thin ($\sim$0.010" diameter) 'Permalloy C' wire. The amplitude of an A.C. signal developed in the secondary winding depends not only on the voltage applied to the primary but also on the incremental permeability ($\left(\frac{\partial B}{\partial H}\right)_{B = B_z}$) of the core. This quantity $B = B_z$ varies rapidly with the strength of the field existing along the core axis see figure 5.4. To measure this field, direct current is passed through the primary core to bring the field back to its original condition. This current is then a measure of the field strength. Figure 5.3 shows a block diagram of the circuitry. The power supplies are fully stabilized. The accuracy of the instrument is $\sim$ 1% at 50 gauss. The range covered by the instrument is approximately 1 $\rightarrow$ 50 gauss although the range may be extended to 100 gauss or more, since the only restriction is set by the power dissipation of the balancing direct current. The lower limit is set by the stability of the balance detector. The probe is highly directional producing a reading of $\sim$ 0.2 gauss for a field of 50 gauss at right angles.

The field was measured with the probe mounted on a jig system (shown in Figure 4.3). The probe was aligned in one of the three perpendicular directions, either radial, 'North-pointing' horizontal, or 'West-pointing'horizontal. The field was, in all cases, measured as close as possible to the position occupied by the electron gun anode during the experiment. All the field measurements were undertaken within the degaussing coils with the terrella in the same

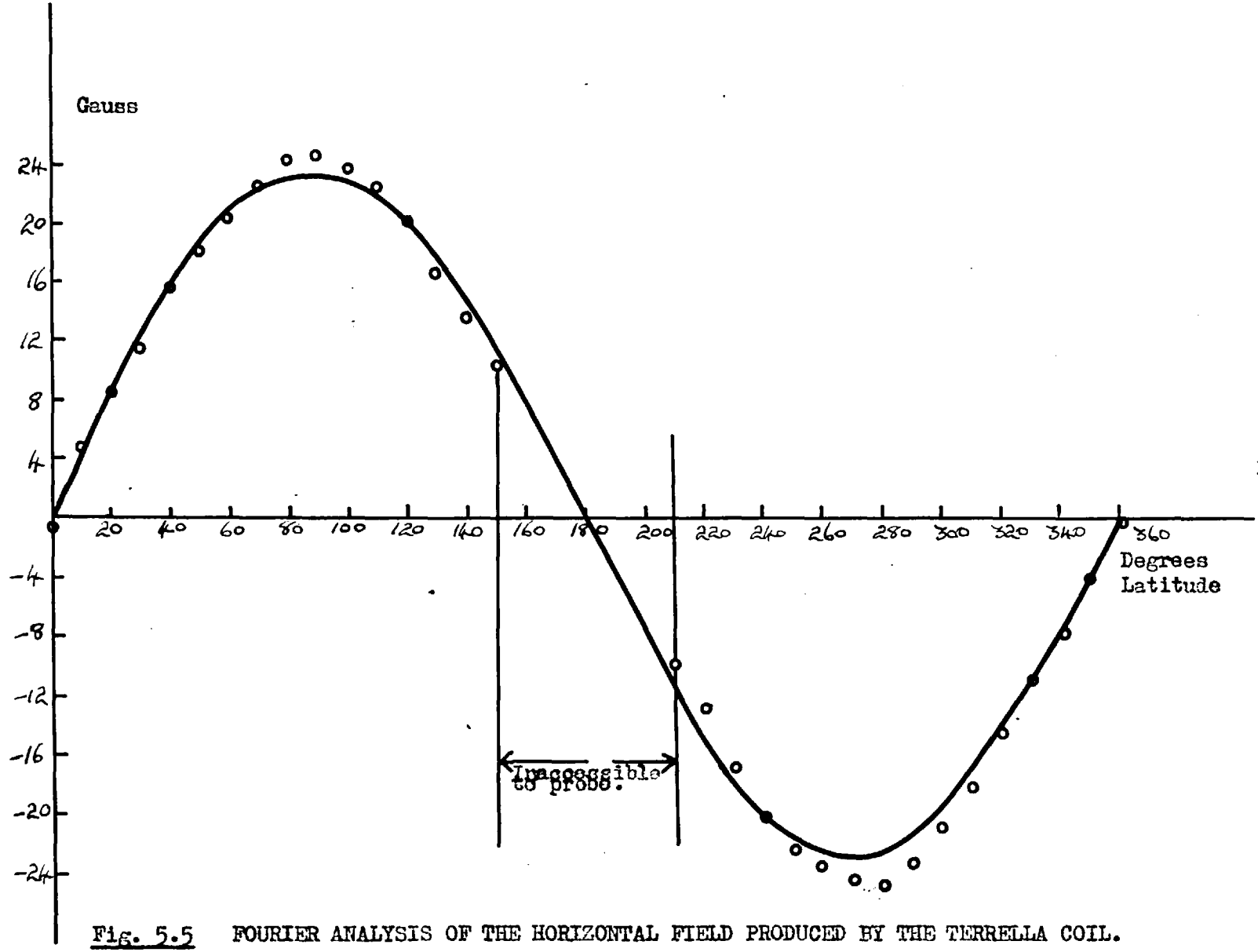

Fig. 5.5 FOURIER ANALYSIS OF THE HORIZONTAL FIELD PRODUCED BY THE TERRELLA COIL.

position as it occupied during the subsequent experiments.

5.5 The Results of the Measurements.

The first measurements of the terrella field due to the coil alone revealed an assymetry in the polar fields showing that the coil centre did not coincide with the terrella casing. This assymetry was removed by grinding down the P.T.F.E. bosses on which the coil assembly revolved.

If the field due to the coil itself is that of a centred dipole, then a set of measurements of either the north-pointing horizontal or the radial component should produce a sinusoidal dependence of field strength on latitude. A Fourier analysis is therefore a means of estimating the extent to which the field is that of a centred dipole. Figure 5.5 shows the result of some measurements, for comparison with the first harmonic derived.

The first harmonic accounts for 96% of the total field. We believe most of the remaining field is due to inaccuracies inherent in the coil design rather than to serious errors in winding. This point is dealt with in Appendix 2 . The dipole moment of the main terrella coil was 30,500 $\pm$ 300 gauss cm^3/amp This figure increased with the fitting of anomaly magnets since these had a substantial dipole component in the direction of the main dipole. We shall deal with this matter presently.

Fig. 5.6 CIRCLES INDICATE McNISH'S RADIAL DIPOLES TO REPRODUCE ANOMALY FIELDS. CROSSES INDICATE POSITION OF MAGNETS USED IN THIS EXPERIMENT.

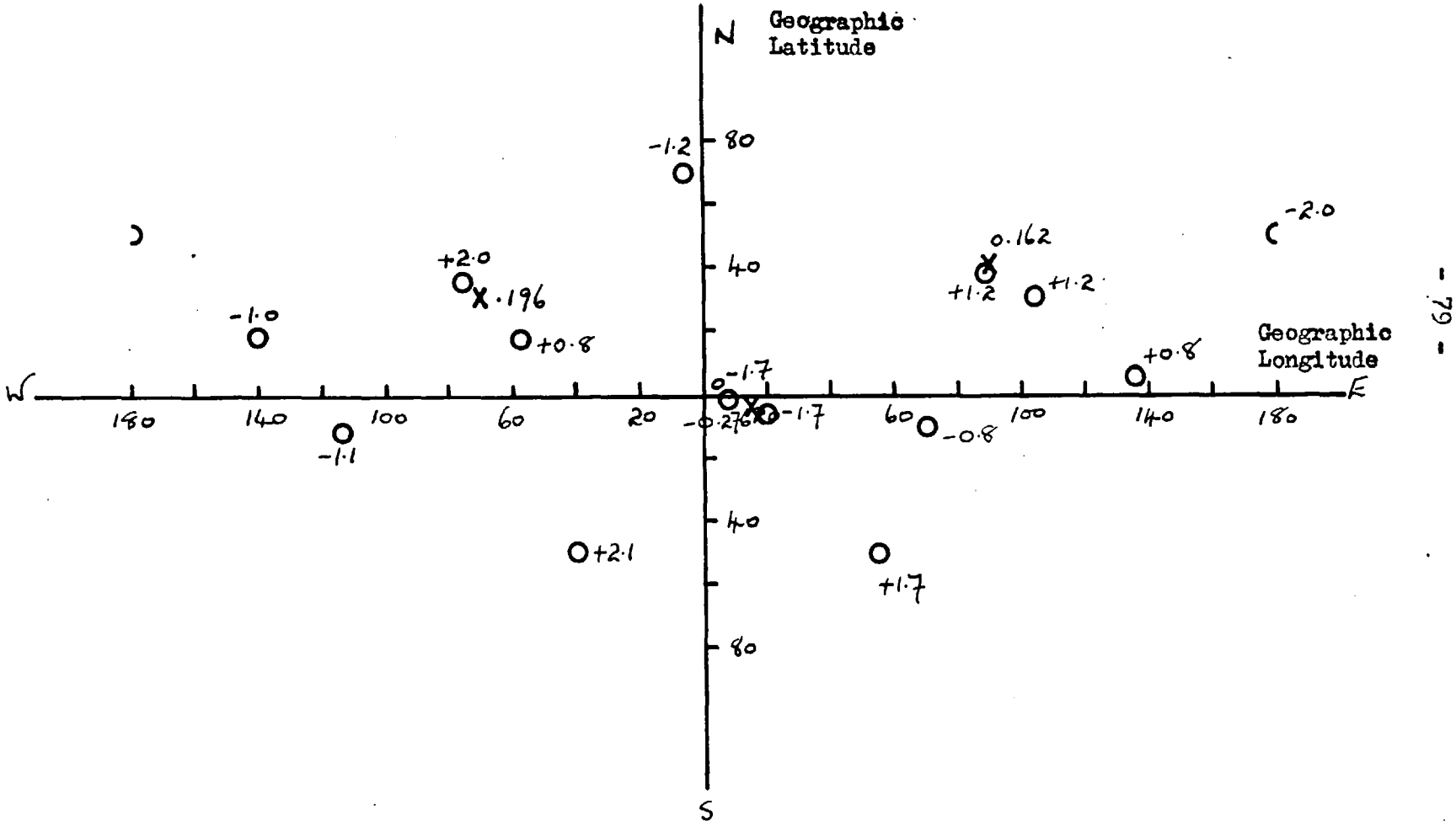

Figure 5.6 indicates the positions and magnitudes of the radial dipoles proposed by McNISH to account for the non-dipole component of the geomagnetic field. For comparison, the three radial dipoles used in this experiment are plotted. The positions and magnitudes of these dipoles were first determined by reference to McNISH. McNISH'S analysis revealed that the grosser components of the anomaly field are reproduced by three aggregates of dipoles which have larger ($\sim$ x 10) dipole moments than the isolated dipoles which represent smaller regional anomalies. The three dipole magnets used in this experiment, were varied in magnitude and position until a best fit was obtained to the geomagnetic field.

It is rather difficult to express the 'goodness' of the fit of the terrella field to the scaled down geomagnetic field. KELLOGG (1960) reproduced the field along the geomagnetic equator, for computer purposes, by the addition of the dipole, quadrapole and octopole terms in the expansion of the geomagnetic field. He expressed the 'goodness' of his fit by simply stating the maximum deviation of the total component of the field.

Before comparing the two fields, we have expressed both in terms of a percentage of the mean polar radial field. This latter field is a measure of the strength of the dipole component.

The field was measured at the equatorial band of latitude, $-30 < \lambda < 30^{\circ}$ at every ten degrees of latitude and longitude. The three mutually perpendicular components viz radial, north pointing

SURVEY OF RADIAL COMPONENT.

TABLE 1A. Terrella Current 1 Amp.1

lat. / long.	+30	+20	+10	0	-10	-20	-30
0	+46.0	+22.4	+13.9	0.1	-19.2	-21.7	-35.1
20	+35.9	+23.0	+11.6	+3.4	-20.8	-27.0	-41.7
40	+32.8	+17.0	+10.5	-6.0	-23.3	-29.0	-40.2
60	+31.4	+16.7	+5.0	-7.9	-25.0	-30.2	-47.4
80	+31.9	+22.4	+6.6	-7.7	-23.0	-30.8	-42.3
100	+32.4	+20.3	+10.2	-4.9	-23.9	-29.1	-39.8
120	+39.9	+24.1	+10.1	-1.0	-18.2	-23.1	-39.9
140	+46.2	+29.0	+17.2	+4.0	-14.5	-21.2	-41.5
160	+47.0	+36.8	+26.4	+5.6	-12.2	-19.6	-37.4
180	+51.2	+35.0	+25.7	+7.3	-11.0	-17.8	-34.0
200	+51.0	+35.8	+25.4	+7.5	-15.7	-19.0	-48.5
220	+50.5	+41.2	+24.0	+6.0	-14.9	-24.3	-47.0
240	+50.0	+36.2	+20.0	+5.1	-16.0	-23.5	-48.9
260	+48.3	+33.9	+19.6	+2.0	-18.1	-23.6	-41.3
280	+48.2	+29.2	+18.7	-1.4	-18.8	-23.8	-40.6
300	+45.7	+30.0	+21.4	-3.0	-17.8	-22.1	-38.4
320	+35.2	+29.2	+19.7	-2.6	-18.0	-23.4	-36.9
340	+45.7	+28.1	+19.4	-3.0	-17.5	-24.9	-33.2

Units of Magnetic Field — gauss
Errors ~4%

SURVEY OF NORTH HORIZONTAL COMPONENT.

TABLE 1B. Terrella Current 1 Amp.

ϕ \ λ	+30	+20	+10	0	-10	-20	-30
0	-25.0	-31.0	-36.2	-34.2	-34.5	-32.6	-28.0
20	-25.5	-31.5	-38.0	-33.3	-26.9	-33.2	-29.1
40	-26.5	-33.0	-40.0	-33.4	-33.0	-32.4	-27.0
60	-27.5	-33.0	-39.0	-36.4	-34.0	-28.1	-26.0
80	-28.0	-33.5	-36.6	-36.2	-32.9	-31.7	-25.9
100	-26.3	-33.0	-36.1	-35.7	-34.9	-35.8	-28.7
120	-25.0	-31.8	-36.0	-36.9	-37.8	-36.0	-33.9
140	-24.0	-31.0	-40.1	-36.5	-50.0	-37.5	-44.0
160	-23.5	-31.0	-38.4	-39.0	-49.4	-38.0	-32.5
180	-23.0	-31.0	-34.8	-39.5	-40.6	-38.1	-31.6
200	-23.5	-31.5	-39.0	-39.4	-39.3	-42.3	-33.1
220	-23.5	-32.0	-45.0	-38.6	-38.6	-45.3	-33.0
240	-24.2	-32.0	-47.5	-38.0	-40.8	-42.2	-31.0
260	-25.0	-31.5	-45.8	-38.4	-37.9	-38.0	-30.6
280	-25.0	-32.0	-39.6	-38.2	-37.4	-37.9	-30.1
300	-25.0	-31.0	-45.0	-36.9	-38.9	-35.2	-31.2
320	-25.0	-29.0	-40.1	-35.8	-37.9	-36.3	-27.0
340	-24.5	-30.1	-38.6	-34.3	-35.1	-37.8	-27.1

SURVEY OF EAST HORIZONTAL COMPONENT.

TABLE 1C. Terrella Current 1 Amp.

X / Ø	+30	+20	+10	0	-10	-20	-30
0	-2.35	-1.85	-3.30	-1.25	2.90	<0.10	<0.10
20	-3.00	-1.40	-2.90	-1.80	-3.80	<0.10	<0.10
40	-3.60	-1.65	-0.30	-0.40	-2.70	-0.10	<0.10
60	<0.10	<0.10	+0.10	<0.10	-0.10	+0.10	+0.40
80	+2.50	+4.00	+2.70	+0.75	0.10	0.10	+4.45
100	+5.75	+7.20	+5.60	+3.80	+1.55	+0.65	+9.40
120	+10.60	+9.40	+7.15	+6.75	+7.30	+7.50	+6.70
140	+10.60	+8.30	+7.40	+3.55	+7.60	+3.40	+6.60
160	+7.15	+8.00	+5.90	+2.35	+3.95	+0.90	+4.65
180	+6.50	+5.10	+1.00	+0.75	+3.30	+2.65	+2.65
200	+5.50	+2.50	<0.10	<0.10	+1.30	+1.95	+1.00
220	+3.45	<0.10	<0.10	<0.10	+0.20	+0.20	+0.30
240	+1.00	<0.10	<0.10	<0.10	+0.10	<0.10	<0.10
260	+0.20	<0.10	<0.10	<0.10	<0.10	<0.10	<0.10
280	<0.10	<0.10	<0.10	<0.10	<0.10	<0.10	<0.10
300	-0.60	<0.10	<0.10	<0.10	<0.10	<0.10	<0.10
320	-2.00	-2.35	-0.60	<0.10	<0.10	-0.10	<0.10
340	-1.40	-2.50	-1.30	-0.60	-0.10	-0.20	<0.10

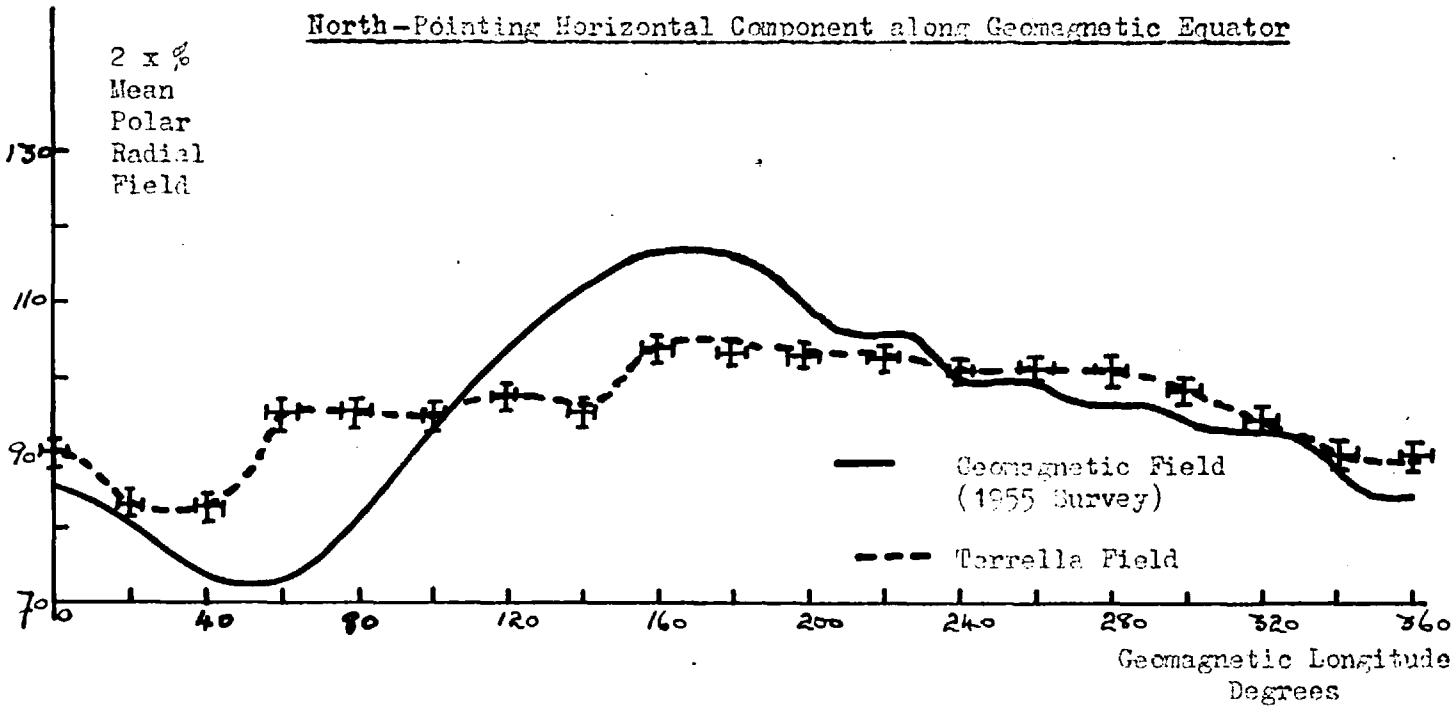

Fig.5.7 COMPARISON OF THE MODEL EXPERIMENT APPROXIMATION TO THE GEOMAGNETIC FIELD GENERATED BY MEANS OF A CENTRED DIPOLE COIL PLUS THREE RADIAL DIPOLE MAGNETS REPRESENTING THE REGIONAL ANOMALIES.

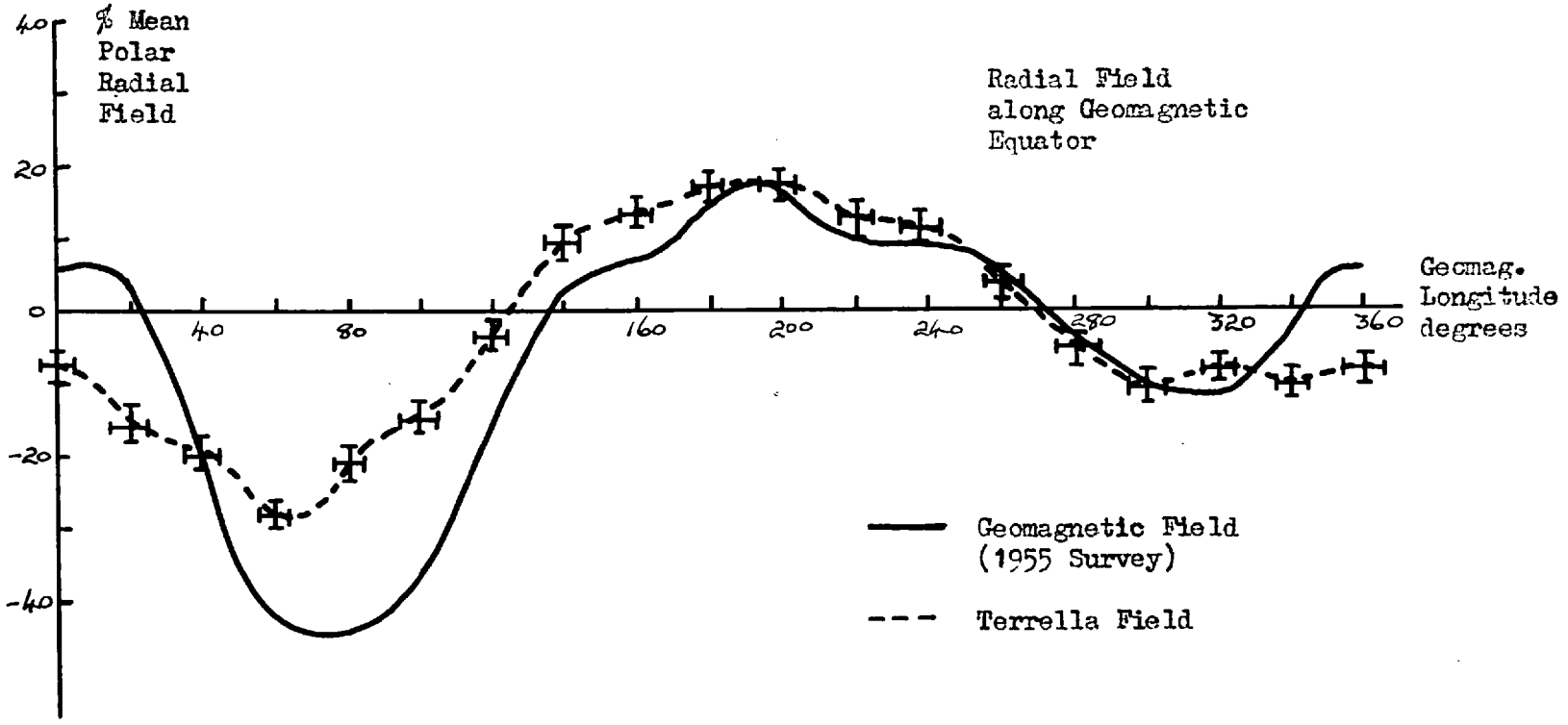

Fig. 5.8 COMPARISON OF THE MODEL EXPERIMENT APPROXIMATION TO THE GEOMAGNETIC FIELD GENERATED BY MEANS OF A CENTRED DIPOLE COIL PLUS THREE RADIAL DIPOLE MAGNETS REPRESENTING THE REGIONAL ANOMALIES.

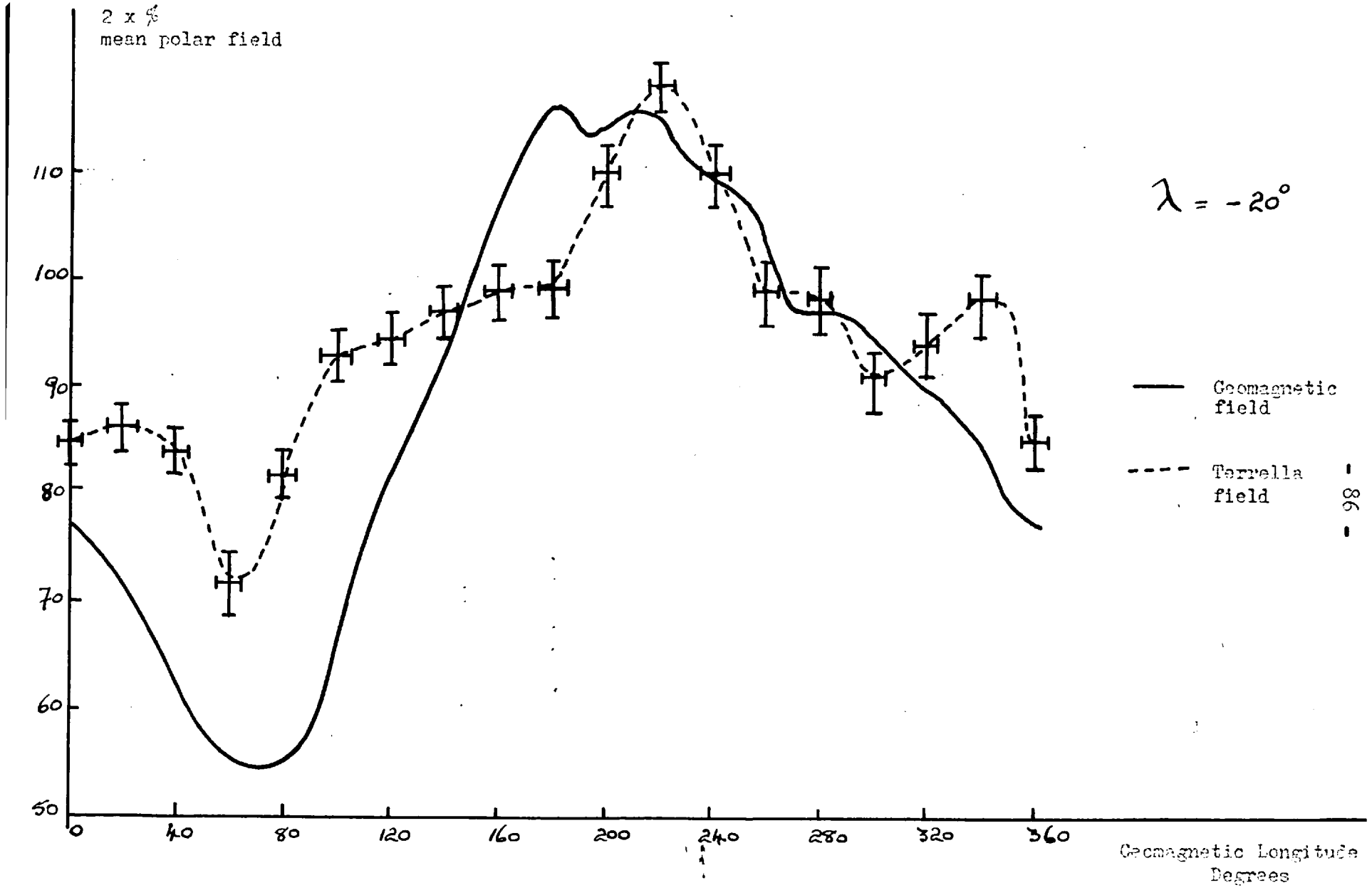

Fig.5.9 COMPARISON OF THE NORTH-POINTING HORIZONTAL FIELD AT λ = 20°S. FOR THE TERRELLA AND THE EARTH.

horizontal, east pointing horizontal were measured. Thus each field survey involved 378 readings. In addition checks were also made on the field at higher latitudes. The north pointing horizontal component is that which requires the most accurate fitting, it being usually at least an order of magnitude bigger than the east pointing horizontal component. Moreover, the horizontal field plays a dominant role in the estimation of 'QUENBY-WEBBER' threshold rigidities in the equatorial regions (see Chapter 1). The maximum deviation of the terrella north pointing horizontal component from the scaled geomagnetic field (taken from the 1955 Admiralty charts) occurs at $\lambda = -20^{\circ}$ and $\varphi = 100^{\circ}$ (φ being the geomagnetic longitude) and amounts to $25 \pm 2\%$; this compares with a maximum deviation of 15% obtained by KELLOGG. In order to indicate the degree of field matching achieved Figures 5.7, 5.8, and 5.9 are reproduced. The r.m.s. deviation of the north pointing horizontal field component over the whole range of latitudes surveyed amounts to $11 \pm 1\%$. Most of this deviation arises in the regions of large regional anomaly. These anomalies were probably reproduced by dipole magnets of insufficient moment, although attempts to increase their contribution to the total field, by decreasing the current to the main dipole field, resulted in a worse fit to the resultant field in regions having a field differing little from the eccentric dipole field, Ideally a complete spherical harmonic analysis should have been used to fully describe the terrella field. Owing to the inaccessability of some parts

Fig. 5.10 SUPERIMPOSED HARMONIC DIALS SHOWING AGREEMENT BETWEEN RADIAL EQUATORIAL FIELDS OF THE TERRELLA AND THE EARTH.

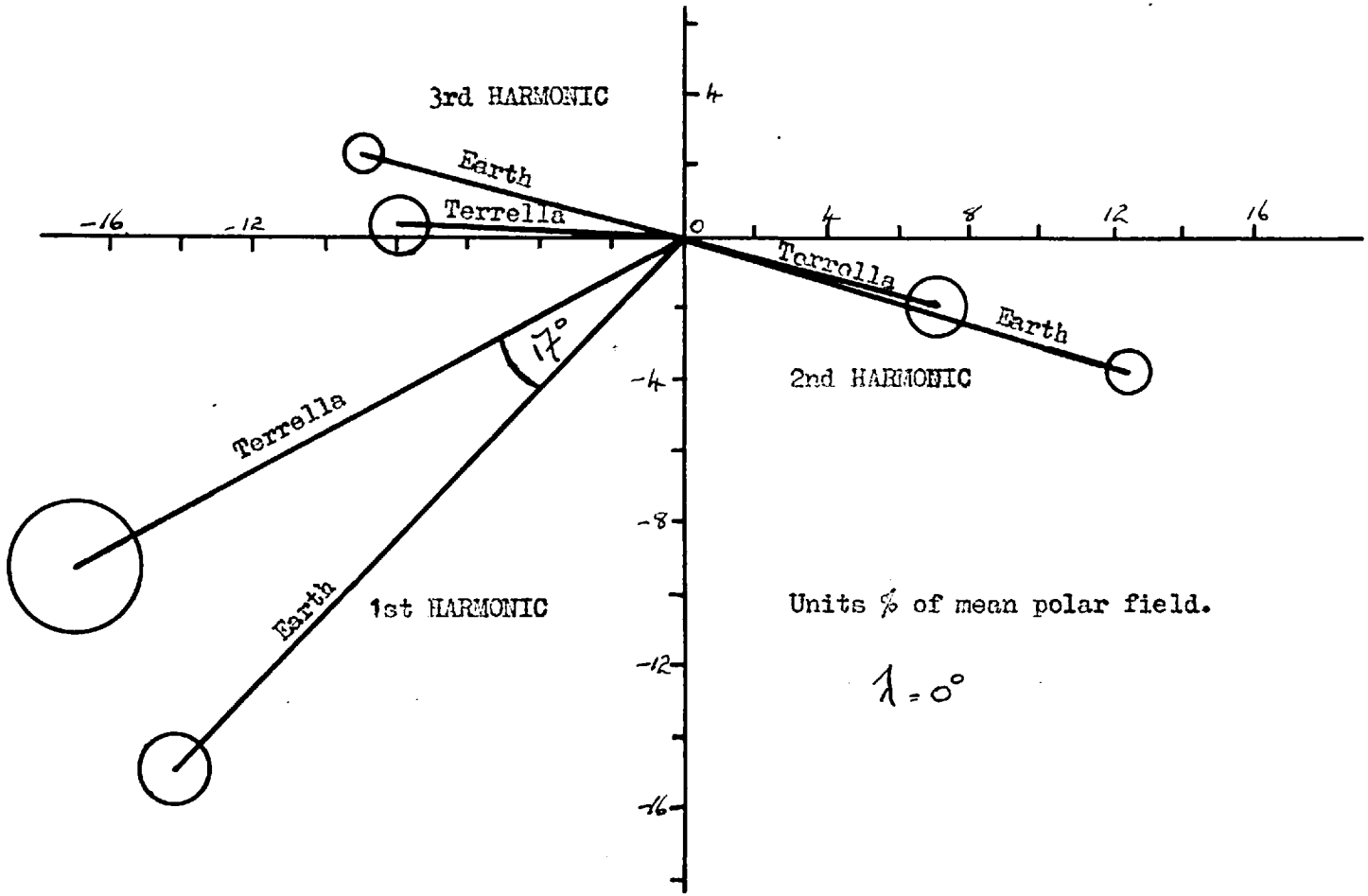

- 38 -

of the terrella field e.g. at the stem of the terrella, and for a variety of technical reasons, no such analysis was possible. In order, therefore, to shed further light on the field matching at the equator, a Fourier analysis was undertaken of the variation of the radial component with geomagnetic longitude. The result was plotted on a harmonic dial with the results from an analysis of the geomagnetic field for comparison (Figure 5.16). The amplitude of each harmonic is a measure of the field described by tesseral terms in the expansion of the complete field. Whilst this information is, itself, of little relevance, a comparison of the two, terrella and geomagnetic, analyses, is certainly indicative of the degree of field matching achieved.

Whilst admitting that the field is only a fair representation of the geomagnetic field, nevertheless the terrella field deviates substantially from that of a dipole and exhibits the gross features of the geomagnetic field. Therefore any inherent errors in the theoretical treatment of geomagnetic effects based on the centred dipole approximation should be evident in experiments made using this terrella field.

CHAPTER 6. DETAILS OF THE PRELIMINARY EXPERIMENTAL PROCEDURE.

6.1 Introduction.

Most of the preliminary experimental work has been described in previous chapters of this thesis. We will therefore summarize the more important aspects adding further information where necessary. After the assembly of the apparatus the following experimental work was carried out:-

6.2 The attainment of high vacuum.

This not only involved the sealing of leaks in the chamber, but also the leak testing of the complete terrella assembly. The larger leaks were found by using hydrogen gas as a probe, and looking for the small drop in pressure indicated on a Pirani gauge. The smaller leaks required the use of a mass spectrometer leak detector, using helium as the probe gas. It is estimated that the total leakage rate is now less than 10^{-2} lusec.

6.3 The measuring of the terrella field; see Chapter 5.

In the first instance, the field was approximately dipole, later when anomalies were added, the survey was repeated.

6.4 The assessment of the optimum current through the degaussing coils.

This necessitated measuring the field over the region in which the electrons move and checking that there were no appreciable fields originating from outside the apparatus. In practice, the only serious stray field arises from A.C. current leaking to earth through the steel frame of the building. Luckily, the magnitude of this current increases towards the lower part of the building, while the apparatus was situated on the top floor. The A.C. field amounts to ~ 0.005 gauss r.m.s. This field however, may account for some of the spread in the threshold rigidities. We shall return to this question presently.

6.5 The testing of the electron gun.

Not only was it necessary to test the optics of the gun, but also to check that the beam emerged from the gun perpendicular to the plane of the anode. Moreover, it was necessary to check that no serious deflection occurred within the gun when it was working in the

magnetic fields produced by the terrella. The former condition was found to be accurately fulfilled, the beam emerging within 2° of the 'vertical'. As regards the second condition, the electrode apertures, to a great extent, define the exit angle of the beam, but when the gun is working at lower voltages and higher fields, then the exit angle will be modified appreciably. Without a knowledge of the details of the electron trajectories, it is, in fact, difficult to make better than an order of magnitude calculation of the deflection inside the gun. If the deflection is small, an approximate value of the angular deflection w is given by:-

$$w = \frac{2a_o H \sin\Psi}{3.37.\sqrt{V_o}}$$

where a_o is the cathode to anode distance

H is the magnetic field

Ψ is the angle between the axis of the gun and the magnetic field

and V_o is the accelerating voltage.

Substituting typical values for H and V_o, one obtains w to be $\sim 20^{\circ}$. We believe that this value is high by a large factor since the application of such magnetic fields across the electron gun caused deflections of less than 5°, (measured during a subsidiary experiment using a post-acceleration target) and moreover the good agreement of the values of Stormer threshold rigidities in the pure dipole field

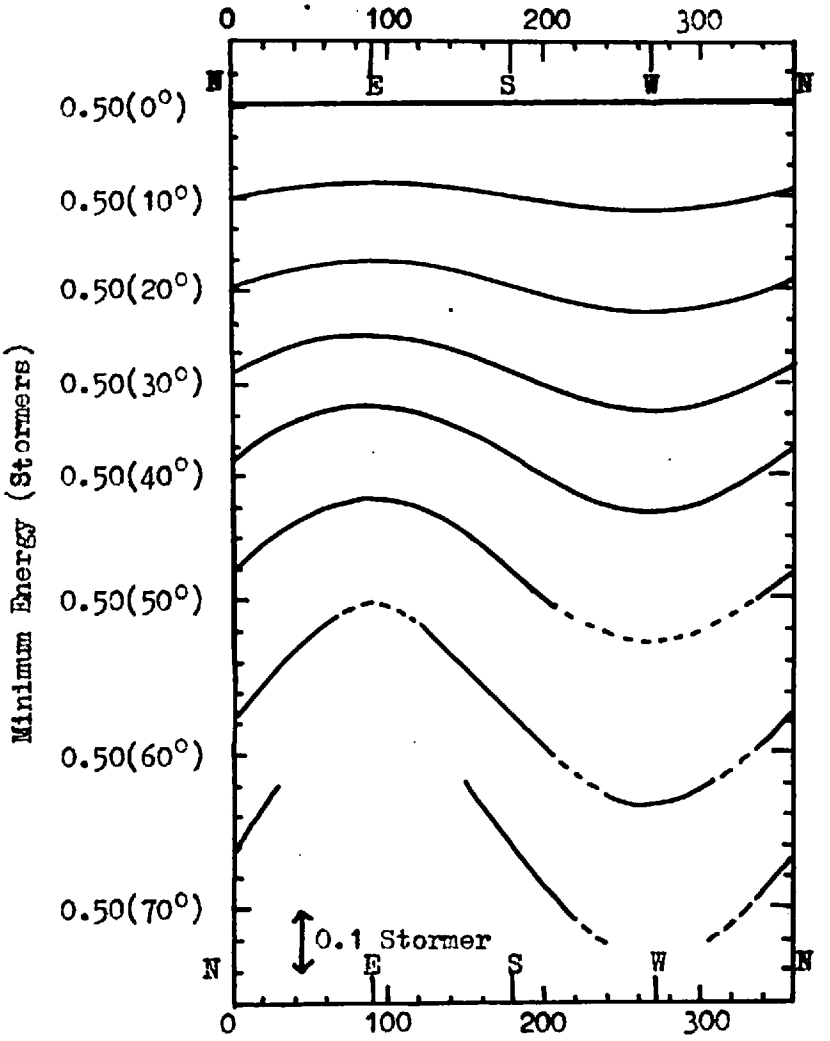

Fig. 6.1 MINIMUM ENERGY OF ARRIVAL, E_{min}, MEASURED IN STORMER UNITS, VERSUS AZIMUTH ANGLE , FOR VARIOUS ZENITH ANGLES , AS DETERMINED BY THE MAIN CONE. GEOMAGNETIC LATITUDE $\lambda = 0°$. (DASHED PORTIONS OF CURVES ARE ESTIMATED.

seems to argue against such a large deflection. The focussing action of the gun would tend to counteract large magnetic deflections within the gun. The small hole in the anode must also select electrons making a small angle to the axis, as is indicated by the sharp fall in emission current as a function of accelerating voltage. This point will be further discussed in the following chapter.

6.6 The alignment of the gun relative to the terrella assembly.

The gun was arranged so that electrons were emitted as close as possible to the normal to the spherical surface of the terrella. In this way the measured threshold rigidities should represent the vertical threshold rigidities. The electron gun had two preset directions of rotation, one in the 'east-west' direction, the other in the 'north-south direction. The Stormer theory of the allowed cone indicates that the cone is symmetrical about an east-west axis. Therefore if the Stormer cone was the only restriction on particles arriving at the earth (or conversely electrons leaving the terrella) then it would only have been necessary to align the gun perpendicular to the east west direction. However the theory of the allowed cone as modified by VALLARTA et al. indicates that a north-south asymetry exists. For this reason, the gun was aligned perpendicular to both the east-west direction and the nort-south direction. The adjustment of the gun perpendicular

to the east-west direction was made as follows:-

The gun was first adjusted by eye and the threshold rigidity at the equator was determined. The centred dipole field was then reversed and the threshold rigidity re-measured. These threshold rigidities differed in value unless the gun was pointing perpendicular to the east-west direction because at the equator the threshold rigidity varies rapidly with zenith angle in the east-west direction. Thus, by trial and error, an accurate setting was obtained. The gun was then locked and maintained in this position throughout the subsequent experiments.

No simple expedient existed for adjusting the gun in the north-south direction. The threshold rigidity curves obtained at higher latitudes with the centred dipole in opposite senses were therefore compared and the north-south angle adjusted until the penumbral modifications were independent of the sense of the dipole.

6.7 Summary.

The above list summarizes the major items of the preliminary experimental work. Other work undertaken included the calibration of measuring instruments, and the checking of subsidiary equipment, e.g. measuring the 'hum' on power packs etc.

A great deal of effort was involved in technical problems particularly the insulation of the terrella coil, outgassing of the

electron gun, and the replacement of burnt-out filaments. However, after the solution of these problems and the completion of the preliminary work, the apparatus worked satisfactorily for periods long enough to obtain a great deal of useful data.

CHAPTER 7. THE OBSERVATION OF THRESHOLD RIGIDITIES.

7.1 General.

According to LIOUVILLES theorem the flux of cosmic rays within an allowed cone should be equal to the flux at infinity. Therefore, a detector of infinitisimal acceptance angle situated at the top of the atmosphere should either see the full cosmic radiation intensity at a given rigidity or zero intensity. Therefore, a graph of intensity versus rigidity would contain a series of step functions representing alternately allowed and forbidden rigidity intervals.

The graph obtained from the analogue computer of the percentage of emission current escaping the environment of the terrella as a function of equivalent proton rigidity will not exhibit the features of the graph obtained with the hypothetical detector. The reasons being that the electron gun has a finite solid angle ($\sim 4^{o}$) and also any measurement made at a mean equivalent proton rigidity is in fact, a reading taken over a finite spread of equivalent rigidities due to the electrons not being monoenergetic, and also because of such factors as 'hum' in the dipole coil. Nevertheless, the trapping of electrons in the terrella field as a function of rigidity certainly indicates the essential features of the restrictions imposed by the geomagnetic

field on particles arriving close to the vertical. Moreover, since any actual cosmic ray detector usually has an acceptance angle much bigger than the electron gun exit angle, then the results obtained with this analogue computer are probably of sufficient accuracy.

7.2 Experimental Technique.

In order to vary the equivalent proton rigidity there are three quantities that may be altered (cf. scaling equations, Chapter 3) in the model experiment, these are the following:-

(1) The electron energy

(2) The magnetic field

(3) The radius of the terrella

The third possibility is not an attractive one, although it was used by MALMFORS, who used a permanent magnet in his terrella and therefore was limited in his choice of variables. The variation of electron energy is rather unsuitable, since the emission current varies as a function of accelerating voltage and furthermore the equivalent proton rigidity varies as the square root of the electron voltage. This mean that a wide range of gun voltages is called for, some of which may lie in regions where the gun optics are significantly modified.

The variation of magnetic field is the most attractive

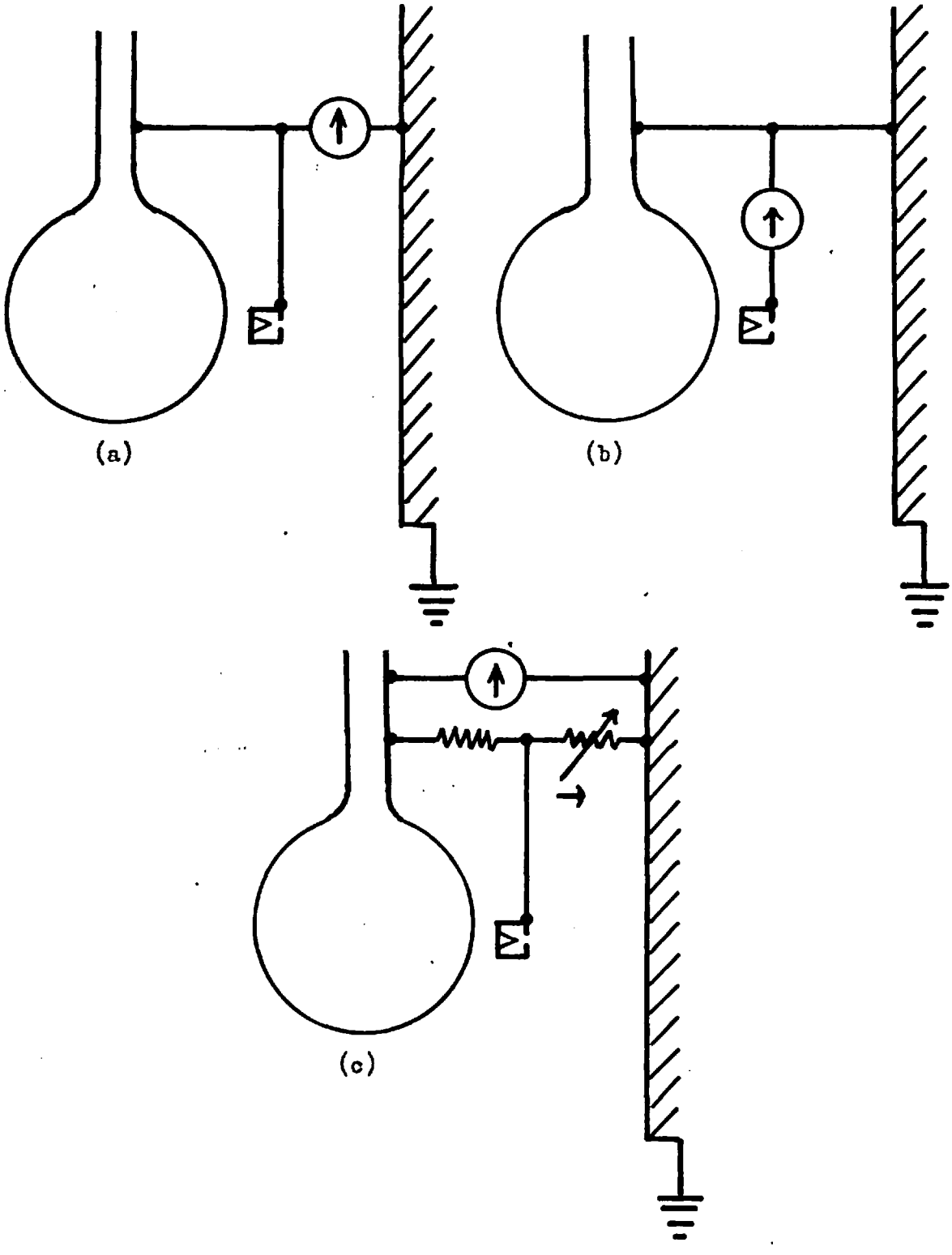

Fig. 7.1 METHOD OF CONNECTION FOR MEASURING:-

(a) TANK CURRENT
(b) TOTAL EMISSION CURRENT
(c) RATIO OF TANK TO TERRELLA CURRENT.

possibility since the equivalent threshold rigidity is a linear function of the magnetic moment and this last can be varied very simply if it is generated by a solenoid, by means of a rheostat in series. This variation was, in fact, used in the pure dipole experiments. In the further experiments with more complex fields generated by a solenoid and permanent magnets the variation of electron energy was employed.

Taking the pure dipole experiment first (figure 7.1 indicates the circuit layout) the current flowing from the gun anode to the tank was measured as a function of the magnetic moment of the terrella (i.e. the terrella coil current), the terrella being connected to the gun anode. The current flowing to the terrella and the tank was then measured (i.e. the total emission current)as a function of the magnetic moment over the same range. The former readings were then each divided by the corresponding latter readings to yield a graph of the percentage emission current leaving the terrella as a function of threshold rigidity. The currents flowing to the stem of the terrella or the electron gun holder were checked from time to time to ensure that these objects were not obscuring some part of the beam. These currents were found to be very low and were measured with the electrometer amplifier. The current to the stem was always $\sim .001$ of the total emission current and the current to the gun holder was $\sim .01$ of the total emission current, although at latitudes $< 20^{\circ}$ it sometimes

rose $\sim$.03 near to the equivalent threshold rigidity. In all the threshold rigidity measurements the stem was connected to the tank and the gun holder to the terrella. It is felt that the net effect of these two obstructions was not significant.

In order to check that there were no appreciable obscuring currents flowing in the measuring circuits due say, to thermo-electric e.m.fs, the current flowing to the tank was added to the current flowing to the terrella and compared with the measured total emission current. It was found that in some cases appreciable leakage currents flowed. In particular, with the cathode at high negative potentials with respect to earth ($\sim$ 500v) a current flowed through the insulation of the filament supply power pack to earth. In such cases, this supply was not used, and was replaced by a supply consisting of lead acid accumulators mounted on sheets of polythene.

The accuracy of results obtained by the above experimental procedure depends largely on how constant the filament temperature is kept. This is the reason for using filament supplies of high stability. It was possible, however, to get over the difficulty of emission current variation in the case of equatorial threshold rigidity measurements, since in this case, the threshold is virtually a step function. For this reason, the ratio of the tank current to the terrella current was measured by means of a bridge circuit (cf. figure 7.1). This ratio varies with equivalent rigidity in a similar

way to the percentage of emission current reaching the tank, but has the great advantage of being independent of the total emission current.

The actual measurements were obtained using a lamp and scale galvanometer, and working with the lowest usuable total emission current. This latter restriction was imposed by the necessity of keeping the filament temperature as low as possible in order to obtain a useful lifetime.

The first equatorial threshold rigidities were observed soon after the preliminary experimental work was completed. Threshold rigidities at higher latitudes were then investigated and found to exhibit more complex structure which was later attributed to the penumbral effect. These were thoroughly investigated at many latitudes up to the upper latitude limit set by the boundary of the tank coinciding with the jaws of the forbidden regions, which turned out to be about 33°, compared with the theoretically predicted value of 34°. The measurements were hampered by the ohmic heating of the terrella. Although the terrella was allowed to reach about $120^{\circ}C$, this temperature was reached after 20 minutes, with 0.6 amp. flowing, this current being the value necessary to obtain a threshold at the equator with 230 volt electrons. By only switching on the terrella during measurements, about two hours of experimental work could be carried out. It was necessary to wait about four hours for the terrella to cool. The working time was further reduced at higher

latitudes, where higher terrella currents were required.

The technique for measuring threshold rigidities was substantially the same in the case of the dipole plus anomaly field, except that the electron voltage was varied. The terrella current was kept constant at 1 Amp, while the electron volts were varied over a range of 200 → 1000 volts. The higher voltages necessitated a supply highly insulated from earth and this was achieved by using nine 120 v dry cell batteries in series with sheets of polythene as insulation. Several high value resistors were wired into this supply in case of accidental shorts!

In passing we mention some work done on the observation of threshold rigidities with an oscilloscope. If the electron voltage is varied by superimposing a waveform derived from an oscilloscope time base on top of the standing voltage, then the application of a voltage proportional to the tank current, to the Y plates should produce a trace resembling the situation around the threshold rigidity. This technique was tried briefly and showed promise. The major difficulty encountered was that of providing enough drive to the Y plates. The voltage to the Y plates should be proportional to the tank current which was generally small ($\sim$ 1 or 2μA).

The other difficulty encountered was the effect of the difference in phase between the X and the Y plates. This tended to distort the trace. Elimination of these difficulties was not

seriously attempted for lack of time. However this technique, once perfected, would provide a very convenient method of observing threshold rigidities. Further investigation may be rewarding if it is proposed to use the apparatus to obtain large quantities of data.

CHAPTER 8. RESULTS OF THE EXPERIMENT.

8.1 Discussion of the Probable Errors involved in measuring Threshold Rigidities.

The salient features of the experimental technique have been mentioned in Chapter 7. We will now consider the various sources of error that arise when threshold rigidities are measured in this manner.

The various sources of systematic error are as follows:-

(i) Errors in measuring the effective distance of the gun anode from the magnetic centre of the terrella.

(ii) Errors due to the gun not emitting electrons exactly normal to the terrella surface.

(iii) Internal deflections occurring within the electron gun. This source of error is most serious close to the geomagnetic equator, where the horizontal field is at its maximum.

(iv) Errors due to the electron beam not being mono-energetic.

(v) Errors due to the terrella field deviating from that of a centred dipole.

(vi) Errors in latitude.

(vii) Errors to magnetic fields.

(viii) Errors in measuring voltages, currents etc. during the determination of the threshold rigidities.

(ix) Errors due to estimation of the threshold rigidity from a curve which differs from the theoretical step function.

By far the most serious errors are those due to the first three causes. The radius of the gun anode is subject to errors due to the centre of the terrella not coinciding with the magnetic centre of the dipole. In order to check this, threshold rigidities were measured at longitudes 0° and 180°. The difference in equivalent threshold rigidity amounted to $0.10 \pm .03$ GV. This therefore must be the upper limit on the error due to this cause. The radius itself was measured to be:-

$$\underline{9.74 \pm .03 \text{ cms.}}$$

This error in the measurement of the radius leads to an error in the equivalent threshold rigidity of approximately

$$\pm 0.10 \text{ GV.}$$

As regards the errors due to (ii) an estimate can be made from the shift in threshold rigidities occurring when the dipole moment was reversed. This was arranged to be a minimum as described in Chapter The shift observed was less than 0.4 GV.

The errors due to (iii) are difficult to assess since, as we have mentioned in the previous chapter, the internal deflection is not easily calculable except for the oversimplified case of an electron

moving in uniform crossed electric and magnetic fields. The evidence obtained from a subs diary experiment, in which the emergent beam was examined by means of a post acceleration target, indicates that the maximum deflection is $\sim 5^{\circ}$ from the vertical. Substitution of this value into the formula derived by STORMER for the evaluation of the threshold rigidity P at geomagnetic latitude and at an angle to the meridian plane i.e.

$$P = P_o \left(\frac{1 - \sqrt{1 - \cos\theta \cos^3\lambda}}{\cos\theta \cos\lambda} \right)^2$$

where P_o is the vertical equatorial threshold rigidity indicates that the maximum error due to this cause is ~ 0.5 GV.

The error due to (iv) is negligible as inspection of the equation giving the equivalent rigidity reveals

$$P_{eq} = 198 \frac{r_m^2}{M_m} \sqrt{V} \quad \text{GV.}$$

The voltage V in the case of the equatorial latitudes was 230 volts. The width of the Maxwellian distribution curve, being a few times KT where K is Boltzmann's constant and T is the temperature of the cathode ($\sim 2700^{\circ}$K) leads to a variation of V of less than one volt and consequently sets an upper limit on the error due to this cause of 0.02 GV.

Errors due to (v) are thought to be negligible. The analysis of the horizontal field survey (cf. Chapter 5) indicated that the first harmonic accounts for 96% of the field. (The maximum deviation

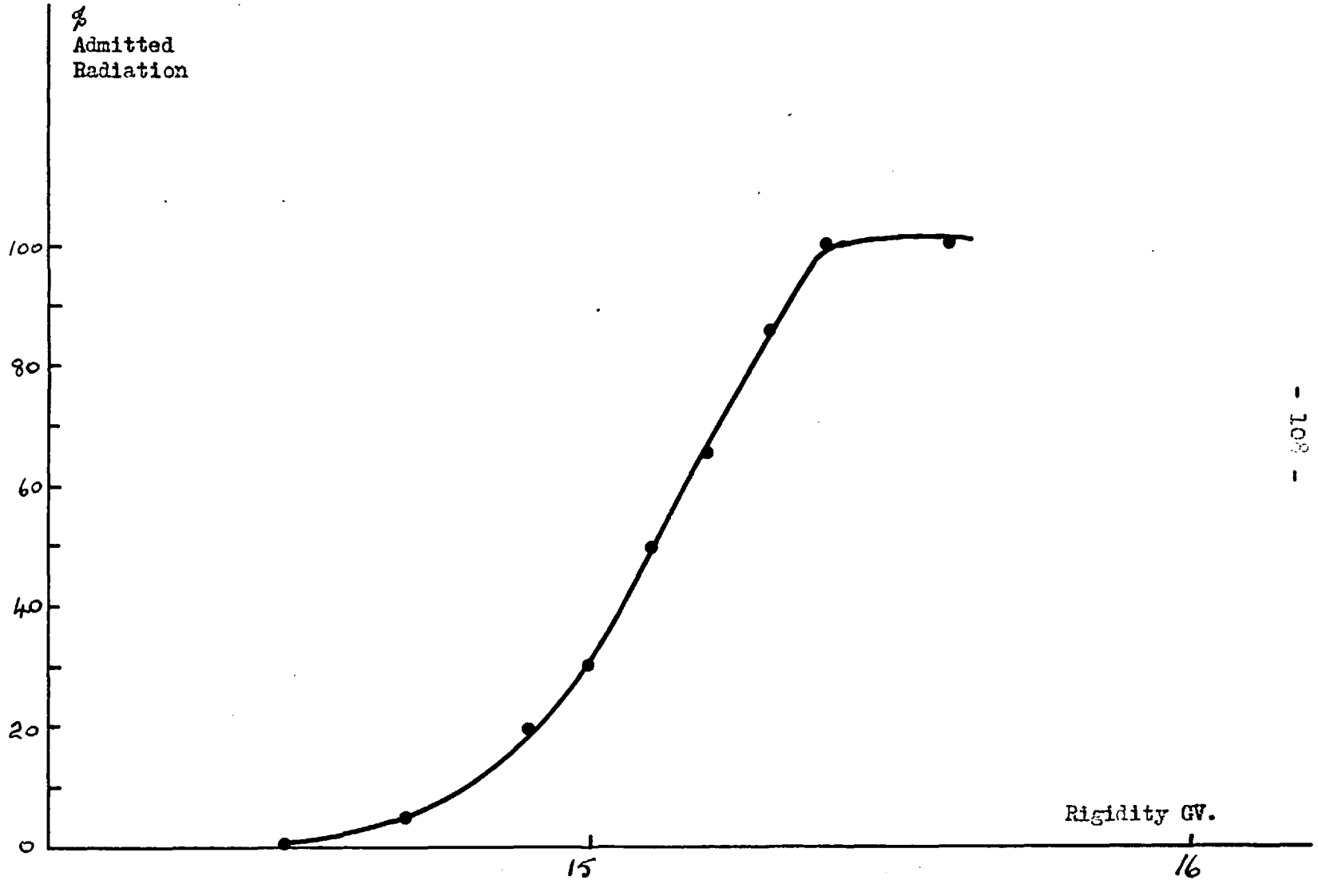

Fig. 8.1 TYPICAL EQUATORIAL THRESHOLD RIGIDITY IN CENTRED DIPOLE FIELD.

from a dipole field occurring at the polar regions). Since the particles near their threshold rigidities at the latitudes measured are confined near to the equatorial plane, the fields they encounter must contain a negligible contribution due to higher order terms.

Errors due to (vi), (vii) and (viii) are presumably random and can therefore be estimated from the standard deviation of the measurements.

Errors due to (ix) are dependent on the error in the area under the threshold curve. This depends on the accuracy of the shape of the curve. Some estimate can be made if the coordinates of the curve are tkane as the upper and lower limit of the error assigned to each experimental point. In practice, it is found that this procedure only shifts the threshold rigidity by ~ 0.05 GV, which is negligible compared with errors due to other sources.

If we sum up all the above sources of systematic error we obtain the probable error in the absolute value of the equatorial threshold rigidity which we found to be:-

$$15.3 \pm 0.7 \text{ GV}.$$

The error is probably pessimistic but nevertheless implies an accuracy of 4.5% in the measurement of the absolute magnitude of the threshold rigidity.

As regards the width of the equatorial threshold rigidity curve itself (fig.8.1) we suggest that it is due to the finite solid angle of the electron beam. The resultant curve is thus a sum of several

threshold rigidity curves contributed by small solid angle increments of the beam.

The threshold rigidities observed at other latitudes were evaluated by measuring the shift from the equatorial threshold. The percentage error in the shift is less than the error in the absolute value of the threshold which is largely a systematic error and sensibly constant for all latitudes. We estimate the error in measuring the shift to be ~ 0.2 GV and to this should be added a further error of ~ 0.2 GV to account for errors in latitude estimated to be $\pm 1^{\circ}$ and also a difference in the angle and magnitude of the magnetic field across the electron gun which must cause different internal deflections within the gun according to the latitude.

The evidence on the latter source of error is scanty, and the uncertainty of internal deflections is one of the weaker aspects of these measurements.

As a check on the degree to which internal deflections may modify the threshold rigidity, several threshold rigidity values were obtained at a given point on the terrella by using different combinations of magnetic field and electron gun voltage. In this way any internal deflection would be modified thereby causing a change in threshold rigidity. In practice such changes were negligibly small (~ 0.10 GV) and it is therefore concluded that internal magnetic deflections were offset by the severe electric field gradients existing within the short electron gun.

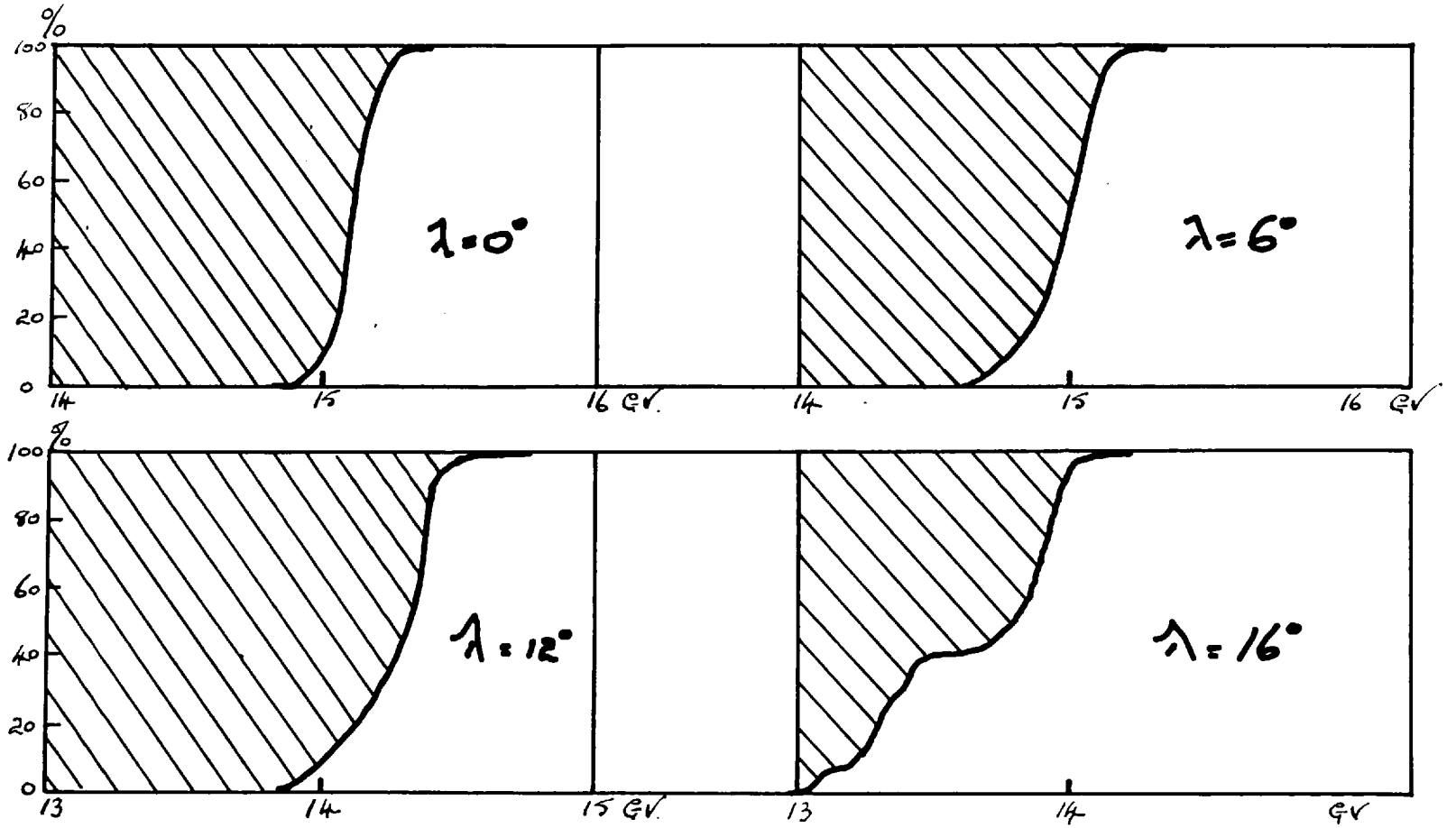

Fig. 8.2 CURVES SHOWING THE PERCENTAGE OF PRIMARY COSMIC RADIATION "SEEN" AT THE SURFACE OF THE EARTH ASSUMING A CENTRED DIPOLE FIELD, AS A FUNCTION OF RIGIDITY EXPRESSED IN GV. FOR SEVERAL GEOMAGNETIC LATITUDES.

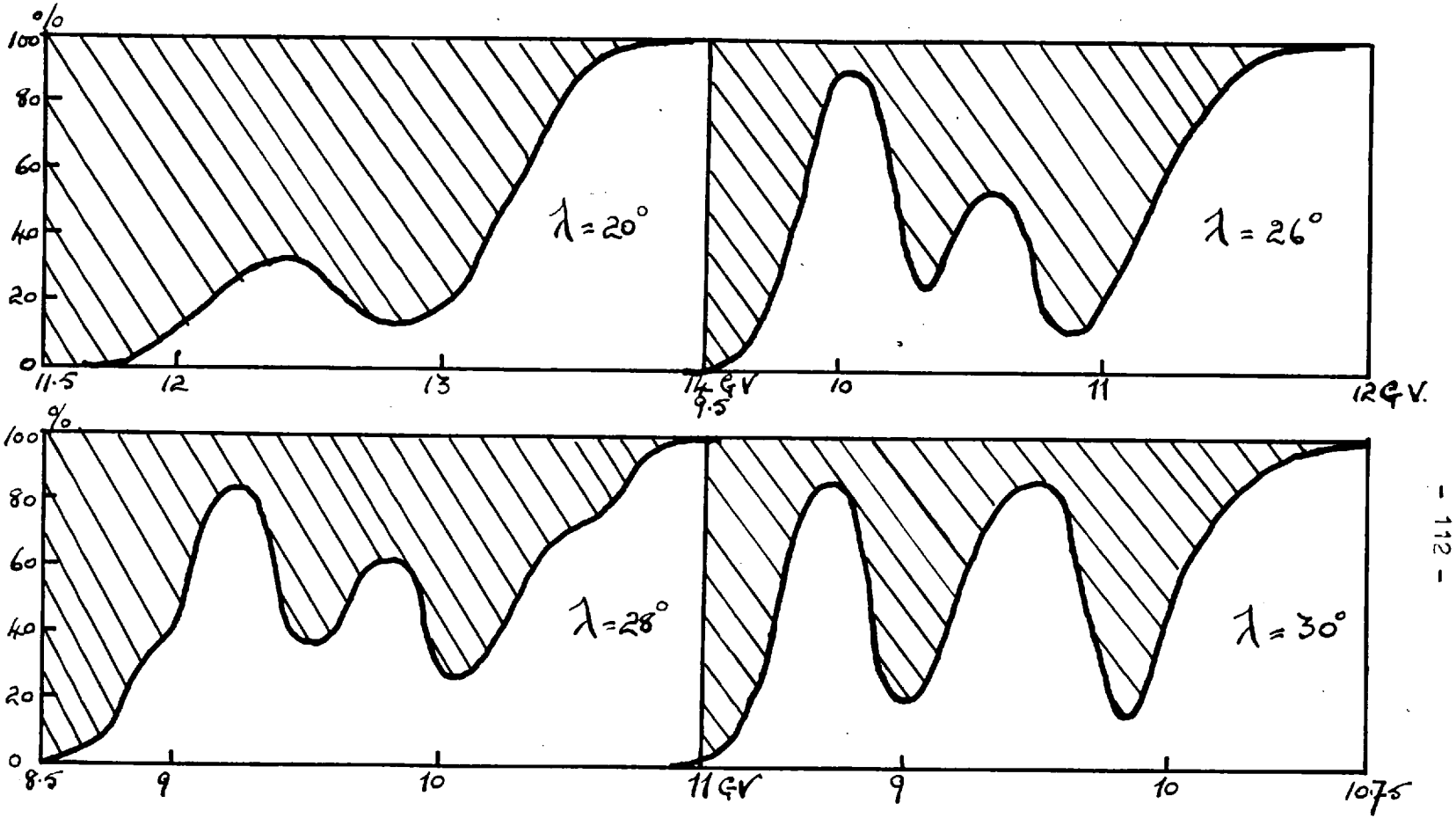

Fig. 8.3 CURVES SHOWING THE PERCENTAGE OF PRIMARY COSMIC RADIATION "SEEN" AT THE SURFACE OF THE EARTH ASSUMING A CENTRED DIPOLE FIELD, AS A FUNCTION OF RIGIDITY EXPRESSED IN GV. FOR SEVERAL GEOMAGNETIC LATITUDES.

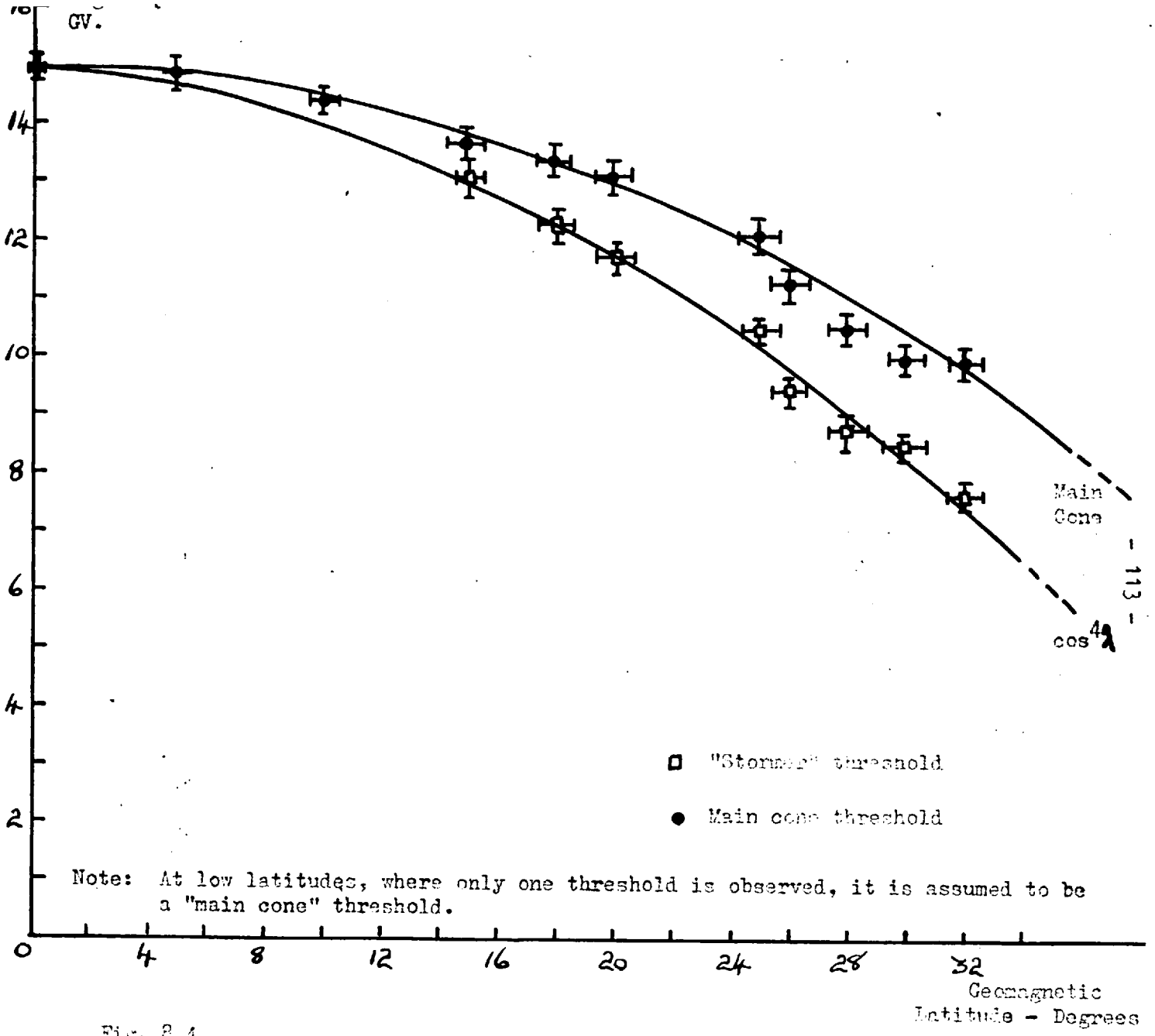

Fig. 8.4

THEORETICAL CURVES SHOWING THE EXPECTED VARIATION OF MAIN CONE AND STORMER CONE THRESHOLD RIGIDITIES WITH GEOMAGNETIC LATITUDE, FOR A CENTRED DIPOLE FIELD. POINTS OBTAINED IN THE MODEL EXPERIMENT ARE PLOTTED FOR COMPARISON.

8.2 Results of Centred Dipole Measurements.

The curves of the percentage of allowed radiation against equivalent rigidity are shown in Figures 8.2, 8.3 above 15° the threshold rigidity is not defined by a simple function but exhibits some irregularities. As the geomagnetic latitude increases the threshold curve breaks up into two distinct parts, the region between them exhibiting features which are similar to the penumbra. We shall assume that the initial decrease is due to the main cone threshold, the final decrease is due to the Stormer cone threshold and the region between, the penumbra. The shift in each latitude curve is measured by drawing tangents to the major decrease and measuring the distance along the x axis from the tangent to the equatorial threshold (see Figure 8.5).

In order to compare the results obtained with the theory of the main cone and the Stormer cone, we plot the points obtained from this experiment together with the theoretical curves (fig 8.4). In order to simplify matters, the equatorial threshold rigidity is arbitrarily assumed to be 14.9 GV and the values obtained at other latitudes are normalized to this value. It will be seen that the agreement with the theoretical curves is good. The transparency of the penumbra can be evaluated by integrating the area under the curve between the main cone and the Stormer cone thresholds.

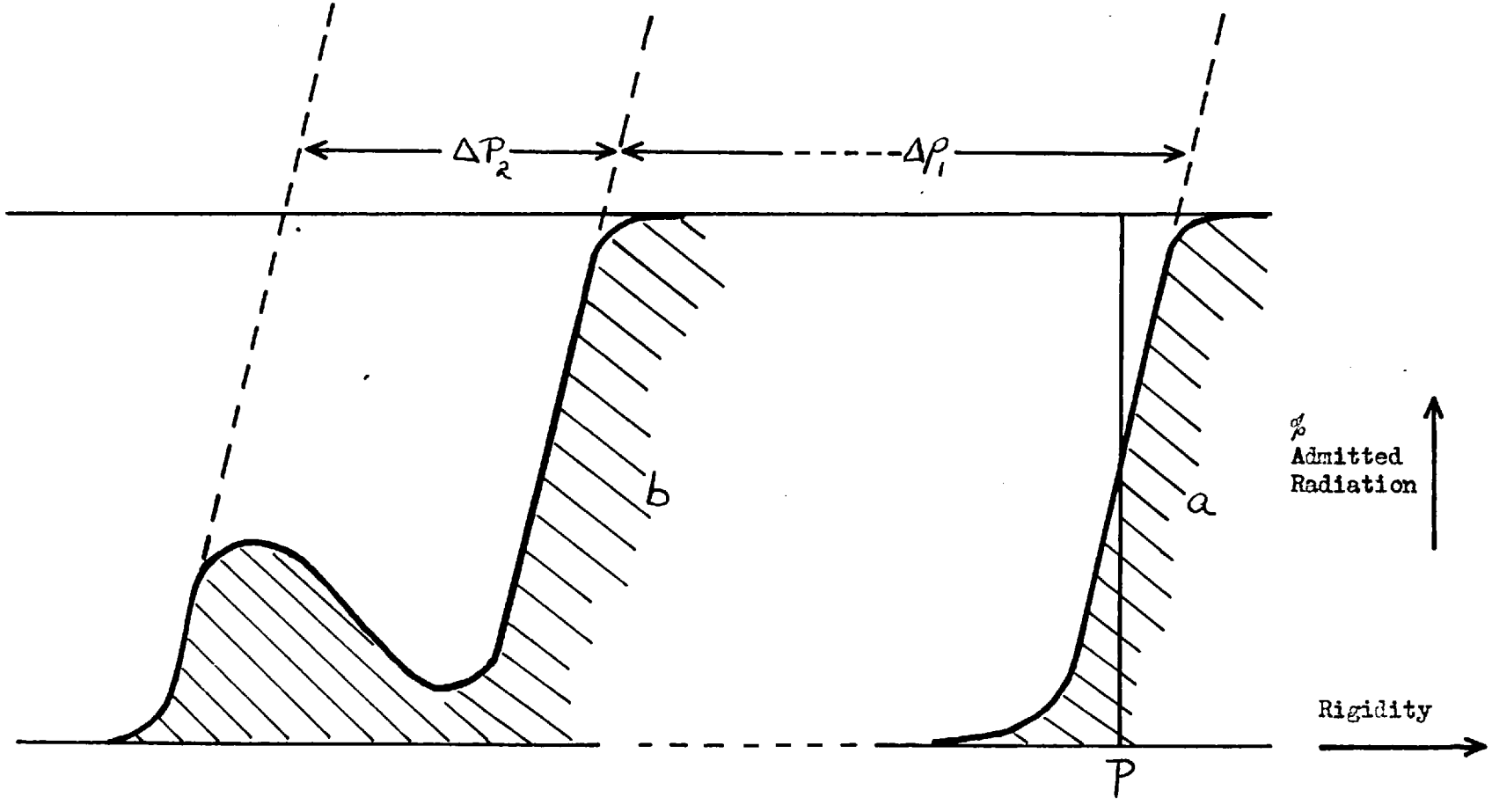

Fig. 8.5 METHOD OF MEASURENG THRESHOLD RIGIDITIES.

Main Cone Threshold = $p + \Delta p_1$

Stormer Cone Threshold = $p + \Delta p_1 + \Delta p_2$

p = Standardized Equatorial Threshold

Penumbral Width = Δp_2

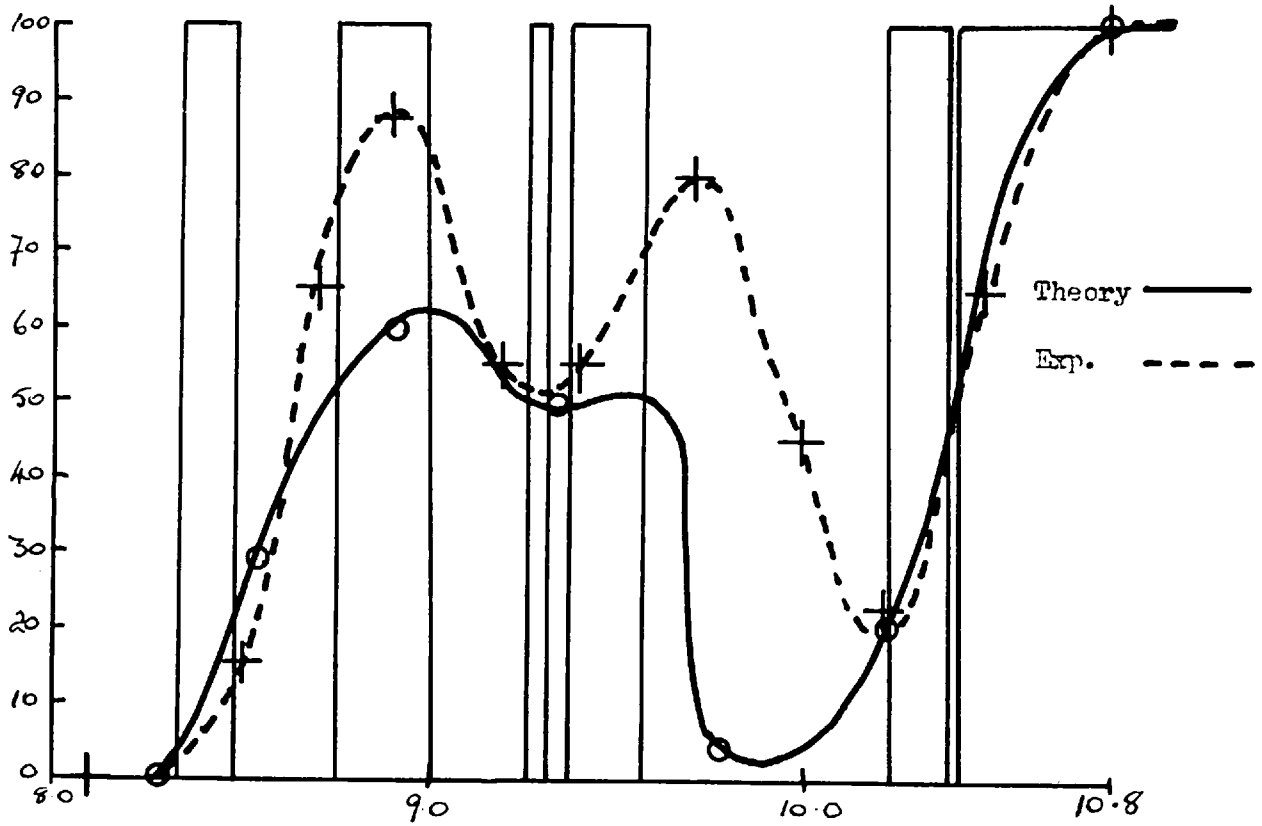

Fig. 8.6 AGREEMENT BETWEEN THRESHOLD RIGIDITY CURVE PREDICTED BY SCHWARTZ ASSUMING 0.4 GV AVERAGING INCREMENT.

these two thresholds is not easily found unless some estimate be made of the "averaging process". By this we mean, that if we were dealing with results obtained from an experiment in which the electron beam was mono-energetic and of an infinitely small solid angle, then these two thresholds would occur as step functions. In practice, the results are averaged over an effective rigidity range, and some estimate must be made of this range before the transparency of the penumbra may be obtained.

Use is therefore made of the results at latitude 30°, where our results overlap with the work of SCHWARTZ who presents his results as a series of completely allowed and completely forbidden bands between the main cone and the Stormer cone. By averaging the transparencies, therefore, over various arbitrary rigidity intervals a fair agreement should be obtained between the experimental curve and the curve obtained by this process. It is found that an interval of 0.4 GV gives a fair agreement, (see Table 8.6). If this interval is now assumed, reversing the aforementioned process will yield precise values for the width of the penumbra thereby allowing an estimate to be made of the penumbral contribution. Table 2 lists the values obtained together with the theoretically predicted values.

It should be mentioned that the shape of the threshold rigidities observed say, in the regions $\lambda = 15^{\circ}$ to $\lambda = 30^{\circ}$ were at first ascribed to the intersection of the electron beam with projections from the spherical surface of the terrella. A drastic change in the

TABLE 2.

Geomagnetic Latitude	Schwartz predicted Transparency	Observed Penumbral Transparency	Implied Threshold Correction
20°	0%	30 ± 8%	0.45 ± 0.15 GV
22°	0%	23 ± 6%	0.35 ± 0.10 GV
26°	1%	52 ± 14%	0.90 ± 0.30 GV
28°		56 ± 14%	1.10 ± 0.30 GV
30°	31%	50 ± 12%	1.00 ± 0.30 GV

configuration of the electron gun and also the monitoring of the current to the gun holder (Chapter 7) revealed that this was not the case.

The poor agreement of the transparency of the penumbra at some latitudes may be due to the penumbra being a sensitive function of zenith angle. For this reason it is likely that contributions from the electron beam that did not leave the terrella surface exactly vertically are responsible for modifying the vertical penumbral picture. Reference to the work of HUTNER (1939) does not support this view. Another possibility is that the path length of electrons in penumbral orbits was long compared with the m.f.p. It is estimated that the m.f.p. was at the worst $\sim 1000 \times r_e$, it is therefore difficult to explain the anomalous result on this basis. We shall consider the matter further in the following chapter.

8.3 The Effect of external Uniform Fields.

The centred dipole threshold rigidity measurements were terminated by an investigation of the effect of external uniform fields parallel to an antiparallel to the dipole axis. This investigation is interesting in the context of the magnetic storm modification of the threshold rigidities. Recently WEBBER & QUENBY (1961) have deduced the effect of likely external fields that may exist during such storms,

and OBAYASHI & HAKURA (1960) have calculated expressions for the change of threshold rigidities due to uniform external fields. They postulate some geocentric cavity in which this uniform magnetic field exists during the magnetic storm. We have mentioned the lowering of thresholds during the main phase of a magnetic storm in the chpater concerned with the effect of geomagnetism on intensity variations. In order to check qualitatively and quantitatively on these effects, the current through the vertical degaussing coils was reduced so that a unfiorm field given by:-

$$H = H_o - \frac{I}{I_d} \cdot H_o = H_o\left(1 - \frac{I}{I_d}\right)$$

was produced over the terrella where

H_o = vertical geomagnetic field

I = actual current through degaussing coils

I_d = current necessary for complete degaussing.

The equivalent external field over the earth was estimated by taking the ratio of the external field to the dipole moment of the terrella and equating to the ratio of an external interplanetary field to the dipole moment of the geomagnetic field. The change in threshold rigidity was estimated by measuring the shift from the threshold in the field free condition. The threshold rigidities were measured by the ratio method mentioned in Chapter 7. Each point on the threshold curve is the average of six readings. The accuracy was sufficient

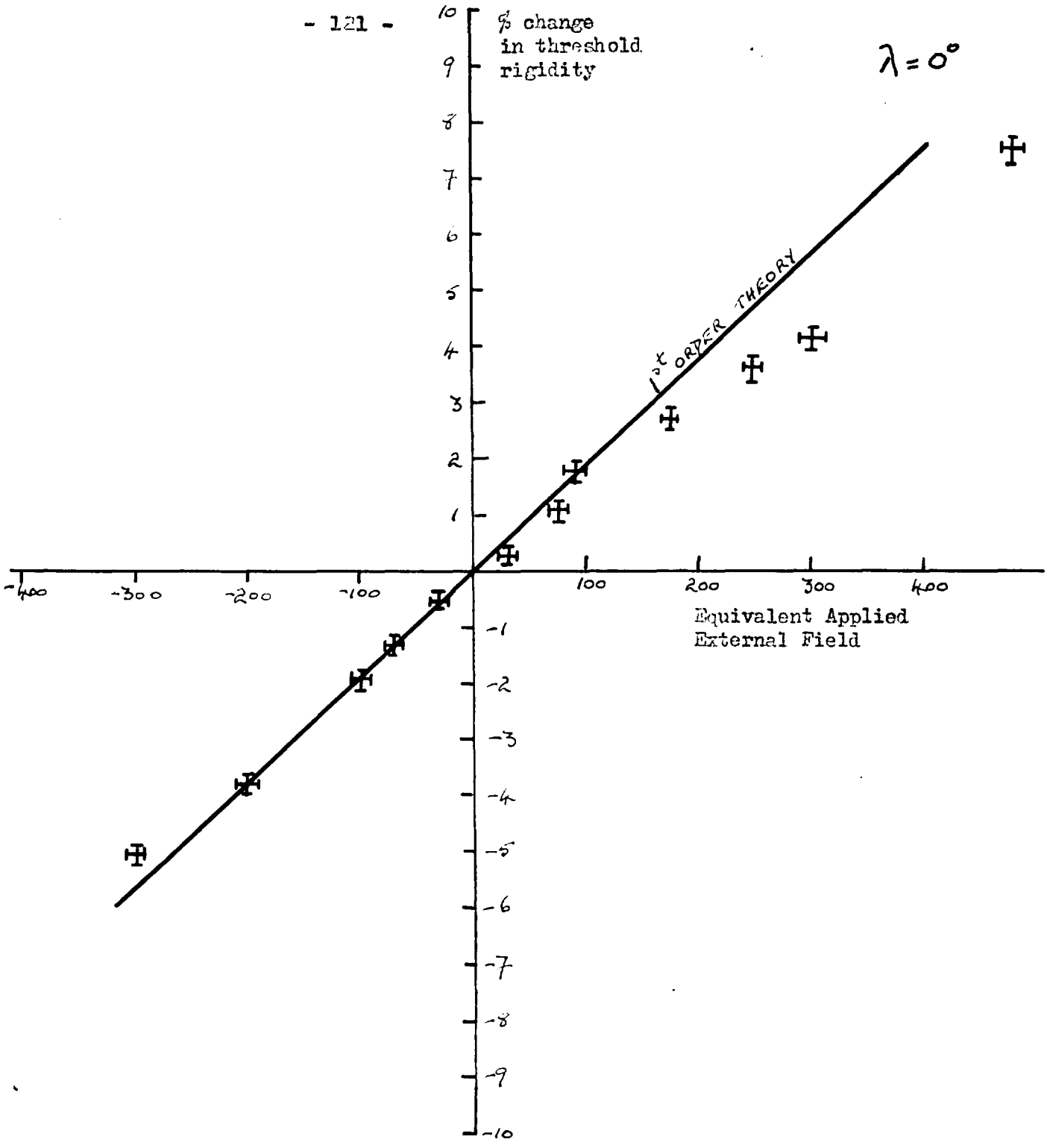

Fig. 8.7 EXPERIMENTAL POINTS OBTAINED FROM MODEL EXPERIMENT, USING A CENTRED DIPOLE TO REPRESENT THE GEOMAGNETIC FIELD. THEY SHOW THE CHANGE OF THRESHOLD RIGIDITY TO BE EXPECTED AT THE EQUATOR WHEN AN EXTERNAL UNIFORM FIELD IS APPLIED. THE SENSE OF THE EXTERNAL FIELD IS TAKEN TO BE POSITIVE WHEN IT IS THE SAME DIRECTION AS THE DIPOLE. THE STRAIGHT LINE PREDICTED BY THE FIRST ORDER THEORY IS PLOTTED FOR COMPARISON.

to detect the change in threshold rigidity of 0.3% due to an external field equivalent to 30γ in the terrestrial case. The agreement with the first order theory (Figure 8.7) is good up to equivalent fields of 200γ. The inclusion of higher order terms would improve the agreement between theory and practice. The relevant theory is developed in Appendix 3.

8.4 Measurements after the Inclusion of Regional Anomalies.

The regional anomalies were inserted without disturbing the zenith angle of the electron gun, since no easy way of aligning the gun vertically is possible when the field is not a centred dipole. The measurements began with a survey of the threshold rigidities along the geomagnetic equator. These were measured by varying the voltage on the electron gun. The deflection inside the electron gun was calculated to be much the same as in the centred dipole experiments despite the increase in the magnetic field over the gun. The magnetic deflection was in fact compensated by the use of higher electrode potentials. In evaluating the threshold rigidities the formula used was as before:-

$$P_{eq} = 198 \frac{r_m^2}{M_m} \sqrt{V} \quad GV.$$

the magnetic moment being replaced by that appropriate to the modified

field, this being $38.5 \pm 0.5 \times 10^3$ gauss cm^3. In order that the gun anode should coincide with the radius at which the field was measured, the radius was increased slightly to 10.02 ± 003 cms.

In order to check on the work of QUENBY & WEBBER on the computation of threshold rigidities in the geomagnetic field, the thresholds measured were compared with the thresholds predicted by calculations, obtained by the methods indicated by QUENBY and WEBBER for the terrella field. It was felt that this was a fairer test of the theory than to directly compare the terrella results with geomagnetic thresholds, since the terrella field only exhibits the gross features of the geomagnetic field. Nevertheless, any agreement between the measurements and the theory for the terrella field is certainly a measure of the reliability of the theory in predicting geomagnetic threshold rigidities. Before summarizing the findings on this subject, we shall deal with the method of calculating the threshold rigidities by the QUENBY-WEBBER method.

8.5 Method of Calculating Threshold Rigidities.

QUENBY and WEBBER derive the following expression for the threshold rigidity between geomagnetic latitudes $\pm 20^{\circ}$:-

$$P_m = \frac{M}{4r_e^2}\left(1 + 0.6\left(\frac{H_a - H_c}{H_c}\right)\right)\cos^4\lambda$$

where $\lambda = \tan^{-1}\left(\frac{\bar{V}}{2\bar{H}}\right)$

and $\bar{V} = V_c + 0.52\Delta V$

$\bar{H} = H_c + 0.52\Delta V$

H_a = actual horizontal field

H_c = horizontal field due to a centred dipole

V_c = vertical field due to a centred dipole

$\Delta H = H_a - H_c$

$\Delta V = V_a - V_c$

The constants 0.6 and 0.52 are worked out by taking weighted means of the contribution due to the various higher order terms. These constants are not necessarily applicable to the terrella field.

The determination of these constants requires an estimation of the contribution to the total field of each of the multipole terms. This is found from a spherical harmonic analysis of the magnetic field. The values of the geomagnetic field have been calculated by FINCH and LEATON (1957) for the 1955 epoch and are therefore readily available. In the terrella case, no simple appraoch is possible and the deduction of the contribution of each multipole term would require field measurements to be made at numerous points over the entire terrella, in addition to the undertaking of an extremely lengthy spherical harmonic analysis.

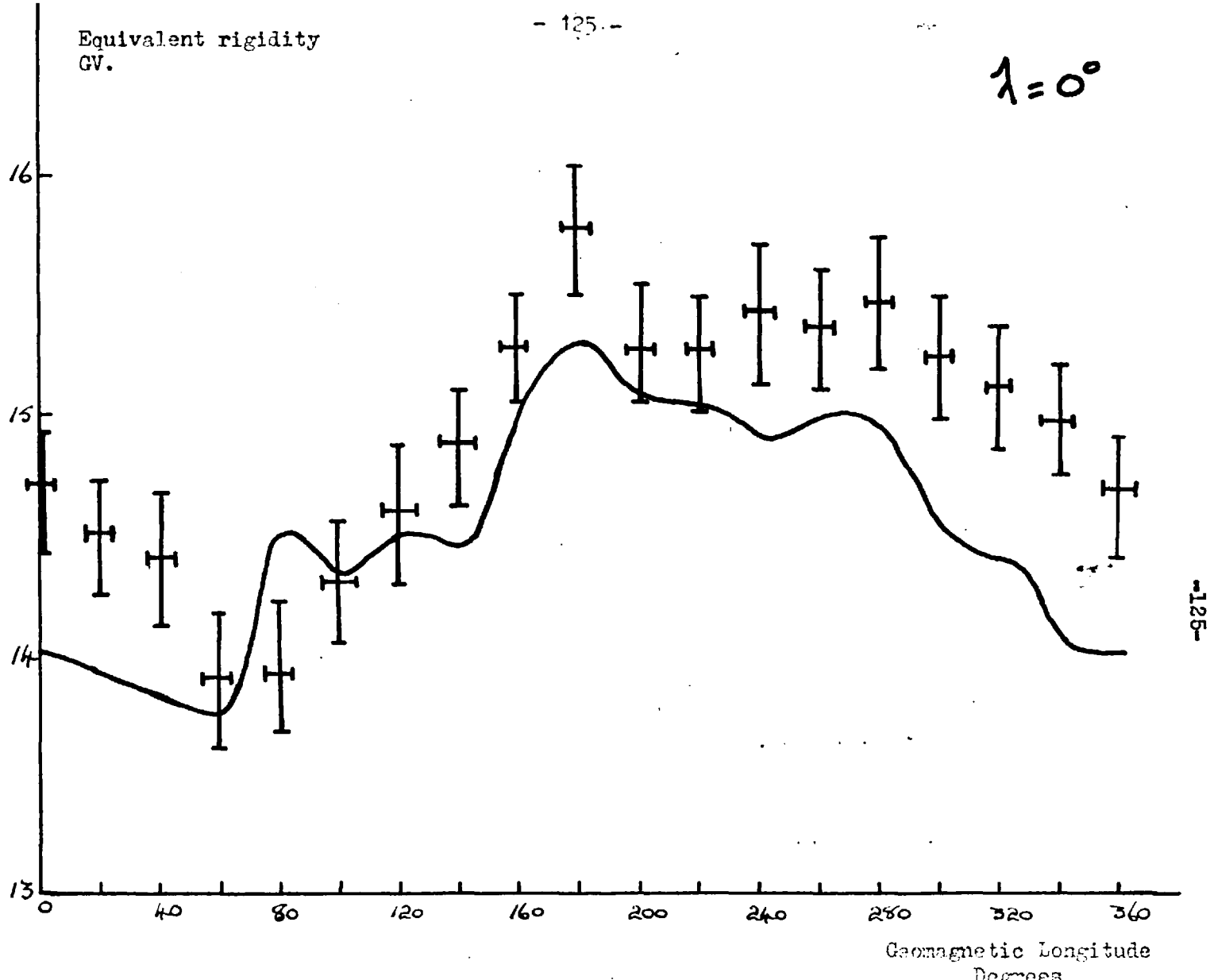

Fig. 8.8

CURVE SHOWS THE EXPECTED EQUIVALENT THRESHOLD RIGIDITIES PREDICTED BY "QUENBY-WEBBER" CALCULATIONS FOR THE TERRELLA APPROXIMATION TO THE GEOMAGNETIC FIELD. EXPERIMENTALLY FOUND VALUES ARE PLOTTED FOR COMPARISON. THE ERRORS IN THE PREDICTED THRESHOLDS PROBABLY AMOUNT TO ~ 0.5 GV. DUE TO INACCURACIES IN THE TERRELLA FIELD MEASUREMENTS AND THE ERRORS INHERENT IN THE THEORETICAL TREATMENT.

Having therefore adjusted the terrella field to reproduce the gross features of the geomagnetic field, the geomagnetic Quenby-Webber constants were straightforwardly used. A check was made by estimating the contribution of each multipole term by means of a limited Fourier analysis in regions where the field is mainly due to sectorial multipoles. In this region the analysis reduces to a Fourier analysis (cf. CHAPMAN & BARTELS, 1953). We estimate the errors in the above constant to be no more than $\sim 5\%$.

8.6 The Survey of Threshold Rigidities around the Geomagnetic Equator.

To return to the equatorial measurements Figure 8.8 shows the results of a survey of threshold rigidities at different longitudes along the geomagnetic equator. The errors on the experimental points are due to the probable error in estimating the shift of one threshold from a standard threshold (here taken as the highest threshold observed at 180° longitude). The values assigned to all the points may be somewhat high, since the theoretical curve is based on the centred dipole. equatorial threshold rigidity being 14.9 GV. In fact, this value, as we have noted, was found to be 15.4 GV, so that all the points should perhaps "come down" by 0.5 GV. Since we have no evidence of the systematic error in the dipole plus anomaly field the

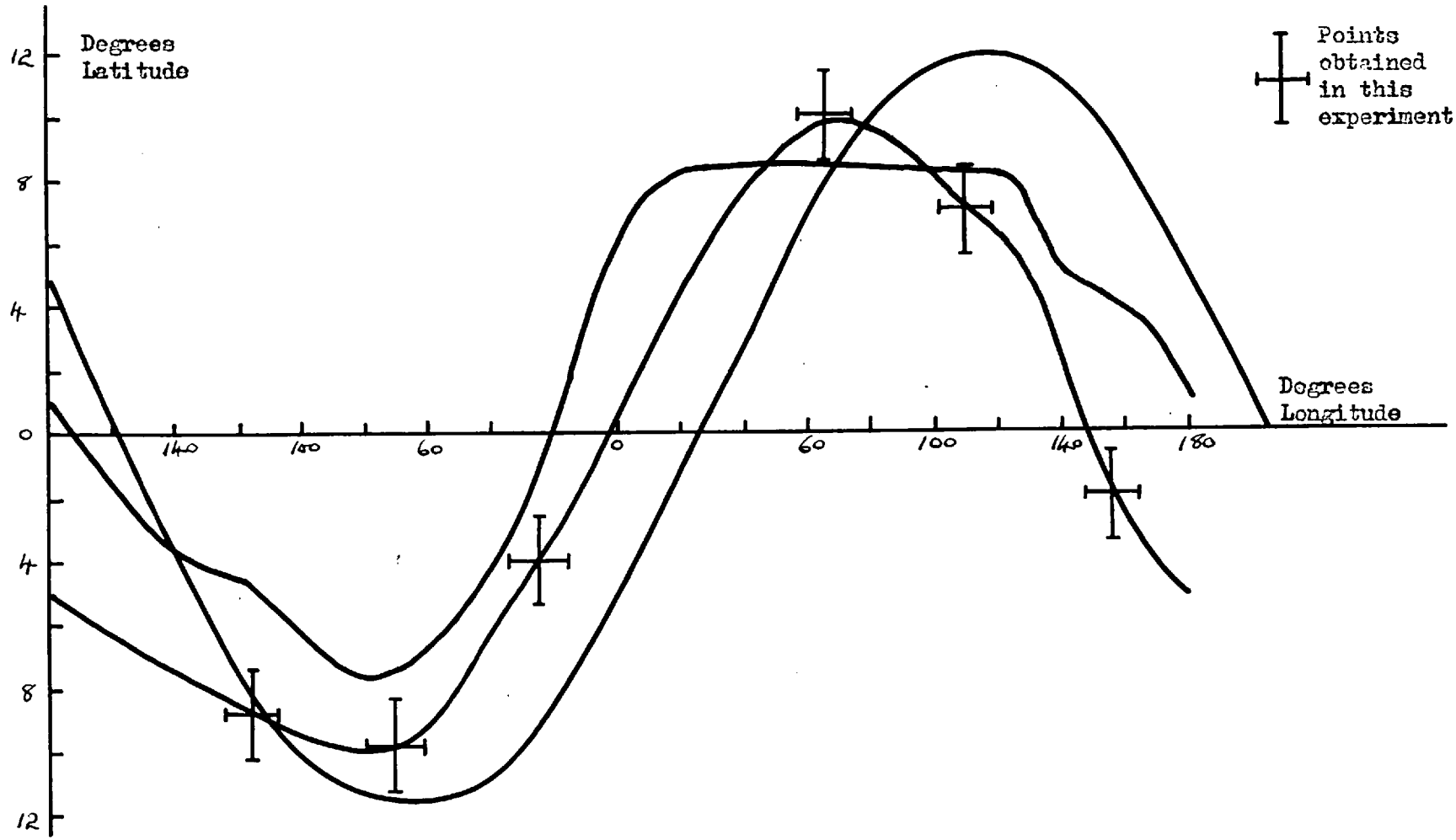

Fig. 8.9 COMPARISON OF TERRELLA "COSMIC RAY EQUATOR" WITH CENTRED DIPOLE AND OBSERVED DEPENDENCE.

theoretical curve is straightforwardly calculated on the basis of this value being 14.9 GV. The agreement is good, bearing in mind that the theoretical curve is probably in error by as much as 0.5 GV in some regions, due to errors in the measurement of the terrella field and errors inherent in the theoretical treatment. The r.m.s. deviation is 2.1%

8.7 The Measurement of the Cosmic Ray Equator.

This measurement is rendered difficult by the fact that not all latitudes of the terrella are accessible. This is because the terrella is mounted in such a way that it is effectively pivoted about an axis at right angles to the rack used for varying the latitude. The cosmic ray equator is found by latitude surveys at several longitudes, an estimate is made by interpolation of the latitude at which the maximum threshold rigidity occurs. Longitude surveys were carried out at six latitudes. The points are plotted in figure 8.9 For comparison the observed cosmic ray equator is plotted as well as the eccentric dipole equator. Also plotted is a curve through the predicted maximum threshold rigidities at the longitudes where the maximum thresholds were measured. The results of these measurements confirm that the 'phase shift' of the cosmic ray equator from the eccentric dipole equator can be accounted for by including the effects

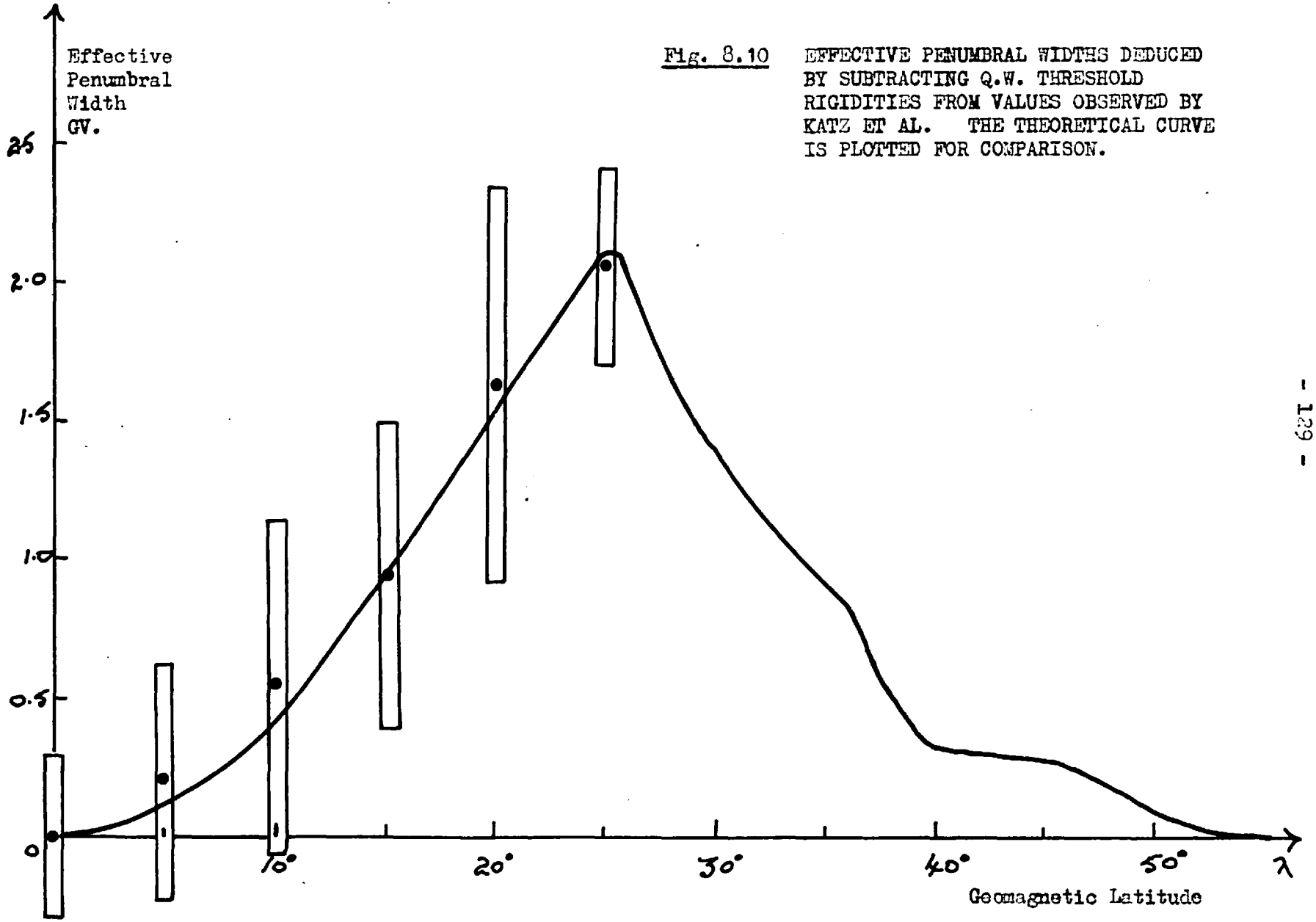

Fig. 8.10 EFFECTIVE PENUMBRAL WIDTHS DEDUCED BY SUBTRACTING Q.W. THRESHOLD RIGIDITIES FROM VALUES OBSERVED BY KATZ ET AL. THE THEORETICAL CURVE IS PLOTTED FOR COMPARISON.

of the higher order contributions to the internal geomagnetic field without recourse to hypothetical external field configurations as suggested by SIMPSON (1954). Moreover, these particular measurements indicate the extent to which the geomagnetic field has been matched by the terrella approximation.

8.8 The Effect of Non-Dipole Fields on the Penumbra.

The investigation of the effect of non-dipole terms in the terrella approximation to the geomagnetic field was of particular interest. In particular, an analysis by QUENBY & WENK (1961) of some results by KATZ, MEYER & SIMPSON (1958) from aeroplane flights in the region of the geomagnetic equator, indicate that the average behaviour of the penumbra is not significantly different from SCHWARTZ'S predicted values, but that there are large differences at individual points. Figure 8.10 illustrates this behaviour. The question arises as to whether these differences are due to the fact that the penumbral corrections are estimated by subtracting possibly incorrect 'Quenby-Webber' threshold rigidities from the observed threshold rigidities, or whether they are due to the use of penumbral corrections which are only appropriate to a centred dipole field.

In order to settle this question complete latitude surveys were first undertaken at longitudes 0° and 180° on the terrella. The

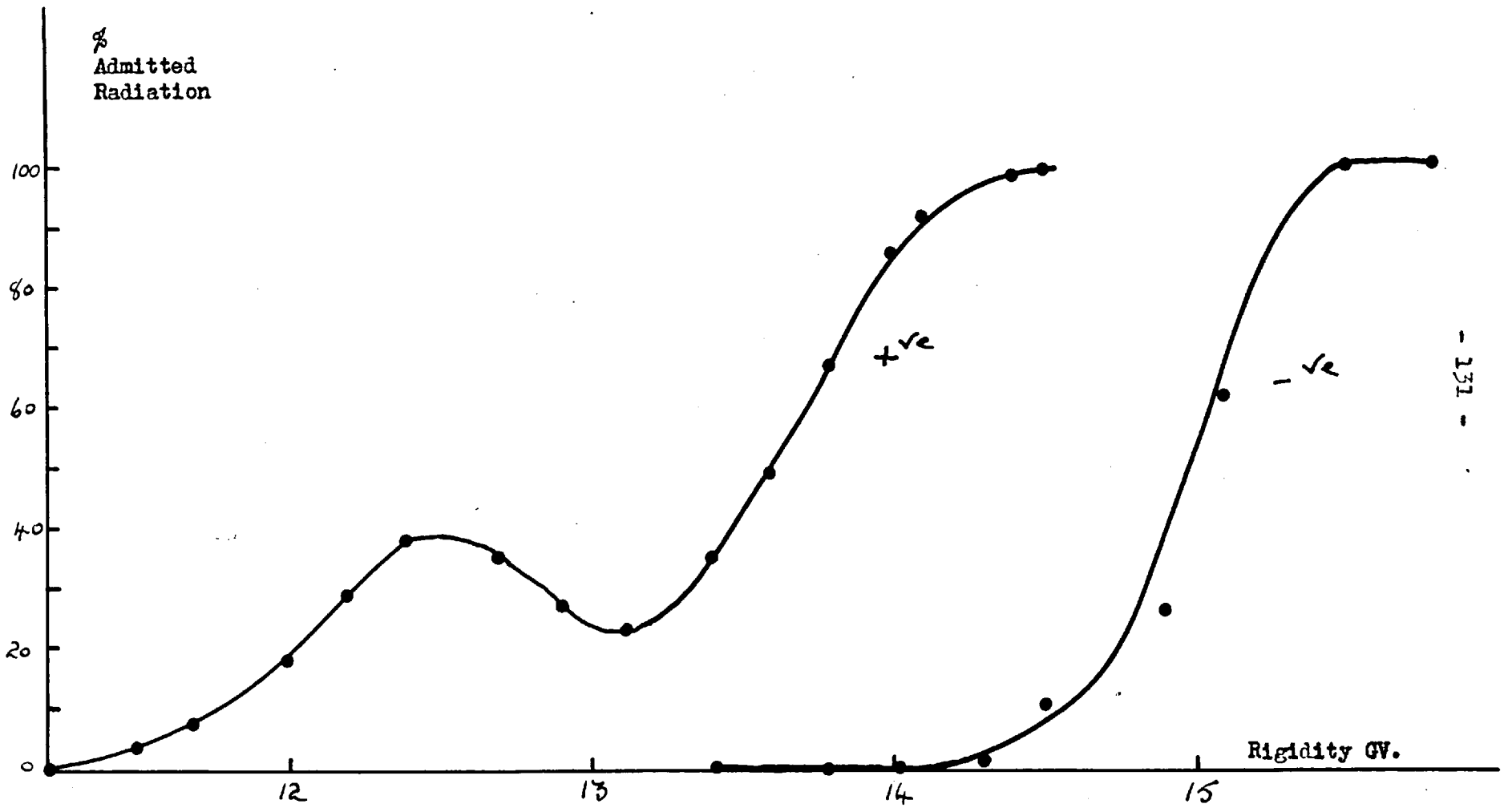

Fig. 8.11 THRESHOLD CURVES OBTAINED AT $\lambda = \pm 18^{\circ}$ AND 180° LONGITUDE, SHOWING HOW THE SHAPES ARE DEPENDENT ON THE VALUE OF THRESHOLD.

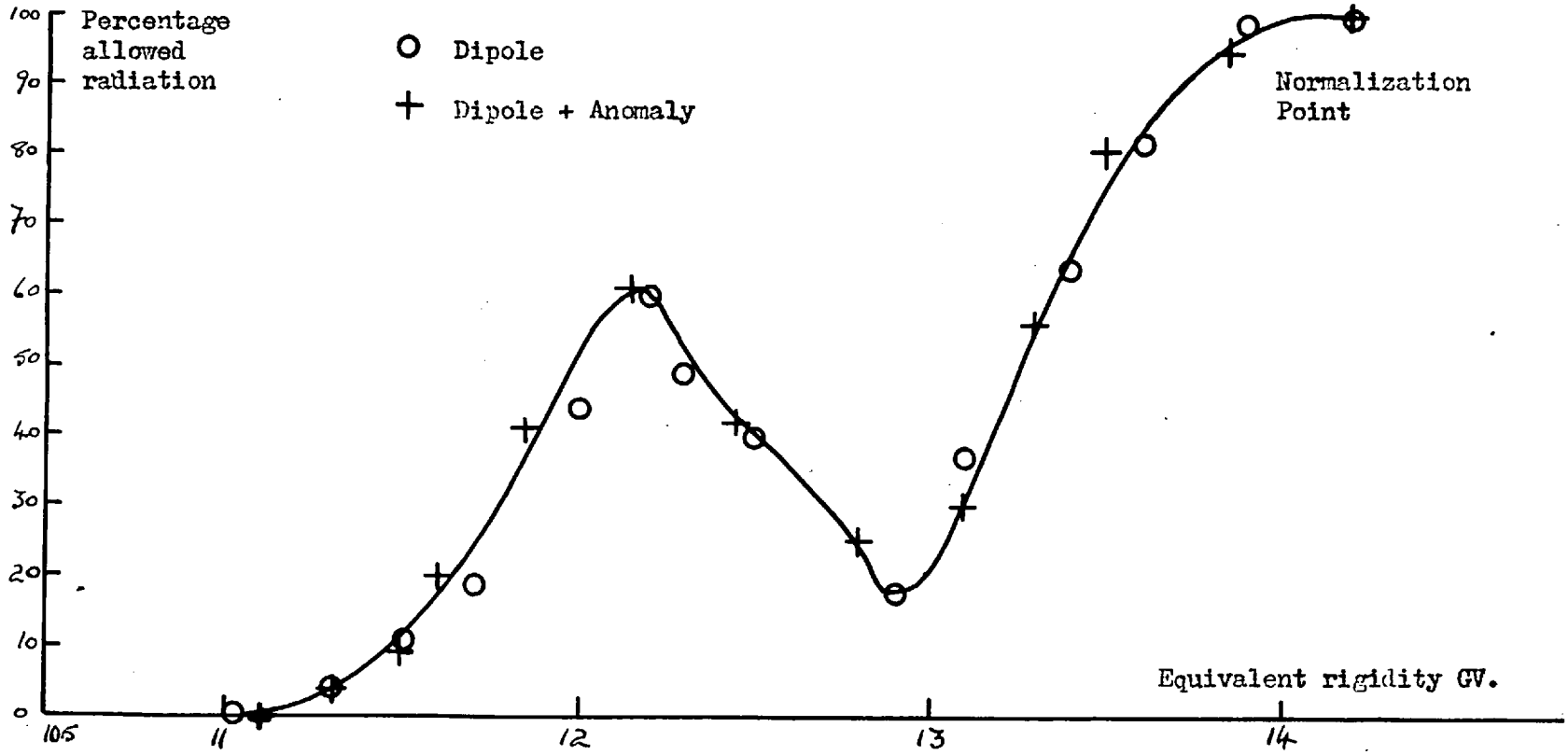

Fig. 8.12 AGREEMENT BETWEEN SHAPE OF PENUMBRA IN CENTRED DIPOLE AND DIPOLE + ANOMALY FIELD AT LATITUDE 22°.

threshold curves obtained with the centred dipole approximation were reproduced in detail. However, between latitudes 10° and 20°, curves were obtained that were previously obtained at other latitudes. For example, Figure 8.11 shows a curve obtained at $\lambda = \pm 18^{\circ}$; very similar curves were obtained at latitudes 0° and 20° in the centred dipole case.

Above 20° the agreement is very close to the centred dipole penumbra both in width, transparency and structure. Figure 8.12 shows curves obtained at $\lambda = 22^{\circ}$ and longitude 180°, for the centred dipole and the dipole plus anomaly field.

It was thought originally that the aforementioned behaviour was due to the fact that above 20°, the field at longitudes 0° and 180° did not deviate substantially from a centred dipole. For this reason, the investigation was repeated at other longitudes, in particular at those where there were strong regional anomalies in the $\lambda \sim 20^{\circ}$ region. The pattern was repeated. Figure 8.13 shows the agreement between the penumbral widths at $20^{\circ} < \lambda < 30^{\circ}$, each point being the average of readings taken at six longitudes, except at $\lambda = 28^{\circ}$, where they are the average of readings taken at four longitudes. The errors are estimated from the r.m.s. deviations from the means as well as the probable error in estimating the penumbra by the method of drawing tangents to the principle decreases.

A further investigation was undertaken in the region $10^{\circ} < \lambda < 20^{\circ}$

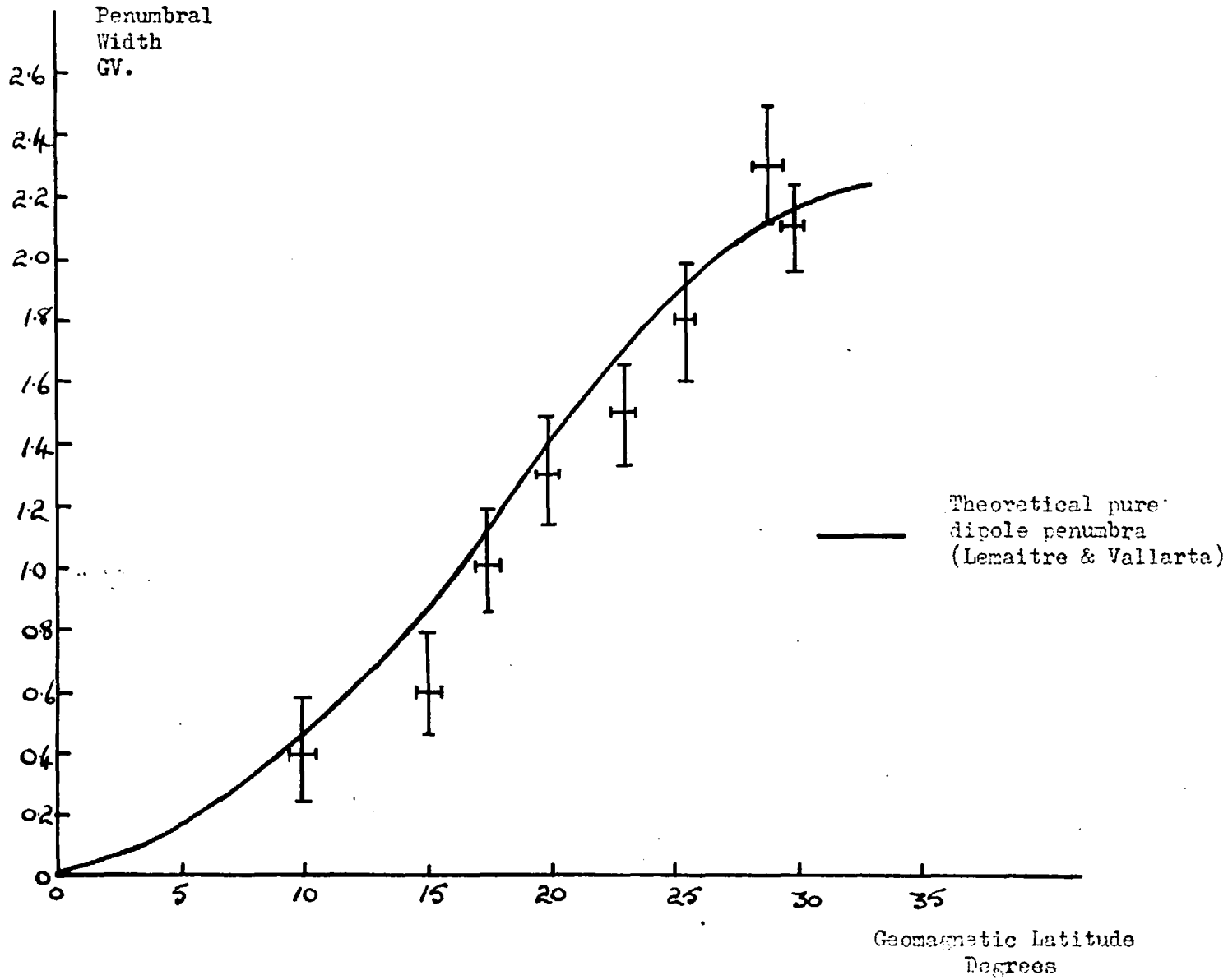

Fig. 8.13

THE PENUMBRAL WIDTHS OBSERVED IN THE MODEL EXPERIMENT APPROXIMATION TO THE GEOMAGNETIC FIELD. EACH POINT IS THE AVERAGE OF SEVERAL LONGITUDES. THE DEVIATION OF THE WIDTHS AT EACH LATITUDE DOES NOT EXCEED THE S.D. OF THE MEASUREMENTS EXCEPT AT LATITUDES BETWEEN $\lambda = 10^{\circ}$ AND $\lambda = 20^{\circ}$. POINTS IN THIS REGION ARE OBTAINED FROM REGIONS WHERE THE THRESHOLD IS NOT SIGNIFICANTLY DIFFERENT FROM THE CENTRED DIPOLE THRESHOLD RIGIDITY.

- 135 -

Fig. 8.14 PENUMBRAL WIDTHS OBSERVED IN THE CENTRED DIPOLE + ANOMALY FIELD AT $17\frac{1}{2}^{o}$ LATITUDE.

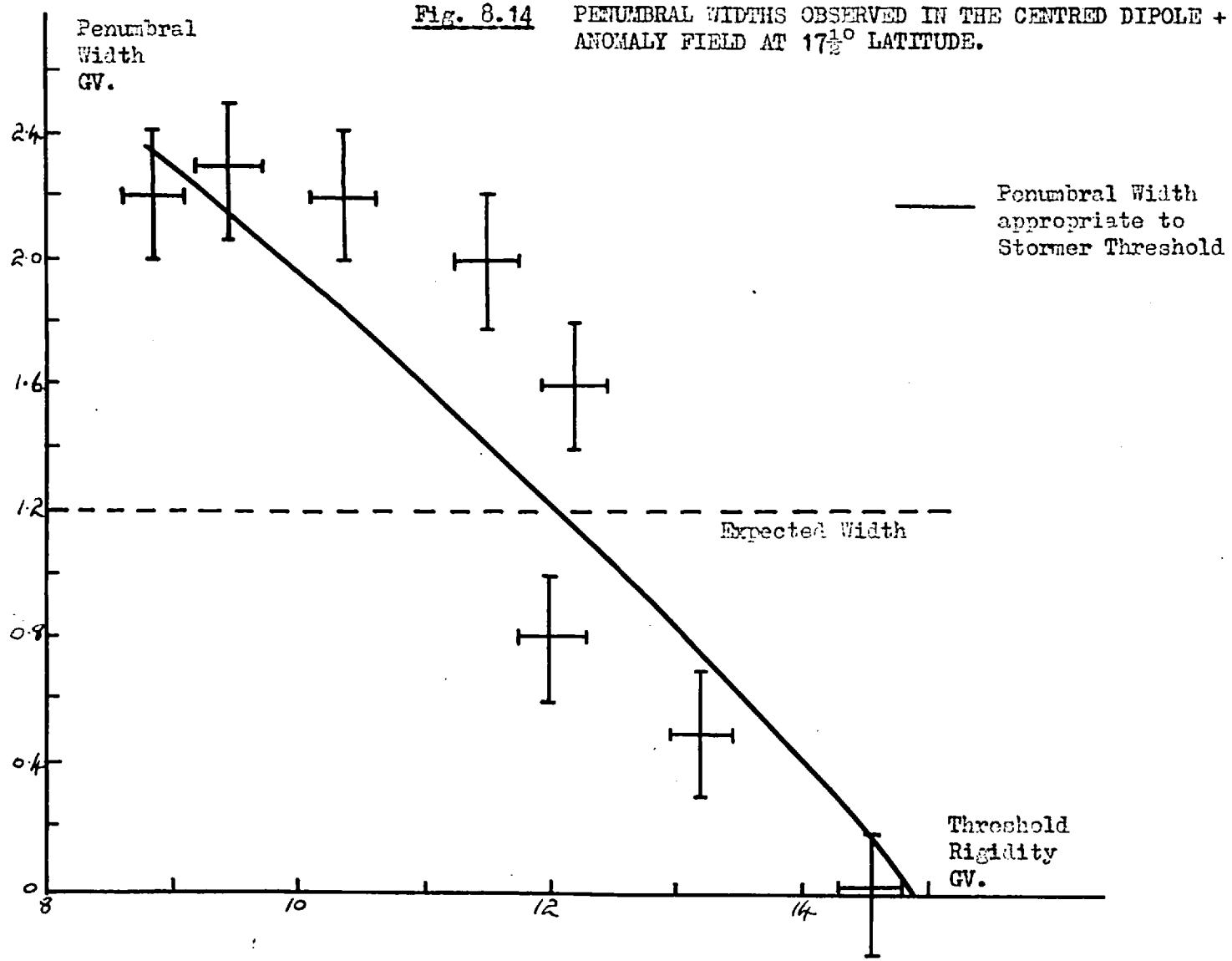

20°, in particular at $\lambda = 15^{\circ}$ and $\lambda = 17\frac{1}{2}^{\circ}$. In the latter case, the penumbra was investigated at eight points on the terrella. The width of penumbra was plotted as a function of 'Stormer' threshold rigidity in this case. Figure 8.14 shows the result of this investigation. If the penumbra were simply a function of geomagnetic latitude, as in the pure dipole case, then all the experimental points should have the same ordinate, quite clearly they differ over a wide range. However, the agreement is much better between a curve assuming that the penumbra is a function of the equivalent latitude λ' *. This function may be an over-simplification of the case, but probably affords a good second order approximation to the first order centred dipole penumbra.

The results of QUENBY & WENK are consistent with the results of these penumbral investigations, in that if we assume that there is no systematic deviation from the centred dipole penumbra and just assign errors big enough to account for the spread in widths observed, then the points obtained agree well with the diagram in Figure . Figure 8.15 shows this agreement. The following three points are relevant to the interpretation of figure 8.15 :-

* Where is given by $P = 14.9 \cos^{4}\lambda'$ GV, where P is the observed Stormer threshold rigidity. When P is above 14.9 GV is assumed to be 0°.

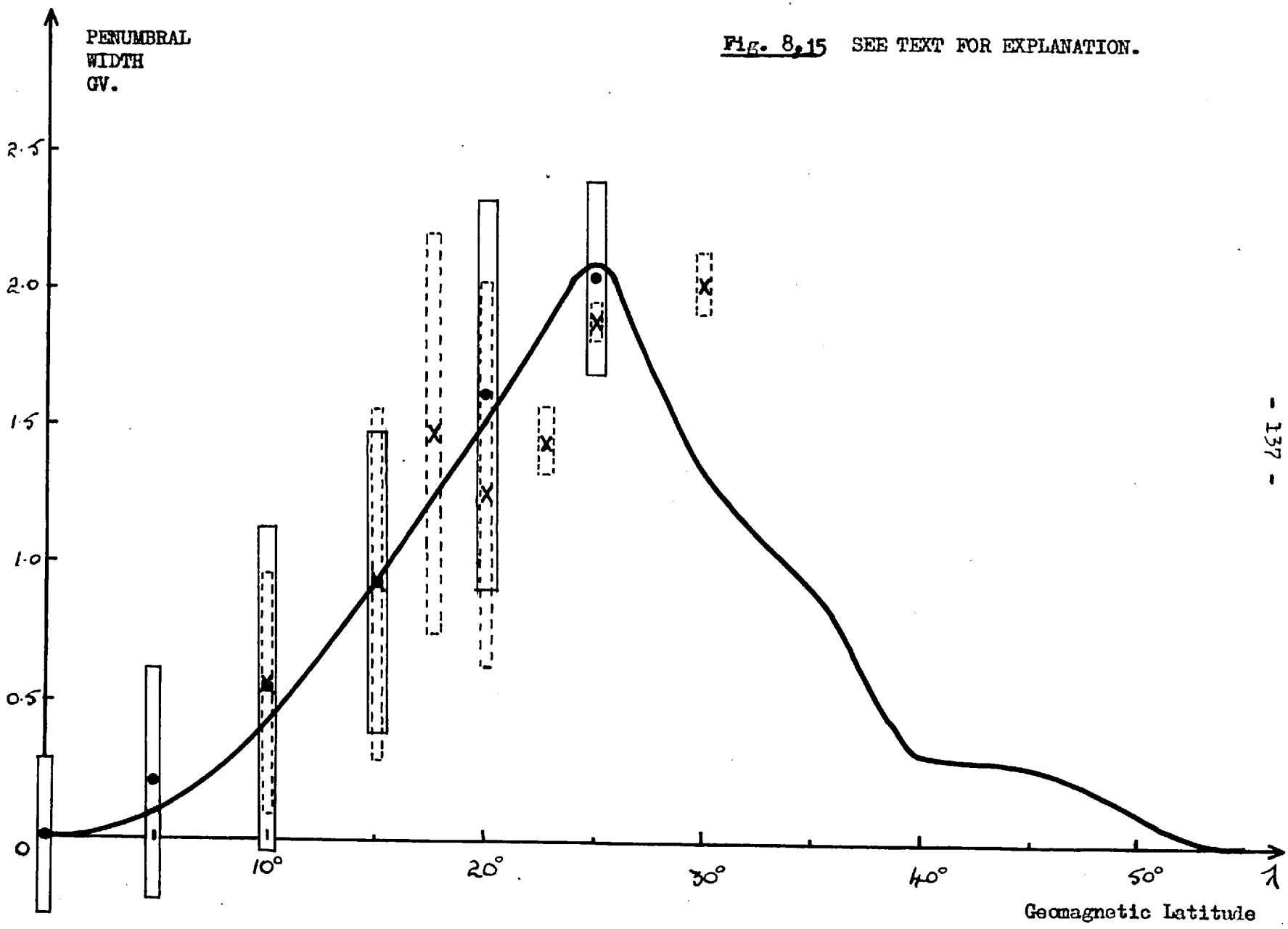

Fig. 8.15 SEE TEXT FOR EXPLANATION.

(1) In the theoretical curve (a) and the points obtained by subtracting 'Quenby-Webber' threshold rigidities from the observed threshold rigidities; both take into account the transparency of the penumbra, whereas our points are simply obtained by subtracting the 'Quenby-Webber' threshold rigidity from the main cone threshold rigidity. This fact is probably only important at $\lambda > 25^{\circ}$.

(2) The experimental point at $\lambda = 10^{\circ}$ is obtained by assuming the predicted Quenby-Webber terrella threshold rigidity is correct and subtracting this value from the observed threshold rigidity. The reason for this procedure is that the threshold rigidities in this region are all higher than predicted and therefore we assume that they are main cone thresholds with a completely 'black' penumbra. The other assumption being that, in this region, the Quenby-Webber thresholds are rather accurate.

(3) At $\lambda = 0^{\circ}$, we can make no estimate of the penumbra since its probable width is of the same order as the spread in the experimental threshold and the probable error in the threshold rigidity value.

We shall presently discuss the implications of figure 8.15 in the chapter dealing with the conclusions drawn from these experiments.

8.9 The Agreement between the Predicted Threshold Rigidities at Latitudes other than the Equator.

The Quenby-Webber approximation predicts threshold rigidities below 20° and above 40°. In these two regions the motion of charged particles can be easily envisaged and suitable approximations made. At latitudes between these limits, interpolation must be used to estimate the threshold rigidities. In the case of the terrella, information concerning the magnetic field above 30° was limited owing to experimental difficulties, and therefore theoretical threshold rigidities were estimated by using a weighted mean of the two expressions used to estimate threshold rigidities. More explicitly if

$$P = \frac{M}{4r_e^2} \cos^4 \bar{\lambda}$$

be the expression to be used at $\lambda > 40^{\circ}$ and

$$P = \frac{M}{4r_e^2} \left(1 + 0.6\left(\frac{H_a - H_c}{H_c}\right) \right) \cos^4 \bar{\lambda}$$

be the expression to be used at $\lambda < 20^{\circ}$ then at some latitude ψ where $20^{\circ} < \lambda < 40^{\circ}$ P is given by:-

$$P = \frac{40 - \psi}{20} \cdot \frac{M}{4r_e^2} \left(1 + 0.6\left(\frac{H_a - H_c}{H_c}\right)\right) \cos^4 \bar{\lambda} + \frac{\psi - 20}{20} \frac{M}{4r_e^2} \cos^4 \bar{\lambda}$$

In evaluating the values of the threshold rigidities found experimentally the procedure of measuring the shift from a standard threshold was adopted. In addition to the errors in determining threshold rigidities

enumerated earlier, it should be noted that an error of 10% at latitudes between 20° and 30° is anticipated by QUENBY (1958) for some predicted values in this region. Moreover this error is anticipated assuming that the geomagnetic field values are very accurate, whereas the terrella field values are subject to experimental errors of larger relative magnitude and moreover the number of field measurements is comparatively small. The agreement between the experimentally found values and the predicted values will therefore give a pessimistic view of the validity of predicting threshold rigidities in this way. Nevertheless any serious discrepancies should be apparent.

Apart from the equatorial surveys of threshold rigidities, 60 threshold rigidities were measured at other latitudes. For experimental convenience, the greater number were measured along longitudes 0° and 180°. In addition, however, threshold rigidity values were investigated in regions of high anomalies as well as at several equidistant longitudes in the range of latitudes $10^{\circ} < \lambda < 20^{\circ}$. This latter survey was made in conjunction with the previously mentioned investigation into the penumbra in this region.

Table 5 shows the r.m.s. deviations of the observed values from the predicted values at several ranges of latitude together with the estimated experimental r.m.s. deviations. It can be seen that the deviations increase as a function of latitude. A fairer picture of the situation is afforded by Figure 8.16 in which the predicted

TABLE 3.

Range of Geomagnetic Latitudes	No. of Threshold Measurements	r.m.s deviation from QW Threshold	Expected Experimental r.m.s. deviation
0°	18	2.1%	4%
$10^\circ \rightarrow 20^\circ$	15	9.8%	9%
$20^\circ \rightarrow 25^\circ$	16	14.8%	12%
$25^\circ \rightarrow 30^\circ$	12	17.6%	13%

Note: The expected experimental r.m.s. deviation also includes an estimate of the error due to the use of inappropriate weighting factors in the Q-W expressions.

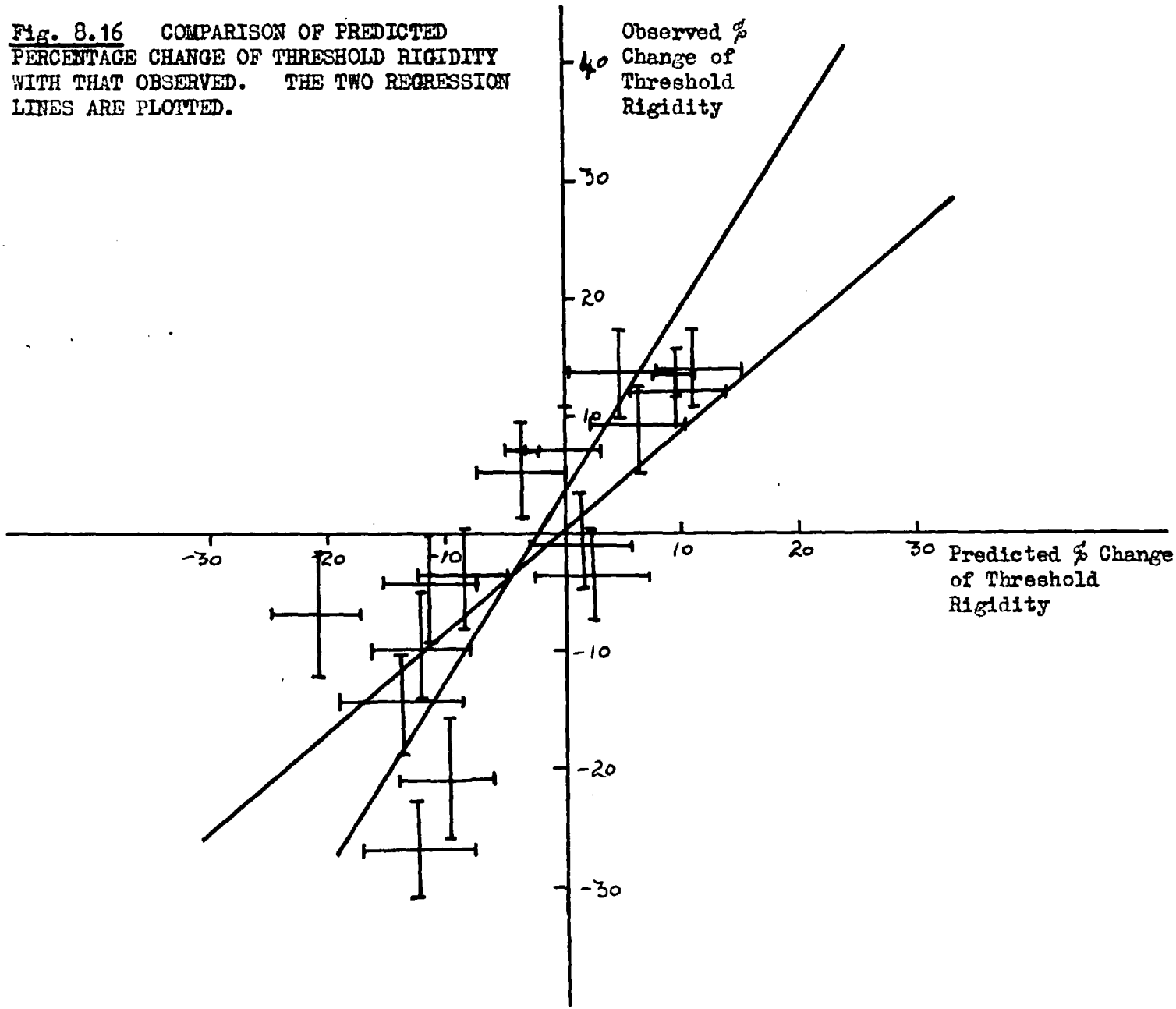

Fig. 8.16 COMPARISON OF PREDICTED PERCENTAGE CHANGE OF THRESHOLD RIGIDITY WITH THAT OBSERVED. THE TWO REGRESSION LINES ARE PLOTTED.

percentage deviations from the mean are plotted against the observed percentage deviations. The points should lie along a line y = x. The regression lines of y upon x and x upon y are plotted and their slopes are not significantly different from unity. The correlation coefficient indicates that the readings lie on the .01 significance level. At the risk of over-generalization, we suggest that the percentage errors are larger where the threshold rigidities deviate most from the centred dipole values. This one would intuitively expect to occur in a theoretical treatment which is based on a perturbation theory.

8.10 Effect of an External Uniform Field on the Perturbed Dipole Field.

Equatorial threshold rigidities were measured as a function of an external uniform field. Essentially this experiment was a repeat of the previous experiment using the centred dipole terrella field. The thresholds were measured on the equator of the terrella at longitudes where the field deviates the most from the dipole field. Fig. 8.7 shows the change in threshold rigidity was a similar function of external uniform field as in the centred dipole case although the scatter about the theoretical linear relationship is larger. The r.m.s. deviation of the experimental values from the predicted values

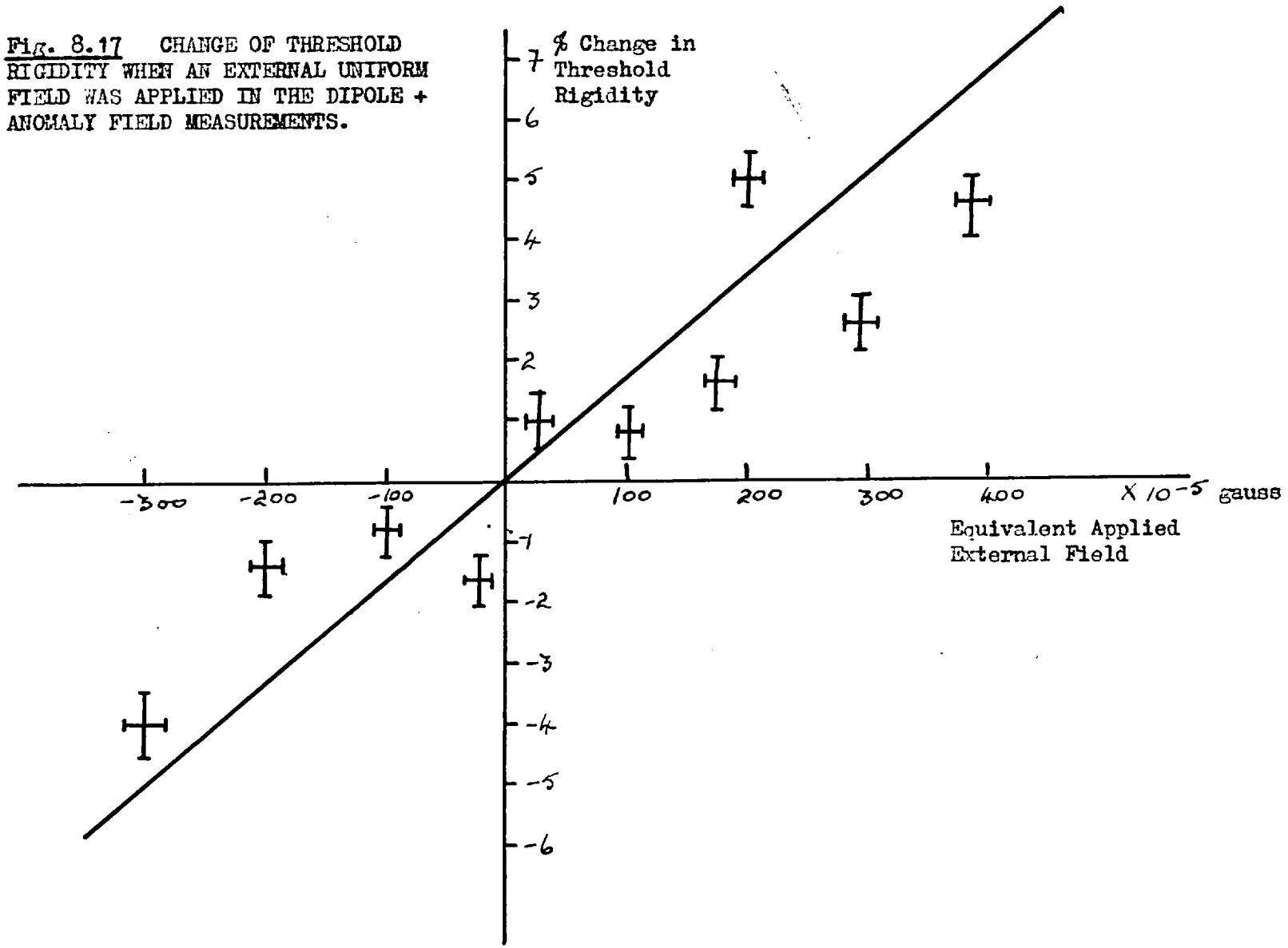

Fig. 8.17 CHANGE OF THRESHOLD RIGIDITY WHEN AN EXTERNAL UNIFORM FIELD WAS APPLIED IN THE DIPOLE + ANOMALY FIELD MEASUREMENTS.

-144-

of threshold shift is 21%. We are not able to account for this larger scatter as time limited the extent of this particular investigation.

CHAPTER 9. DISCUSSION OF THE RESULTS.

9.1 Introduction.

Whilst many points arising from this work have been discussed during the presentation of the results, there are some outstanding questions which require a more amplified discussion and which we shall deal with in this chapter.

9.2 The Transparency of the Penumbra.

Inspection of Table 2 (page 118) indicates some discrepancies in the neasured penumbral transparencies compared with those predicted theoretically. Whilst the causes of these discrepancies are no doubt rather complex, the following three possible causes will be considered. These are:-

(1) Scattering of the electrons executing penumbral orbits by residual gas molecules.

(2) The measured transparency is a mean over the solid angle of the electron beam and differs from the transparency appropriate to the vertical direction.

(3) Some penumbral orbits which would be blocked by the terrella surface, are not blocked because the gun anode does not coincide with the terrella surface.

The first possible origin of error necessitates an estimation of the path length of electrons executing penumbral orbits. By reference to the work of JUAREZ (1949) we estimate that this path length is unlikely to exceed a maximum value of about 100 terrella radii, the mean free path is at the worst $\sim$ 1000 x terrella radius. Severe scattering should therefore be negligible and we find difficulty in believing that scattering is a serious contributary factor to this anomolous result. Experimental confirmation of this view comes from the fact that a penumbral transparency measured at $\lambda = 20^{\circ}$ differed by less than 2% when the pressure was increased from $2 \pm 1 \times 10^{-6}$ mm. Hg to $9 \pm 1 \times 10^{-6}$ mm. Hg.

If the second possibility accounts for the severe difference between penumbral transparencies observed at $\lambda > 20^{\circ}$, it seems difficult to reconcile this fact with the fair agreement with SCHWARTZ'S results observed at $\lambda = 30^{\circ}$. It seems fair to assume that the penumbral transparencies observed with an electron beam of finite solid angle are values averaged over the beam and differ very little from the values appropriate to the vertical direction.

The investigation of the third possibility requires some knowledge of the features of penumbral orbits which intersect the earth. Such knowledge is not readily available since in general most workers who have dealt with this type of problem have been more interested in those orbits which form the shadow cone. Alternatively, authors like SCHWARTZ have not been interested in the topology of the orbits themselves but have simply programmed a computer to count the number of intersecting orbits.

Intuitively one would expect that the location of the electron gun (corresponding to a detector high above the earth in the real case) would lead to results that indicate a more transparent penumbra than if the electron gun anode coincided with the terrella surface. The main reason for this effect being that the earth (or terrella) subtends a smaller solid angle than it would do in the latter case.

KASPER (1960) comes to a similar conclusion. We have no evidence of how much the transparency is altered by this effect, but on the other hand it is difficult to believe that discrepancies at $\lambda \sim 20^{\circ}$ are entirely due to this cause for the following reasons:-

(i) The fact that the agreement is fair at $\lambda = 30^{\circ}$

(ii) The negligible effect on penumbral transparencies (cf. page 132) by higher order terms, which would be difficult to

understand if the intersecting penumbral orbits just grazed the surface of the terrella.

(iii) Some doubt on the part of the author concerning the validity of the transparencies calculated for the $\lambda \sim 20^{\circ}$ region. The latter reason is mentioned because all the evidence concerning penumbral transparencies at $\lambda = 20^{\circ}$ was derived by HUTNER (1939). Now one would perhaps expect the penumbral transparency to be a smoothly varying function of geomagnetic latitude. SCHWARTZ, using some results by HUTNER, indicates that the penumbral transparency suddenly changes from near zero to about 30% in the region $\lambda \sim 26^{\circ}$. Whilst holding reservations about the applicability of these results to the problem of geomagnetic effects at sea level, the results of these experiments are almost certainly applicable to the equivalent altitude of the electron gun. This equivalent height turns out to be $\sim$ 640 Km. which is a typical satellite altitude. Since a precise knowledge of geomagnetic effects is required for satellite cosmic ray experiments, the present results are therefore of particular relevance. It remains to be seen whether penumbral investigations now being planned by HEDGECOCK (1961), using a terrella assembly in which the gun anode coincides with the terrella surface, reveal a different set of penumbral transparencies.

9.3 The agreement between the values of Threshold Rigidities predicted by the Quenby-Webber method and the measured values.

It has been shown by several workers e.g. CARMICHAEL & STELJES (1961) that the Quenby-Webber treatment is very satisfactory for the evaluation of high latitude threshold rigidities. Quantitative checking in the region of $\lambda = 25^{\circ}$ has been hampered by an inadequate knowledge of the penumbral contribution to the threshold rigidity.

Inspection of Table 3 (page 141) indicates that, in general, threshold rigidities predicted for the terrella by the Quenby-Webber method lie within the limits of the expected experimental error. In the case of those values obtained in the range $25^{\circ} < \lambda < 30^{\circ}$, the values obtained are in error by slightly more than the estimated experimental error. Since the latter is itself probably in error by as much as 30% owing to uncertainties about weighting factors, deflections inside the electron gun etc., it is not justified to draw any definite conclusion from this result. Nevertheless if the estimated experimental error is accepted as realistic, the accuracy of threshold rigidities in this range is somewhat better than $\sim$ 10%; the latter value being estimated by QUENBY (1959) as typical in this region. Consideration of the approximations in the Quenby-Webber treatment suggests that this sort of error is not

unrealistic. Indeed, it is gratifying that the Quenby-Webber treatment is capable of such accuracy in this particular region where it is necessary to interpolate between threshold rigidities calculated by the method applicable to the equatorial band of latitudes and that applicable to high latitudes.

9.4 The Effect of Higher Order Terms on the Penumbra.

The result of investigations on this particular subject have been given in the previous chapter. One essential feature that has been demonstrated is that the centred dipole penumbra is not completely modified when the essential cylindrical symmetry of the centred dipole is removed. It therefore appears that the penumbra is a relatively stable phenomena.

The fact that the penumbra in the region $10^{o} < \lambda < 20^{o}$ is that appropriate to the equivalent latitude (see page 136) may be due to the fact that, here, penumbral orbits are confined close to the equatorial plane and therefore pass many times over regional anomolies.

Preliminary investigations by WENK (1961) indicate that, at present, this second order effect is of small consequence due to the uncertainties in the 'Stormer-type' threshold and in the penumbral corrections themselves.

9.5 Conclusion.

In this chapter we have only discussed some of the more important questions arising from this work. It is hoped, however, that the suitability of this type of analogue computer has been demonstrated.

There are many questions that remained unanswered on geomagnetic effects despite nearly half a century of work on this type of problem. It is clear that before such questions as why solar protons seem to arrive below their geomagnetic threshold, are answered, a much fuller understanding of how the huge geomagnetic spectrometer works is necessary.

Now that sophisticated apparatus may be placed at well defined positions in interplanetary space, the effects of geomagnetism must be well understood, before we can understand how the interplanetary and perhaps planetary magnetic fields govern the radiation that such apparatus will record.

ACKNOWLEDGEMENTS.

I am indebted to Professor P.M.S. Blackett for the privilege of working in his laboratories. I have been fortunate in working under the supervision of Professor H. Elliot at whose suggestion this work was carried out, and from whom I have received much help and encouragement.

I am grateful for many helpful suggestions from Dr. J.J. Quenby and particularly for much constructive criticism during the preparation of this thesis.

The successful working of the apparatus was made possible by the valuable assistance of my colleague Mr. P.C. Hedgecock.

I wish to thank the Misses A. Benton, J. Bradshaw, P. Cronk, C. Fogg and H. Keane, particularly for their practical assistance during the production of this thesis.

It is not possible to list everyone to whom I am indebted for assisting me in this work. I hope the omissions will be forgiven.

Finally, I wish to thank the Department of Scientific and Industrial Research for grants for my maintenance and for the construction of the apparatus.

REFERENCES.

Alfven H., 1950. Cosmical Electrodynamics. O.U.P.

Bailey, D.K., 1959, Proc. I.R.E., 47, 2, 255.

Bennett W.H. 1959, Rev. Sci. Inst. 30, 2.

Birkeland K. 1901. Vid. Selsk. Skr. Math. Nat.Kl. 1.
(In Norwegian, translation of some of text appears in Stormer's books on Polar Aurora)

Block, L. I.A.U. Symposium No. 6. Electromagnetic Phenomena in Cosmical Physics, 1958.

Bothe W. and Kolhorster W, 1929, Z.f. Physik, 56, 751.

Bozorth R.M. 1951, Ferromagnetism, Van Nostrand, London.

Brown W.E. and Sweer J.H. 1945. Rev. Sci. Inst., 16, 10, 276.

Bruche E., 1931. Terr. Mag. 36, no. 1., 41.

Brunberg, E.A. and Dattner A. 1953a, Tellus, 5, 135.

Brunberg E.A. and Dattner A. 1954, Tellus 6, 73.

Carmichael, H. and Steljes J.F. 1960, Proc. XII, General Assembly I.U.G.G., Helsinki.

Chapman S., and Bartels J. 1940. Geomagnetism O.U.P.

Chapman S. and Ferraro V.C.A., 1931, J. Terr. Mag. Atmos. and Elec., 36, 171

Clay J., 1928, Proc. Roy. Acad. Amsterdam, 30, 1115.

Cocconi G., Gold T., Greisen K., Hayakawa S. and Morrison, P. I.U.P.A.P C.R. conf. Varenna, 1957.

Cogger L.L., 1960. Atomic Energy of Canada Ltd. Rep.. CRGP - 965.

Craig H., 1947, Proc. Phys. Soc. 59, 804.

Danielson R.E. and Freier P.S., 1958. Phys. Rev. 109, 151.

Dushman S., 1947. Vacuum Technique, Chapman Hall, London.

Elliot, H., 1960., Phil. Mag. 5, 60.

Elliot H., Hynds R.J., Quenby J.J., and Wenk, G.J., 1959. Proc. I.U.P.A.P. conf. Moscow.

Fenton A.G., McCracken K.G., Rose, D.C., and Wilson B.G. 1959, Can. J. Phys., 37, 5, 569.

Finch H.P., and Leaton B.R., 1957, Mon. Not. Roy. Astronomical Soc., Geophys. Supp. 1, 1, 314.

Firor, J., 1954, Phys. Rev. 94, 1017.

Freier P.S., Ney, E.P., and Winkler J.R., 1959a. J. Geophys. Res. 64, 685.

Freon A., and McCracken K.G., 1961. (to be published).

Gall A., and Lifschitz J., 1956. Phys. Rev. 101.

Gill P.S., 1939. Phys. Rev. 55, 429.

Gold R., and Elliot H., 1957. "The Solar Cosmic Ray Outburst of 23 Feb., 1956. (unpublished)

Gregg J., 1947. Rev. Sci. Inst. 18, 2, 77.

Haas G.A., Jensen G.T., 1957., Rev. Sci. Inst. 28, No. 12.

Haynes S.K., and Wedding J.W., 1951. Rev. Sci. Inst. 22, .

Hedgecock P.C., 1961. Private Communications.

Hultqvist B., 1958. Arkiv. for Geofysik 3, 4.

Hutner R.A. 1939. Phys. Rev. 55, 15.

Hynds R.J., 1961. (to be published)

Johnson T.H. and Read D.N. 1937. Phys. Rev. 51, 557

Jory F.S. 1956, Phys. Rev. 102, 4, 1167.

Juarez A.R. 1949, Phys. Rev. 75, 1, 137.

Kasper J.E. 1959. Il Nuovo Cimento, Ser. 10. Supp. 11, No. 1.

Kasper J.E. 1960. J. Geophys. Res. 65, 1, 39.

Katz L., Meyer P., and Simpson J.A. 1958. Il Nuovo Cimento, 8, supp. II, 277.

Kellogg P. 1959. Il Nuovo Cimento, 13, 4.

Kellogg P. 1960. J. Geophys. Res. 65, 9, 2701.

Kitamura M. 1954. Ind. J. of Met. and Geophys. 5, 153.

Klemperer O. 1960. Private Communication.

Kodama M., Kondo I., and Wada M. 1957. J. Sci. Res. Inst., Japan, 51, 138.

Kodama M., and Miyazaki Y. 1957, Rep. of Ion. Res. in Japan, 11, 99.

Kondo I., Nagashima K., Yoshida L., and Wada M. 1960. Planet Space Sc. (in press)

Leck J.H., and Austin W.E., 1960. Electronic Engineering, Feb. 1960.

Lemaitre G. 1935. Ann. Soc. Sci. Bruxelles, 54, 162.

Lemaitre G., and Vallarta M.S. 1933. Phys. Rev. 43, 87.

Lemaitre G., and Vallarta M.S. 1936a. Phys. Rev. 49, 719.

Lemaitre, G., and Vallarta, M.S. 1936b. Phys. Rev. 50, 493.

McCracken, K.G. 1961. (to be published)

McDonald F.B. 1956, Phys. Rev., 104, 1723.

McDonald F.B., 1957, Phys Rev., 107, 1386.

McDonald, F.B., and Webber, W.R., 1960. Proc. 1st. Space Sci.

McNish, A.G., 1936. Terr. Mag., 41, 37.

McNish, A.G., 1940. Trans. American Geophys. Union, (1940), 287.

Malmfors, K.G. 1945. Arkiv. for Math o Fysik. 32A, 8.

Martyn, D.F. 1951, Nature, 167, 92.

Mathews, T., Thambyahpillai, T., and Webber, W.R., 1961, Monthly Notices of Royal Astronomical Soc. (in press).

Meyer, P., 1959. Phys. Rev., 115, 1734.

Millikan, R.A., and Neher, H.V., 1936. Phys. Rev., 50, 15.

Neher, H.V., 1952. Progress in C.R. Physics, Vol. I. North Holland Publishing Company, Amsterdam.

Obayashi, T., and Hakura, Y., 1960. J. Atm. and Terr. phys., 18, 101.

Pfotzer, G.P., 1956. Mitt. Max-Planet Inst. Phys. Stratosphere, No. 9, 13.

Quenby J.J., 1958. Ph.D. Thesis. University of London (unpublished)

Quenby, J.J., and Thambyahpillai, T., 1960. Phil. Mag., 5, 585.

Quenby, J.J., and Webber, W.R., 1959. Phil. Mag., 4, 90.

Quenby, J.J., and Wenk, G.J., 1961. (unpublished).

Quenby, J.J., and Wenk, G.J., 1961. I.U.P.A.P. conference, Kyoto.

Ray, E.C., 1956. Phys. Rev., 101, 3, 1142.

Reid, G.C., and Leinbach H., 1959. J. Geophys. Res. 64, 1801.

Rose D.C., Fenton A.G., Katzman J., and Simpson J.A., 1956, Can. J. Phys., 34, 968.

Rothwell P., 1958, Phil. Mag., Ser. 8, 3, 961.

Rothwell P., and Quenby J.J. 1958, Il Nuovo Cimento, Supp. 8, 249.

Sandstrom A.E. 1958. Il Nuovo Cimento, 8, Supp. 2, 263.

Sarabhai V., 1956, Ann. Rev. Nucl Sci. 6, 1.

Schluter A. 1958, Il Nuovo Cimento, 8, Supp. II, 263.

Schmidt A. 1934, Beit. Angew. Geophys. 41, 346.

Schremp E.J., 1938. Phys. Rev. 54, 158.

Schwartz M. 1959. Il Nuovo Cimento, Ser. 10, Supp. 11, No. 1.

Sekido Y., and Yoshida S. 1950., Rept. on Ions. Res. in Japan, 4, 37.

Simpson J.A. 1954. Phys. Rev. 94, 426.

Simpson J.A., Fenton K.B., Katzman J., and Rose D.C. 1956. Phys. Rev. 102, 1648.

Skobelzyn D. 1929. Z.f. Physik, 54, 686.

Sonnet C.P., Smith E.J., Judge P.H., and Coleman P.J., 1960. J. Geophys. Res. 65, 1331.

Steljes J.F., Carmichael H., and McCracken K.G. 1961, J. Geophys. Res. 66, 5.

Storey J.R., 1959. Phys. Rev. 113, 297 and 302.

Storner C. 1955. Polar Aurora. O.U.P.

Thambyahpillai T., and Elliot H. 1953. Nature, 171, 918.

Treiman S.B. 1953. Phys. Rev. 89, 130.

Vallarta M.S. 1935, Phys. Rev. 47, 647.

Vallarta M.S. 1961, Handbuch der Physik, 46, 1, Springer-Verlag.

Vallarta M.S., Gall R., and Liftschitz J. 1958, Phys. Rev. 109, 1403.

van Heerden I.J., and Thambyahpillai T., 1955., Phil. Mag. 7, 46, 1238.

Villard M.P., 1906, Ann. de Chimie et de Physique, 8 series, 9.

Waddington C.J., 1956, Il Nuovo Cimento, X, 3, 930.

Webber W.R. 1961. Progress in Cosmic Ray Physics, No. 6, North Holland Publishing Co. (in press)

Webber W.R., and Quenby J.J. 1961, Progress in Cosmic Ray Physics, No. 6. North Holland Publishing Co. (in press).

Wenk G.J. 1961. Private Communications.

Wilson B.G., Rose D.C., and Pomerantz M.A. 1960. Can. J. Phys., 38, 328.

Winkler J.R. 1960. J. Geophys. Res. 65, 1331.

Winkler J.R., and Anderson K.A. 1954. Phys. Rev. 93, 596.

Winkler J.R., and Bhavsar P.D. 1960. J. Geophys. Res. 65, 2637.

Winkler J.R., Bhavsar P.D., and Peterson L. 1961. J. Geophys. Res. 66.

APPENDIX 1

THE GEOMAGNETIC FIELD.

The mathematical analysis of the earth's field was first undertaken by GAUSS. He assumed that if the field is not generated by magnetic matter near the ground or currents from the atmosphere to the ground then the field must possess a potential function which satisfies LAPLACE'S equation.

This potential function must therefore be expressible in terms of spherical harmonics. A convenient representation was suggested by SCHMIDT (1934), in which if V be the potential function then V is given by:-

$$V = \sum_{n=1}^{\infty} V_n$$

where

$$V_n = r_e \left(\frac{r_e}{r}\right)^{n+1} T_n$$

where r is the distance from the centre of the earth and r_e is the radius of the earth and

$$T_n = \sum_{m=0}^{n} \left(g_n^m \cos mw + h_n^m \sin m w\right) P_n^m(\theta)$$

g_n^m and h_n^m are known as the gauss coefficients.

w is the geographic longitude and

θ is the geographic colatitude.

The coefficients g_n^m and h_n^m are determined from measurements made at many points. Their values are found by minimizing the differences between the field measurements and grad V.

It is found that most of the field ($\sim$80% at $r = r_e$) is represented by the n = 1 terms. These terms describe a field due to a magnetic dipole situated at the centre of the earth and tilted with respect to the polar axis. The position of tilt is such that the geomagnetic axis intersects the earth's surface at two antipodal points, approximately at 79°S 111°E and 79°N 69°W in the southern and northern hemispheres respectively. These positions are subject to a secular variation.

The dipole component has a moment of 8.1×10^{25} gauss cm^3.

The axis of the centred dipole defines a set of spherical coordinates. These geomagnetic coordinates are extremely useful in cosmic ray work as they allow a rough estimate of the threshold rigidity to be made using the equation

$$P = 14.9 \cos^4 \bar{\lambda} \text{ GV}$$

$\bar{\lambda}$ being the geomagnetic latitude.

McNISH (1936) has prepared nomographs from which can be easily found for any point on the earth.

The second order terms describe a set of quadrapoles of different configuration and orientation. There are five quadrapole terms in all. It is found that three of them tend to zero, if the magnetic centre of the earth is slightly displaced from the geomagnetic

centre. This displacement amounts to 0.054 r_e or 340 Km towards the position 6.5° north, 161.8° east. (These coordinates being geographic).

The remaining two quadrapole and higher order terms describe the residual fields which reside in the regional anomalies. These regional anomalies are large scale deformations in the geomagnetic field and are not to be confused with local anomalies which are attributable to deposits of iron ore etc.

The relative importance of the various order terms are shown in table 4 (reproduced from the paper by QUENBY & WEBBER, 1959).

TABLE 4.

Distance	V_2	V_3	V_4	V_5	V_6		ΣV_n
1.0 r_e	10.4	5.9	2.8	0.9	0.4	n =1	20.4
1.2 r_e	8.7	4.1	1.6	0.4	0.2		15.0
1.5 r_e	6.8	2.6	0.8	0.2	0.1		10.5
2.0 r_e	5.2	1.5	0.3	0.1	0.1		7.0
3.0 r_e	3.5	0.7	0.1	0.1	0.1		4.2

In addition to the geomagnetic field of internal origin there are fields of external origin which are particularly evident during magnetic storms. The 'quiet-time' large scale external field (as opposed to local external fields due to electrojets and ionospheric currents) is still partly a matter of conjecture.

Pioneer V results indicate fields of the order of 10^{-5} to 10^{-6} gauss at large distances from the earth ($\sim 5r_e$). Recent measurements by Explorer X indicate that these fields may be greater by a factor of ten or so. No attempt was made to permanently incorporate fields of this kind in this experiment.

APPENDIX 2.

THE WINDING OF A COIL TO PRODUCE A DIPOLE FIELD.

We here reproduce the theory relevant to the winding of the terrella coil. A dipole field is reproduced if the current flowing over a spherical surface has a particular configuration. This configuration is deduced as follows:-

If j be the surface current density, and H_o be the magnetic field outside, and H_i the field inside, then the normal component of H must be continuous through the spherical surface i.e.

$$\underline{r} \cdot \underline{H}_o = \underline{r} \cdot \underline{H}_i \qquad (1)$$

where r is the radius of the sphere and r a unit radial vector and the tangential component must suffer a discontinuity equal in magnitude to the current density i.e.

$$\hat{\underline{r}} \wedge (\underline{H}_o - \underline{H}_i) = \underline{j} \qquad (2)$$

Now if we require H_o to be of a dipole character

$$\hat{\underline{r}} \cdot \underline{H}_o = \frac{2m \sin \lambda}{4\pi r^3} \quad \text{- 'vertical component} \qquad (3)$$

and

$$\left| \underline{r} \wedge \underline{H}_o \right| = \frac{2m \cos \lambda}{4\pi r^3} \quad \text{- 'horizontal component} \qquad (4)$$

λ being the geomagnetic latitude and M the magnetic moment.

Combining equations (1) and (3)

$$\hat{\underline{r}} \cdot \underline{H}_i = \frac{2m \sin \lambda}{4\pi r^3} \qquad (5)$$

and combining equations (2) and (4)

$$\underline{r} \wedge \underline{H}_i \hat{\underline{\phi}} = \frac{m \cos \lambda}{4 \pi r^3} \hat{\underline{\Phi}} - \underline{j} \qquad (6)$$

If now we multiply equation (5) by ~~sin~~ cos λ and a unit vector $\hat{\underline{\Phi}}$ in the direction of $\underline{r} \wedge \underline{H}_o$ and equation (6) by 2 ~~cos~~ sin λ and subtract the resultant equations from each other, we obtain

$$\hat{\underline{r}} \cdot H_i \cos \lambda \hat{\underline{\Phi}} - 2 \hat{\underline{r}} \wedge \underline{H}_i \sin \lambda \hat{\underline{\phi}} = 2 \underline{j} \sin \lambda \qquad (7)$$

If H_i is assumed to be uniform and equal to $\frac{2m}{4\pi r^3}$ as it would be within a unfformly magnetised sphere. Then:

$$\underline{j} = \frac{3m}{4 \pi r^3} \cos \lambda \hat{\underline{\Phi}} \qquad (8)$$

It will be seen therefore that the current flows in circles of latitude and varies as the cosine of the latitude. Whilst we have not specified the thickness of the current sheet it is clear that the superposition of several spherical current sheets will also produce a dipole field.

In order to estimate the number of segments required in the terrella coil (see Figure 5.1), the following procedure was adopted. Suppose due to the construction of the coil the current density at a latitude λ, is that appropriate to another latitude λ, substitution of equation (8) into equation (2) and evaluation of $\hat{\underline{r}} \wedge \underline{H}$. yields the following equation:-

$$\left| \hat{\underline{r}} \wedge \underline{H}_o \right| = \frac{3m \cos \lambda^1}{4 \pi r^3} - H_i \cos \lambda = H_{o\ horizontal} \qquad (9)$$

substituting $H_i = \dfrac{2m}{4\pi r^3}$

$$H_o = \frac{3m \cos \lambda^1}{4\pi r^3} - \frac{2m \cos \lambda}{4\pi r^3}$$

Now the horizontal field at should be

$$H_\lambda = \frac{m \cos \lambda}{4\pi r^3}$$

The difference $H_o - H = \Delta H$ is given by:-

$$\Delta H = \frac{3m \cos \lambda^1}{4\pi r^3} - \frac{3m \cos \lambda}{4\pi r^3}$$

rearranging

$$\Delta H = \frac{3m (\cos \lambda^1 - \cos \lambda)}{4\pi r^3} \simeq \frac{6m \sin \lambda \Delta \lambda}{4\pi r^3} \qquad (10)$$

Equation 10 therefore indicates the error to be expected in the field if the current density at a latitude is in error so that it is that appropriate to another latitude $\lambda = \lambda + \Delta \lambda$

This equation allows one to compute how many segments are required on the terrella design shown in Figure 5.1 (Page 65) if a maximum value is placed on the percentage error:-

$$\frac{\Delta H}{H_\lambda} \times 100 \simeq 600 \tan \lambda \Delta \lambda \qquad (11)$$

APPENDIX III.

An Approximate Theory of the Effect of an External Uniform Field on the Equatorial Threshold Rigidity in a Centred Dipole Field.

We shall use the same coordinate system as in Figure The vector potential of the combined dipole and external uniform field may be written:-

$$A = \frac{M \cos\lambda}{r^2} i_w - i_w \frac{rH_z \cos\lambda}{2} \qquad (1)$$

where the symbols have the same meaning as in the original Stormer treatment (pages 13-16) except H_z which equals the uniform external field along the dipole axis.

The first integral of motion in the ϕ direction is:-

$$b = r \cos\lambda \sin\theta + \left(\frac{M}{r^2} - \frac{rH_z}{2} \right) \frac{r \cos^2 \lambda}{P} \qquad (2)$$

We now make the substitution:

$$R = \sqrt{\frac{P}{M}}\, r$$

where R is now in Stormer units and Put

$$\sqrt{\frac{P}{m}}\, b = 2\gamma$$

Pages 168, 169 are in the reversed order

to:- $Y = X + 3YX$

i.e. $Y = \dfrac{X}{1 - 3X}$

Therefore $R = 1 + \dfrac{X}{1 - 3X} = \dfrac{1 + 2X}{1 - 3X}$ (8)

Substituting (8) into (4) and putting $\cos = 1$ and $\sin\theta = 1$

$$\frac{1 + 2X}{1 - 3X} + \frac{1 - 3X}{1 + 2X} - X\left(\frac{1 + 2X}{1 - 3X}\right)^2 = 2$$

$$(1 - 3X)(1 + 2X)^2 + (1 - 3X)^3 - X(1 + 2X)^3 = 2 \quad (1 + 2X)(1 - 3X)^2$$

Using the binomial expansion the equation reduces to:-

$$= \frac{1\ (2 + 3X)}{2\ (1 + 2X)}$$

Substituting into equation (4) with $\sin\theta = 0$ (vertical incidence)

$$\frac{(2 + 3X)}{(1 + 2X)} = \frac{1}{R} - R^2X$$

Assuming $R = \frac{1}{2}(1 + B)$ and solving for B we obtain:-

$$B = \frac{X(3 - 2X)}{2(1 + 2X)(4 + X)}$$

Using a binomial approximation we obtain:-

$$R = \frac{1}{2}\left(1 + \frac{X}{z}\,\frac{(3 - 2X)}{2(4 + 9X)(1 + 2X)}\right)$$

(2) then reduces to:-

$$2\gamma = R\cos\lambda\sin\theta + \frac{\cos^2\lambda}{R} - \frac{M^{1/2}\cos^2\lambda}{2P^{3/2}} R^2 H_z \qquad (3)$$

Substituting: $\frac{MH_z}{2P^{3/2}} = X$

$$2\gamma = R\cos\lambda\sin\theta + \frac{\cos^2\lambda}{R} - XR^2\cos^2\lambda \qquad (4)$$

Putting the condition $\sin\theta < 1$. We now wish to find the minimum in the R - γ curve which will indicate the position of the inner pass point. We therefore equate $\frac{d\gamma}{dR} = 0$

$$\frac{d\gamma}{dR} = \frac{1}{2}(\cos\lambda\sin\theta - \frac{\cos^2\lambda}{R^2} - 2XR\cos^2\lambda) = 0 \qquad (5)$$

At the equator equation (5) reduces to:-

$$1 - \frac{1}{R^2} - 2XR = 0 \qquad (6)$$

$(\sin\theta = 1)$

or

$$R^2 - 1 - 2XR^3 = 0 \qquad (7)$$

Let us assume to a first order:-

$$R = 1 + Y$$

Using the first terms of the binomial expansion equation (7) reduces

$$R = \sqrt{\frac{P}{M}}\, r$$

so that at $r = r_e$, r_e being the radius of the earth

$$P = \frac{M}{r_e^2} R^2$$

$$P = \frac{M}{4r_e^2}\left(1 + \frac{X(3 - 2X)}{2(1 + 2X)(4 + 9X)}\right)^2$$

This approximately reduces to:-

$$P = \frac{M}{4r_e^2}\left(1 + \frac{3}{4} X\right)$$

Now $$X = \frac{M H_z}{2P^{3/2}}$$

If we make the substitution $P = \frac{M}{4r_e^2}$

$$X = \frac{4H_z}{H_e}$$

where H_e is the horizontal field at the equator due to the centred dipole alone. Substitution of $H_z = 100\gamma$ (10^{-3} gauss) indicates a change in P of about 1%.